LIBRARY
Michigan State
University

PLACE IN RETURN BOX
to remove this checkout from your record.
TO AVOID FINES return on or before date due.

DATE DUE	DATE DUE	DATE DUE
JAN 11 2000		
NOV 08 2002 11 08 02		

1/98 c:/CIRC/DateDue.p65-p.14

PRODUCT/PACKAGE INTERACTION: EFFECT OF PHYSICAL, CHEMICAL, AND CLIMATIC ENVIRONMENTS

By

Mark David Newsham

A DISSERTATION

Submitted to
Michigan State University
in partial fulfillment of the requirements
for the degree of

DOCTOR OF PHILOSOPHY

School of Packaging

1998

ABSTRACT

PRODUCT/PACKAGE INTERACTION:
EFFECT OF
PHYSICAL, CHEMICAL, AND CLIMATIC ENVIRONMENTS

By

Mark David Newsham

As the use of plastics in packaging proliferates, there is an increasing need to be able to determine *a priori* what types of plastics are likely to provide suitable shelf lives and product integrity under a variety of environmental conditions. The research presented provides initial steps towards the fundamental understanding of interactions between products, packages, and their storage and physical environments.

Product/package interactions were evaluated for three product/package systems: a bleach alternative laundry additive, an anti-bacterial surface cleaner, and a glass surface cleaner. The package system was comprised of high density polyethylene bottles with induction sealed closures. The physical environment was studied by comparing product/package systems that were exposed to simulated distribution testing to those that were not. The storage environments were ambient conditions, 100, 120, and 140 °F.

Damage caused by distribution testing occurred in the bottle or closure component of the package. Bottle defects resulting from distribution testing were dents, abrasions, and creases. Closure defects resulted in sheared off closures, cracks in the closure body, or nozzle cover damage.

Product/package systems exposed to the four storage environments were inspected for failure, defined as product leaking from the package, during the six month study. All systems failed due to environmental stress cracking. Dents in the shoulder and bottom region of the bottle were the only simulated distribution defects that impacted the storage stability of the product/package systems, which often resulted in reduced shelf life. The primary location of all other failures was near the center of the bottle bottom edge, which was the thinnest region of the bottle. The bleach alternative laundry additive was the most aggressive product, while the two surface cleaners exhibited similar storage stability.

Performance criteria of failed bottles were evaluated to study the impact of package system properties on product/package integrity. Yield strength, modulus of elasticity, and dynamic mechanical properties of failed samples acquired from bottle side panels did not change significantly from control samples. However, modest increases of ~10% in yield strength and modulus were observed for select systems. Color changes were monitored by measuring interior and exterior surface yellowness indices of bottle side panels. Although observed spectrophotometrically, these changes were not detected visually.

To my wife.

ACKNOWLEDGMENTS

I would like to thank my entire family for all their support and encouragement during my second Ph.D. adventure. Above all, my wife Sharon deserves the biggest credit of all for her unending love, devotion, and understanding. Special thanks to Kelli and David for allowing me to be their part-time roommate during the past several months, to MaryAnne for her support and help finding my way around the department, and to Brandi for taking care of Sharon when I was away from home. I would also like to acknowledge my parents for the years of support and encouragement they have provided me.

I need to give special thanks to all the professors in The School of Packaging at Michigan State University. I cannot express how much they have helped me with my research, faculty responsibilities, job search, etc. I would especially like to thank Bruce Harte, Jack Giacin, Paul Singh, and Tee Downes for the special effort they put forth on my behalf.

I would also like to acknowledge several colleagues that have helped me with various aspects of the research. Thanks to DeLynne Vail and Jeff Wolford for the hours they spent filling bottles with product, Mike Rich for his help in the Composite Materials and Structures Center, Rob Tempelman for help with the statistical analysis of the data, and Teerapong Laoharavee for performing all the d-limonene GC analyses. Finally, I

would like to thank all my friends throughout the Dow Chemical organization, especially Scott Silvenis, Marilyn Shope, Chuck Broomall, Dee Strand, and Charlie Berglund, for all the technical support they provided.

TABLE OF CONTENTS

Page

LIST OF TABLES ix

LIST OF FIGURES xi

LIST OF ABBREVIATIONS xv

INTRODUCTION 1

CHAPTER 1 - BACKGROUND 5

CHAPTER 2 - EXPERIMENTAL 10
A. Materials 10
1. Bottles and Closures 10
2. Polymer Resins 12
3. Cleaning Products 13
4. Corrugated Shipping Containers 14
B. Methods 14
1. Preparation of Product/Package Systems 14
2. Simulated Distribution Testing 15
3. Storage of Product/Package Systems 18
4. Tensile Testing 18
5. Dynamic Mechanical Analysis 19
6. Yellowness Index Determination 19
7. Percent Crystallinity Determination 20
8. Sorption of d-Limonene 20
9. Density Measurement 22
10. Optical Photographs 23
11. Bottle Dimensions 23
12. Molecular Weight Measurement 23

CHAPTER 3 - RESULTS AND DISCUSSION 25
A. Empty Control Bottle Properties 25
1. Introduction 25
2. Mechanical Properties 26

3. Dynamic Mechanical Properties 30
4. Percent Crystallinity 31
5. Yellowness Index 34
6. Sorption of d-Limonene for Anti-Bacterial Surface Cleaner 35
7. Summary of Empty Control Bottle Properties 35
B. Effect of Simulated Distribution Testing 36
1. Introduction 36
2. Package System Defects Caused by Simulated Distribution Testing 39
C. Package System Weight Loss During Storage 51
1. Introduction 51
2. Percent Weight Loss Results 52
3. Weight Loss Rates 57
D. Characterization of Package System Failure During Storage 60
1. Introduction 60
2. Characterization of Failure Modes 62
3. Quantification of Product/Package System Integrity 80
4. General Cumulative Failure vs. Time Behavior 95
E. Environmental Effects on Package System Properties 97
1. Mechanical Properties 97
2. Dynamic Mechanical Properties 115
3. Yellowness Index 126
4. Crystallinity 137
5. Sorption of d-Limonene for Anti-Bacterial Surface Cleaner 139

CHAPTER 4 - CONCLUSIONS 143

LIST OF REFERENCES 147

LIST OF TABLES

Page

Table 1. Properties of virgin and PCR HDPE resins. 13

Table 2. Weights of shipping containers....16

Table 3. Properties of empty HDPE control bottles. 35

Table 4. Breakpoints of truck/air vibration spectrum. 38

Table 5. Characteristic package system defects from Simulated Distribution Testing. ...47

Table 6. Number of package systems with characteristic defects....51

Table 7. Percent weight loss at the end of storage. 57

Table 8. Weight loss rates during aging....58

Table 9. Failure modes observed at 140 °F....63

Table 10. Failure modes observed at 120 °F and totals. 63

Table 11. Fisher's Exact Test results for failure mode analysis. 69

Table 12. Thickness measurements of bottles used for the product/package systems....72

Table 13. *Initiation periods* during storage....90

Table 14. Failure rates during storage....90

Table 15. Analysis of covariance results for cumulative failure vs. time plots. 90

Table 16. t-Test results for tensile yield stress....102

Table 17. Mechanical properties of product/package systems at the end of the study...106

Table 18. t-Test results for yield stress at the end of the study....106

Table 19. t-Test results for modulus of elasticity. 108

Table 20. t-Test results for modulus of elasticity at the end of the study. 114

Table 21. t-Test results for exterior surface yellowness index measurements. 126

Table 22. t-Test results for interior surface yellowness index measurements. 126

Table 23. Percent crystallinity of 140 °F samples. 137

Table 24. Percent crystallinity of 120 °F samples. 138

Table 25. Percent crystallinity at the end of study of 100 °F and ambient samples. 139

LIST OF FIGURES

Page

Figure 1. View of HDPE bottle used in the study.....11

Figure 2. Stress vs. strain plot for empty control bottle panel sample.....28

Figure 3. Modulus of elasticity determination for empty control bottle panel sample.....29

Figure 4. DMA plot for empty control bottle front panel sample.....32

Figure 5. Typical DSC plot for empty control bottle front panel sample.....33

Figure 6. Shoulder dent in laundry additive bottle placed in storage at 140 °F.....40

Figure 7. Shoulder dent in anti-bacterial cleaner bottle placed in storage at 140 °F. 41

Figure 8. Shoulder dent in anti-bacterial cleaner bottle placed in storage at 120 °F. 42

Figure 9. Shoulder dent in glass surface cleaner bottle placed in storage at 120 °F.....43

Figure 10. Shoulder dent in anti-bacterial cleaner bottle placed in storage at 100 °F. 44

Figure 11. Bottom dent in anti-bacterial cleaner bottle placed in storage at 120 °F.....45

Figure 12. Bottle defects in product/package systems from distribution testing.....48

Figure 13. Closure defects in product/package systems from distribution testing. 50

Figure 14. % weight loss vs. time for laundry additive. 53

Figure 15. % weight loss vs. time for anti-bacterial cleaner.....54

Figure 16. % weight loss vs. time for glass surface cleaner. 55

Figure 17. Number of failures for product/package systems stored at 140 °F.....64

Figure 18. Number of failures for laundry additive system stored at 120 °F. 65

Figure 19. View of bottle with vertically oriented stress crack. 67

Figure 20. Detailed view of bottle with vertically oriented stress crack.....68

Figure 21. Detailed view of laundry additive bottle shoulder dent of Figure 6.....74

Figure 22. Detailed view of anti-bacterial cleaner bottle shoulder dent of Figure 7. 75

Figure 23. Detailed view of anti-bacterial cleaner bottle shoulder dent of Figure 8. 76

Figure 24. Detailed view of glass surface cleaner bottle shoulder dent of Figure 9.....77

Figure 25. Detailed view of anti-bacterial cleaner bottle shoulder dent of Figure 10. 78

Figure 26. Detailed view of anti-bacterial cleaner bottle bottom dent of Figure 11.....79

Figure 27. Cumulative failure vs. time for laundry additive at 140 °F.....81

Figure 28. Expanded cumulative failure vs. time for laundry additive at 140 °F.....82

Figure 29. Cumulative failure vs. time for laundry additive at 120 °F.....83

Figure 30. Expanded cumulative failure vs. time for laundry additive at 120 °F.....84

Figure 31. Cumulative failure vs. time for anti-bacterial cleaner at 140 °F. 85

Figure 32. Expanded cumulative failure vs. time for anti-bacterial cleaner at 140 °F. 86

Figure 33. Cumulative failure vs. time for glass surface cleaner at 140 °F.....87

Figure 34. Expanded cumulative failure vs. time for glass surface cleaner at 140 °F.....88

Figure 35. General cumulative failure vs. time plot as a function of temperature.....96

Figure 36. Yield stress vs. time for laundry additive bottle panels stored at 140 °F. 98

Figure 37. Yield stress vs. time for laundry additive bottle panels stored at 120 °F. 99

Figure 38. Yield stress vs. time for anti-bacterial cleaner bottle panels stored at 140 °F.....100

Figure 39. Yield stress vs. time for glass surface cleaner bottle panels stored at 140 °F.....101

Figure 40. Modulus of elasticity vs. time for laundry additive bottle panels stored at 140 °F.....109

Figure 41. Modulus of elasticity vs. time for laundry additive bottle panels stored at 120 °F. 110

Figure 42. Modulus of elasticity vs. time for anti-bacterial cleaner bottle panels stored at 140 °F. 111

Figure 43. Modulus of elasticity vs. time for glass surface cleaner bottle panels stored at 140 °F. 112

Figure 44. DMA plot for failed laundry additive bottle panel after 27 days at 140 °F... 117

Figure 45. DMA plot for failed laundry additive bottle panel after 90 days at 120 °F... 118

Figure 46. DMA plot for failed anti-bacterial cleaner bottle panel after 109 days at 140 °F. 119

Figure 47. DMA plot for anti-bacterial cleaner bottle panel after 180 days at 120 °F. .. 120

Figure 48. DMA plot for failed glass surface cleaner bottle panel after 87 days at 140 °F. 121

Figure 49. DMA plot for glass surface cleaner bottle panel after 180 days at 120 °F.... 122

Figure 50. Tan δ plots of bottle panels for product/package systems stored at 140 °F. . 124

Figure 51. Tan δ plots of bottle panels for product/package systems stored at 120 °F. . 125

Figure 52. Exterior surface yellowness index vs. time for laundry additive bottles stored at 140 °F. 127

Figure 53. Interior surface yellowness index vs. time for laundry additive bottles stored at 140 °F. 128

Figure 54. Exterior surface yellowness index vs. time for laundry additive bottles stored at 120 °F. 129

Figure 55. Interior surface yellowness index vs. time for laundry additive bottles stored at 120 °F. 130

Figure 56. Exterior surface yellowness index vs. time for anti-bacterial cleaner bottles stored at 140 °F. 131

Figure 57. Interior surface yellowness index vs. time for anti-bacterial cleaner bottles stored at 140 °F. 132

Figure 58. Exterior surface yellowness index vs. time for glass surface cleaner bottles stored at 140 °F. 133

Figure 59. Interior surface yellowness index vs. time for glass surface cleaner bottles stored at 140 °F. 134

Figure 60. d-Limonene concentration in bottle panels of anti-bacterial cleaner product/package system as a function of temperature. 141

LIST OF ABBREVIATIONS

ASTM	American Society for Testing and Materials
CIE	Commission International de l'Éclairage (International Commission on Illumination)
DSC	differential scanning calorimetry
ESC	environmental stress cracking
HDPE	high density polyethylene
ISTA	International Safe Transit Association
MEK	methyl ethyl ketone
PCR	post-consumer recycled
RH	relative humidity
SDT	Simulated Distribution Testing (procedure used for this research)
TIP	torque-inch-pound
YI	yellowness index

INTRODUCTION

As the use of plastics in packaging applications proliferates, there is an increasing need to be able to determine *a priori* what types of plastics are likely to provide suitable shelf lives and product integrity for specific products under a variety of environmental conditions. Manufacturers often cannot afford to invest time and money in evaluating candidate materials for new products. In addition, the number of available resins, including the use of post-consumer recycled (PCR) resins, continues to expand at a rapid pace. If there were a thorough fundamental understanding of the interactions between products, packages, and their storage and distribution environments, then manufacturers could use knowledge about their product to determine, without a substantial investment in testing, whether a particular plastic package was likely to meet their needs. This would reduce the need for extensive testing of package systems for new products and enhance the likelihood of successful performance of those packages, thus providing significant time and economic benefits. The research described in this dissertation provides the initial steps towards the development of this type of fundamental understanding. The ultimate outcome of studies of this kind, if successful, will be a model for package selection and design based on product characteristics.

This study investigates the effect of chemical, physical, and climatic environmental factors on the storage stability of well-characterized product/package systems. Chemical factors were controlled by varying the nature of the contact phase (i.e., the product). Three different commercially available cleaning products were selected. First, a bleach alternative laundry additive was studied because it is known to be a very aggressive product towards plastics. Second, an anti-bacterial surface cleaner was used because it contains d-limonene, a chemical known to affect properties of plastics by sorption into the packaging material. Third, a glass surface cleaner that is a mildly aggressive product, especially when compared to the bleach alternative laundry additive product, was investigated.

The package system was comprised of rigid high density polyethylene (HDPE) bottles with heat-sealed foil membranes as the closures. HDPE bottles were chosen as the primary packaging component because they are widely used in the industry for a variety of applications ranging from milk to cleaning product packaging. A heat-sealed foil membrane was used as the closure in an effort to eliminate the influence of closure on product/package system integrity for this initial study.

The effect of the physical environment was investigated by subjecting product/package systems to simulated shock and vibration forces that would represent typical handling and transportation environments. Following simulated distribution testing, the product/package systems were stored under four different environmental conditions. These conditions were ambient conditions of approximately 72 °F and 50 % RH, and 100, 120, and 140 °F, which were representative of abusive storage temperatures

(RH was not controlled in any of these environments). The study was conducted over a period of six months. The product/package systems were inspected for structural integrity after exposure to physical and climatic environments. Failure analysis for systems exposed to simulated distribution testing were compared to systems that did not experience distribution testing.

In addition to performing a failure analysis on product/package systems stored under the different environmental conditions, performance criteria of failed systems were evaluated. The objective was to initiate a fundamental understanding that relates package properties to performance during long-term storage.

Performance criteria for the product/package systems included failure mode determination, bottle mechanical properties, and color changes. In addition, percent crystallinity was monitored, as it is an important physical characteristic of plastics. Failure of the packaging system was defined as the occurrence of a leak in the package system, which was accomplished by visual inspection. This included inspecting the package systems for visual cracks and failures in the body, base, and neck region of the bottle. Mechanical properties investigated included the yield stress and modulus of elasticity of bottle front and back panels, the strength of side and bottom seams, and dynamic mechanical properties. In addition, yellowness indices (YI) of the interior and exterior surfaces of the package structure were measured.

Product compositional changes were monitored by measuring the pH of the product. In addition, the level of d-limonene sorption by the package structure for the

anti-bacterial surface cleaner was investigated. Weight loss was also used to gain an understanding of package integrity.

In summary, the research described is the initial stage in the development of a more fundamental understanding of the interactions between packages, products, and the distribution environment. The methodology developed can be used as a guideline for further research and in-depth investigations. The results have both practical and theoretical significance. In terms of practical importance, this research is the initial step in determining the general utility and applicability of an experimental design which evaluates package performance as a function of the product/package system and environmental conditions. In terms of theoretical importance, the results presented here help provide a better understanding of the interaction between package structures, the chemical nature of the contact phase, and environmental factors which can impact the quality of product/package systems. It is hoped that the work described in this dissertation can provide the basis for the successful development of a model for package selection and design.

CHAPTER 1

BACKGROUND

The use of plastics in packaging continues to grow and develop at a rapid pace. New plastic packaging materials are continually being developed for applications ranging from food packaging to cushioning. In addition to the continued number of virgin plastic packaging materials available, there is a concurrent drive to increase the use of recycled plastic resins. Clorox claims to use up to 27% recycled plastics in their packaging applications which totals more than 100 million pounds per year - for Clorox alone [1]! Finally, the continual drive towards cost savings results in manufacturers using as little packaging material as possible [2]. For example, "thinwalling", which is the reduction in wall thickness of packaging components such as bottles, can be used to reduce packaging material. These combined factors have increased the importance of being able to predict the long-term stability of product/package systems and how environmental and physical factors impact this stability.

It has long been known that many polymeric materials such as high density polyethylene are susceptible to failure due to cracking when exposed to mechanical stress in combination with certain kinds of liquids [3]. This phenomenon, called environmental stress cracking (ESC), occurs only when a material is under stress and in contact with specific liquids. In other words, ESC is failure associated with cracking which is due to

the simultaneous action of mechanical stress and specific liquids. It has been estimated that approximately 15% of all failures of plastic components in service are due to ESC [4]. Indeed, one of the primary technical challenges in developing bottles using PCR high density polyethylene is to minimize failure resulting from ESC [5]. Not surprisingly, this has been an area of extensive research in the past, and continues to be an important issue for the successful use of many plastic packaging materials.

The source of stress in a plastic packaging material can be from a number of different sources. Stress is often unavoidable since it is processed into the packaging component, such as a bottle, during the molding process. Therefore, applied stress is not always necessary because stress is already present in the package system. The stress can also be due to and/or increased from other post-processing events such as pressure build-up inside sealed systems. The pressure build-up can result from volatile components of the product and will be dependent on product composition and the environmental conditions to which the product/package system is exposed.

Fluid contact with a plastic packaging material can be either from primary or secondary sources. Primary fluid contact occurs due to immersion or containment of the product in packages such as bottles, tubes, etc. and secondary sources result when the intended function indirectly causes fluid contact. Examples of secondary sources include adhesives, paints, lacquers, lubricants, cleaning agents, aerosol spray, plasticizers, and inks. Severe ESC agents include fluids that are readily adsorbed by a plastic. Typically, a plastic packaging material will not readily adsorb the product in which it is in contact with, otherwise it would create a poor product/package system. Moderate ESC agents are

responsible for a large percentage of the practical problems associated with ESC, including packaging-related failures. In this case, the fluid and plastic are classified as compatible. However, the fluid in the presence of stress leads to cracking. Mild ESC agents will tend to reduce extremely long service lives. For example, service life may be reduced from 20 to 10 years [4].

In addition to the environmental factors such as ESC that can impact the long-term stability of product/package systems, the physical environment can also influence package integrity. The most significant physical condition that impacts product/package systems is the distribution environment to which most products are exposed. Choudhry *et al.* [6] studied the influence of mechanical stresses and vibrations associated with product transport on the migration of plastic components from PVC. Global migration, as determined by total organic carbon, was affected by transport simulation. However, this is one of the only published research papers that characterizes the impact of distribution forces on the fundamental properties of product/package systems. Singh *et al.* [7] studied the effect of closure type in gallon-size plastic bottles in a simulated small parcel test environment. Schluter *et al.* [8] investigated the effect of distribution packaging method on the physical properties and retail display characteristics of pork.

Simulated distribution testing is often performed to assess the impact of shock and vibration type physical forces on packaging systems, and to aid in material selection to ensure a package withstands these types of forces. There are two standards that are commonly used in the United States to perform simulated distribution testing. The standard developed by the American Society for Testing and Materials (ASTM), ASTM

D-4169 [9], is used to provide a uniform basis of evaluating the ability of shipping containers, in a laboratory environment, to withstand typical distribution environments. The second set of standards, which were developed by the International Safe Transit Association (ISTA), are the "Preshipment Test Procedures" [10, 11] which are used in a similar manner to provide a laboratory procedure which assesses the probability of safe arrival of a packaged product at the ultimate destination.

Each standard describes the necessary laboratory procedures for subjecting shipping containers to the shock and vibration forces associated with the transportation environment. The ISTA procedure, which is more severe than the corresponding ASTM test, generates impact forces (drops) that will be experienced by less than approximately 5 to 10% of packaged products in an actual distribution environment [12]. Therefore, this procedure is typically used for high-end, or more severe, testing.

Of further interest is the relationship between package system properties and the failure of product/package systems. Mechanical properties are known to be affected by exposure to certain types of chemical environments. Tensile yield strength is reduced by the sorption of fluid plasticizers by polymers [4]. The modulus of elasticity was shown to decrease in low density polyethylene films with the sorption of d-limonene [13]. However, limited published work is available on the relationship between failure of product/package systems during long-term storage and the physical properties of the components comprising the package.

Accelerated aging studies are frequently used to predict the integrity of product/package systems during long-term aging under actual storage conditions.

Accelerated aging conditions will vary depending on product and manufacturer, but typically utilize elevated storage conditions for short periods of time. Typical conditions for commercial cleaning products are 120 °F for about 3 months. Package systems that survive the accelerated test are considered acceptable for the particular product studied. Other accelerated aging tests expose test samples to a 140 °F environment or a temperature cycling procedure.

Expanding the understanding of the effect of environmental and physical conditions on the integrity of product/package systems can help develop the necessary knowledge for a rational selection of appropriate packaging materials for a wide variety of products. Although studies have been done separately in the different areas, limited work is available which combines the above described disciplines.

CHAPTER 2

EXPERIMENTAL

A. Materials

1. Bottles and Closures

White HDPE bottles (22 oz) were received from an external supplier. The bottles were extrusion blow molded and had a standard 28-400 finish. They were a three layer structure, consisting of virgin HDPE as the two external layers and PCR HDPE as the internal layer. Figure 1 shows a photograph of a typical bottle used in this study. The arrow points to the location of failure which is discussed in Chapter 3.D.2. and the number was used for sample identification. Several terms and their definitions that relate to the bottle and are used throughout the dissertation are given below.

1. Bottom: The bottom surface of the bottle.
2. Horizontal and Vertical: Horizontal and vertical samples were taken from the front or back panels with the long axis of the samples oriented horizontal and vertical, respectively.
3. Mold Seam: A line formed at the point of contact of the mold halves [14]. This will also be called a side seam throughout this report. It is also often referred to as the "mold parting line".

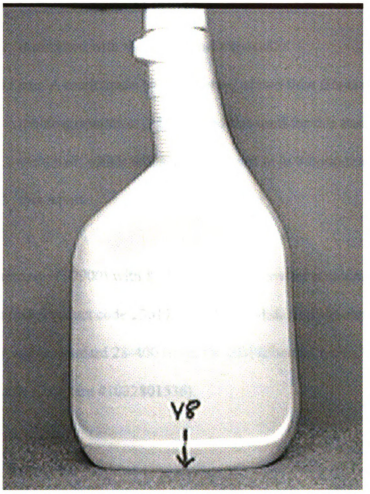

Figure 1. View of HDPE bottle used in the study.

4. Neck: The region between the bottle finish and shoulder.
5. Panels: The two sides of the bottle with the largest surface area. These are classified as the front or back. The front is that which is facing forwards when a right-handed person is holding the bottle, and the back is the back-side for this same orientation. The bottle in Figure 1 is oriented with the front panel exposed.
6. Weld Line: A mark made by the meeting of two flow fronts during the molding operation [14]. The bottles used for this study have a bottom weld line, which will also be referred to as a bottom seam throughout this report.

Trigger sprayers (T7900) with 8 11/16 in dip tubes were obtained from Continental Sprayers (Product code 23017929). Plain white, pulp-backed induction sealable closures with a standard 28-400 finish for HDPE bottles were obtained from Northwestern Bottle Co. (Item #1032801536).

2. Polymer Resins

Resin samples of both the virgin HDPE and PCR HDPE were provided by the supplier of the bottles. The virgin resin, which was a high density polyethylene copolymer, was white in color, while the recycled resin appeared greenish. The properties of each resin are shown in Table 1. Molecular weight values were determined as described in Chapter 2.B.12., and are reported as apparent molecular weights based on

k and a values for polyethylene/polystyrene universal calibration. Percent crystallinity was obtained as described in Chapter 2.B.7. The melt flow index was determined by using ASTM D-1238 [15] as a guideline. The temperature and total load used were 190 °C and 2.16 kg, respectively. The melt flow values obtained are consistent with those reported for polyethylene resins of similar molecular weight and percent crystallinity [16].

Table 1. Properties of virgin and PCR HDPE resins.

Resin Property	Virgin HDPE	PCR HDPE
Density (g/cm^3)	0.9457	0.9454
M_n	11,400	20,000
M_w	121,000	117,000
M_z	742,000	508,000
M_w/M_n	10.6	5.9
Percent crystallinity	60 ± 3	59 ± 3
Melt flow index	3.02	2.87

3. Cleaning Products

Three different household cleaning products were obtained from the supplier of the HDPE bottles: 1) a bleach alternative laundry additive, 2) an anti-bacterial surface cleaner, and 3) a glass surface cleaner. The chemical composition of each product was not made available since this type of information is classified as proprietary. However, the pH specification ranges for research-grade samples were provided so product quality could be monitored by using pH measurements. The ranges for the laundry additive,

anti-bacterial cleaner, and glass surface cleaner were 3.5 - 4.4, 12.0 - 12.3, and 9.4 - 9.7, respectively.

During the six month study, the laundry additive product system remained within specification under all environmental conditions. However, both surface cleaner products did not fall within the research sample specification limits. The initial pH of the anti-bacterial and glass surface cleaner products was 11.92 and 9.00, respectively. This may be due to the fact that the products were received from the production facility, where it is known that the pH may be slightly different than for research samples. During the course of the study, however, the pH did not change significantly for each of these products. The range was 11.87 - 11.98 for the anti-bacterial cleaner and 8.91 - 9.07 for the glass surface cleaner.

4. Corrugated Shipping Containers

Knocked-down corrugated shipping containers were obtained from the supplier of the HDPE bottles. The shippers were used for simulated distribution testing of the product/package systems. They were designed to hold 12 - 22 oz bottles with trigger sprayer closures.

B. Methods

1. Preparation of Product/Package Systems

The HDPE bottles were manually filled with each product using 1000 mL graduated cylinders to measure the volume of 22 oz (651 mL). The bottles were filled,

and the induction sealable closures were manually applied with a torque of ~16 - 17 torque-inch-lb (TIP) using a Secure Pak, Inc. electronic torque tester to measure the torque. The induction seals were then made using an Enercon Industries Corp. induction sealer (Model LM2543-2) with timer and power control settings of 2 s and 8, respectively. Finally, the trigger sprayers (with dip tube removed) were manually applied with a torque of ~17 - 19 TIP using the same procedure as for the induction sealable closures. These were applied to reduce excessive headspace in the corrugated shipping containers since the shippers were designed to hold 22 oz bottles with trigger sprayers.

The filled product/package systems were placed in corrugated shipping containers so simulated distribution testing could be performed. The knocked-down corrugated boxes were first manually assembled using a 3M Polygun II glue gun and 3M Jet-melt 3762-PG hot melt adhesive. The adhesive contains ethylene-vinyl acetate polymer, hydrocarbon, hydrocarbon resin, paraffin wax, and vinyl acetate. The filled bottles, with trigger sprayer closures, were then loaded into the cases and the outer flap was sealed using the same glue gun and hot melt adhesive. The weight of each case was then measured so the appropriate distribution testing procedure could be determined. Table 2 shows the results of the weight measurements.

2. Simulated Distribution Testing

Simulated distribution testing was performed by using the ISTA "Preshipment Test Procedures - For Domestic Shipments Within the Continent of Origin" standard [10]. Test Procedure 1A (Method B) in this standard was used as a guideline. A detailed

Table 2. Weights of shipping containers.

	Weight of Shipping Container		
Shipping Container #	**Laundry Additive**	**Anti-bacterial Surface Cleaner**	**Glass Surface Cleaner**
1	20 lb 4 oz	20 lb 2 oz	19 lb 15 oz
2	20 lb 3 oz	20 lb 2 oz	19 lb 14 oz
3	20 lb 5 oz	20 lb 0 oz	20 lb 0 oz
4	20 lb 5 oz	20 lb 2 oz	20 lb 0 oz
5	20 lb 4 oz	20 lb 1 oz	20 lb 1 oz
6	20 lb 4 oz	20 lb 0 oz	20 lb 0 oz
7	20 lb 4 oz	20 lb 1 oz	20 lb 0 oz
8	20 lb 3 oz	20 lb 2 oz	19 lb 15 oz
9	20 lb 6 oz	20 lb 1 oz	20 lb 0 oz
10	20 lb 4 oz	20 lb 0 oz	20 lb 0 oz
11	20 lb 5 oz	20 lb 2 oz	20 lb 0 oz
12	20 lb 5 oz	20 lb 2 oz	20 lb 0 oz
13	20 lb 4 oz	20 lb 1 oz	19 lb 14 oz
14	20 lb 4 oz	20 lb 2 oz	20 lb 0 oz
15	20 lb 5 oz	20 lb 2 oz	19 lb 15 oz

discussion of the methodology used is given in Chapter 3.B.1. Vibration and impact testing were performed by using a Lansmont Corp. hydraulic vibration test system (Model 10,000 - 10) and a Lansmont Corp. precision drop tester (Model PDT56EX), respectively. Up to nine shipping containers were simultaneously subjected to vibration testing using the random vibration spectrum described in [10].

The following sequence for vibration testing was used. The containers were placed on the vibration table in the bottom down orientation and subjected to the random vibration test for 30 min. The containers were then inverted (top down) and tested for an additional 10 min. The two remaining orientations (both ends) were then tested for 10 min each to give a total test time of 60 min.

After the shipping containers were exposed to vibration testing, they were given ten impacts from a drop height of 30 in (1 - 20.99 lb package weight) using the precision drop tester according to the sequence described in [10]. The numbering system used for the containers is shown below:

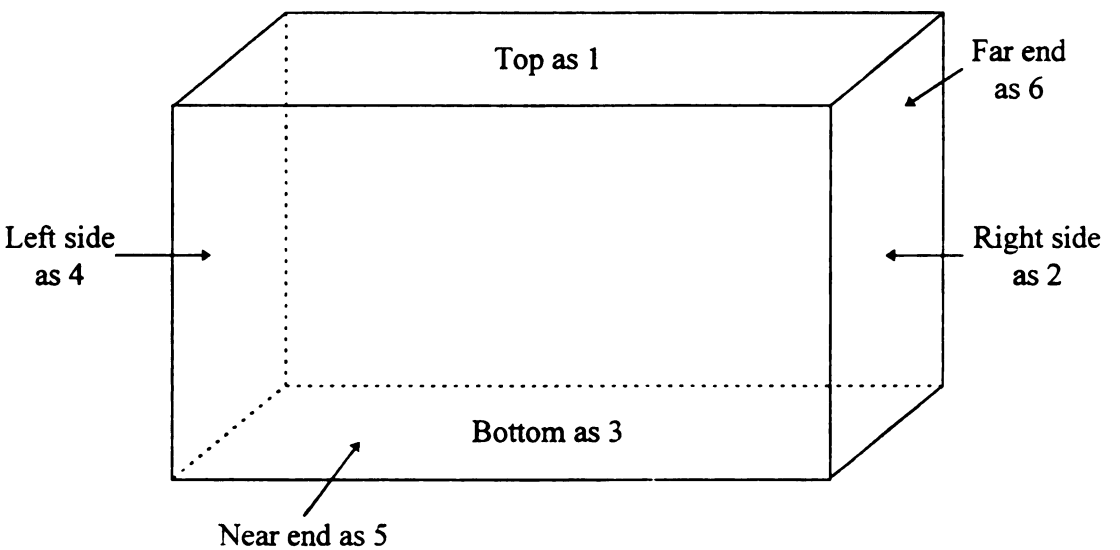

The drop sequence was:

1. 2-3-5 corner
2. the shortest edge radiating from the 2-3-5 corner (edge 2-3)
3. the next longest edge from the corner tested (2-5)
4. the longest edge radiating from the corner tested (3-5)
5. flat on one of the smallest faces (face 2)
6. flat on the opposite small face (face 4)
7. flat on one of the medium faces (face 1)
8. flat on the opposite small face (face 3)
9. flat on one of the largest faces (face 5)
10. flat on the opposite large face (face 6)

This specific ISTA test procedure used will be referred to as Simulated Distribution Testing (SDT) throughout this dissertation.

3. Storage of Product/Package Systems

Following Simulated Distribution Testing, the product/package systems were removed from the corrugated shipping containers and inspected for defects. The trigger sprayer closures were then removed and standard 28-400 continuous thread closures were applied before being placed into storage chambers.

Four different storage environments were used: 1) ambient conditions of approximately 72 °F and 50 % RH, 2) 100 °F, 3) 120 °F, and 4) 140 °F. The storage chambers used for the elevated storage conditions were Environette Controlled Environment Rooms (Model 702-1 and 703-1) and were manufactured by Lab-Line Instruments, Inc. (Melrose Park, Ill.). They were equipped with temperature range of ambient to 60 °C and did not have humidity control.

4. Tensile Testing

Tensile testing was performed using a United Calibration Corp. mechanical test machine (Model SFM-20) equipped with a 20 lb load cell. ASTM D 638-91 [17] was used as a guideline for the test procedure. Type V specimens (gauge length = 0.300 in) were cut from several different bottle locations. A jaw separation of 1 in was used. A pre-load force of 0.100 lb was applied to each sample at 0.15 in/min before the test was initiated. The tests were then performed using a strain rate of 0.15 in/min up to a strain of

100%. This procedure permitted a determination of the yield stress and modulus of elasticity, which was obtained from the linear region of the stress vs. strain curve. The linear region was considered to be up to a strain of 0.05 in/in for all samples.

5. Dynamic Mechanical Analysis

Dynamic mechanical temperature testing was conducted using a Rheometric's RDS-2 running under Rhios 4.4.4 software for machine control and data collection. The geometry was torsion rectangular with a sample size of 0.5 in x 2.5 in. A frequency of 1 rad/s and strain of 0.2% were used. The temperature range was -100 to 130 °C ramped at 10 °C/step.

6. Yellowness Index Determination

Yellowness index measurements were performed using a Hunter Associates Laboratory, Inc. HunterLab Colorquest 45/0 Spectrophotometer. ASTM D 1925-70 [18] was used as a guideline for the measurement. Illuminant C and the 2° observer were used to determine the CIE tri-stimulus values (i.e., X_{CIE}, Y_{CIE}, Z_{CIE}). The yellowness index was then calculated by using eq 1.

$$YI = [100 \times (1.28\, X_{CIE} - 1.06\, Z_{CIE})] / Y_{CIE} \qquad (1)$$

Five replicates where measured on the interior and exterior surface of each bottle sample.

7. Percent Crystallinity Determination

Percent crystallinity was determined using a TA Instruments 2200 differential scanning calorimeter (DSC). The following method was used:

1. Data storage: Off
2. Equilibrate at 20.00 °C
3. Ramp 10.00 °C/min to 0.00 °C
4. Isothermal for 1.00 min
5. Data storage: On
6. Ramp 10.00 °C/min to 170.00 °C
7. Data storage: Off
8. Initial temperature: 20.00 °C

The percent crystallinity was then calculated by using eq 2,

$$\text{Percent crystallinity} = \Delta H / \Delta H_{100} \quad (2)$$

where ΔH is the enthalpy of melt for the sample and ΔH_{100} represents the heat of fusion of theoretically 100% crystalline polyethylene. ΔH for the sample is determined by integrating the area under the melt endotherm and was determined by integrating from 50 to 150 °C. ΔH_{100}, as obtained from the literature [19], was taken to be 294 J/g.

8. Sorption of d-Limonene

Sorption of d-limonene into the HDPE bottles was determined by slightly modifying a technique previously developed by Imai [13]. Samples that were cut from

the front or back panel of each bottle were placed in 25 mL acetonitrile. The samples were allowed to equilibrate for at least 36 hr before measurements were made to permit any sorbed d-limonene to diffuse out of the HDPE and into solution.

The concentration of d-limonene in acetonitrile was determined by the published gas chromatographic procedure [13]. Standard solutions of d-limonene in carbon tetrachloride were prepared for determination of a calibration curve using the following analytical conditions:

Injection temperature:	220 °C
Detector temperature:	250 °C
Head pressure:	10 psi
Total flow port (split vent):	27.8 ml/min
Septum purge (purge vent):	2.76 ml/min
Helium flow rate:	1 ml/min

The following temperature programming conditions were utilized:

Initial oven temperature:	50 °C
Initial time:	2 min
Rate:	7 °C/min
Final temperature:	110 °C
Final time:	0 min
Rate A:	30 °C/min
Final temperature A:	200 °C
Final time A:	3 min
Total run time:	16.58 min

The above conditions gave a retention time for d-limonene of 8.94 min. The d-limonene concentration in the HDPE was then calculated by solution of eq 3,

$$\text{Conc. d-limonene (ppm)} = CF \times AU \times 10^6/wt \quad (3)$$

where CF is the calibration factor for d-limonene, AU is the area units associated with the peak in the chromatogram that is due to d-limonene, and wt is the weight of the sample that was added to acetonitrile.

9. Density Measurement

Density of the virgin and recycled HDPE resins used to fabricate the bottles was determined using a Mettler system designed to measure density. The system consisted of a Mettler AM100 balance, Mettler GA44 printer, and Mettler XPac-M module. The balance was first tared with the beaker filled with methyl ethyl ketone (MEK). Approximately 0.10 - 0.15 g of polymer was then placed on the top pan and the weight was entered into the XPac-M module. The polymer was then placed on the pan, submersed in MEK, and the weight entered into the XPac-M. The XPac-M then calculated the density given a known density of MEK (0.800 g/mL at 25 °C).

10. Optical Photographs

Photographs of product/package systems were taken using an IBM desktop personal computer (Model 750-P100) equipped with a video camera and the Snappy™ software program (version 1.0) by Play Inc.

Snappy settings were:

Video source: live camera
Image type: color
Image size: 640x480
Snap type: still video
New image: use correct window

11. Bottle Dimensions

Bottle dimensions were determined by using a Magna-Mike Hall effect thickness gage manufactured by Panametrics (Model 8000). Ten randomly selected bottles were evaluated by measuring the thickness in several different locations including the front and back panels, front and back bottom edges, and neck region.

12. Molecular Weight Measurement

The molecular weight of the virgin HDPE resin was obtained using a Waters 150C gel permeation chromatographic system. Samples (15 ± 1 mg) were dissolved in 13.0 mL of 1, 2, 4-trichlorobenzene containing 100 ppm w/w Ionol. Samples were then heated at 160 °C for 2 hr with gentle shaking to ensure dissolution. Hot samples were

filtered using a 0.5 μm stainless steel filter. Samples were then evaluated using the following analytical conditions:

Pump:	nominal flow rate 1.0 mL/min, 60 °C
Eluent:	1, 2, 4-trichlorobenzene containing 200 ppm w/w Ionol
Injector:	135 °C, 150 μL
Detection:	differential refractive index, sensitivity = 32, scale factor = 10
Data system:	Polymer Laboratories, Calibre V6.0

Calibration was accomplished using polystyrene/polyethylene universal calibration based on anionic polystyrene molecular weight standards from Polymer Laboratories (polystyrene; k = 12.6, a = 0.702 and polyethylene; k = 51.0, a = 0.706).

CHAPTER 3

RESULTS AND DISCUSSION

A. Empty Control Bottle Properties

1. Introduction

In an effort to develop a fundamental understanding relating package properties to performance during long-term storage, several performance criteria were evaluated. These criteria included mechanical properties, and yellowness indices of the exterior and interior surfaces of the bottles. For comparison, ten bottles were randomly selected for characterization of empty bottle properties and the mean and standard deviation of each property were determined. These bottles will be referred to as the control bottles throughout the dissertation. In addition, the sorption of d-limonene for the anti-bacterial surface cleaner product/package system was evaluated.

The properties of failed product/package systems were compared to the values of the control bottles in an attempt to gain an understanding of the relationship between package properties and product/package system integrity (see Chapter 3.E.). In addition, the effect of Simulated Distribution Testing on the performance criteria was determined by comparing properties of failed systems exposed to Simulated Distribution Testing to those that did not experience the testing.

2. Mechanical Properties

Mechanical properties of package system components are very important to ensure that the packaging system performs as intended. Change in mechanical properties could cause unexpected package system failure due to a variety of factors. For example, the strength of a package may be severely reduced if the tensile strength of the packaging material decreases significantly. Similarly, an increase in the modulus of elasticity would cause a material to become more brittle, and thus the package may have a greater tendency to crack from thermal and/or physical stresses.

Therefore, several different mechanical properties of samples taken from the bottle panels were measured. The yield stress was measured to provide an indication of overall bottle strength. Yield stress was determined instead of tensile strength because this property is more closely related to package system integrity, as HDPE can stretch many times its original length before it breaks, which is not possible in a bottle. In addition, tensile modulus was used as a measure of stiffness. Yield stress and tensile modulus were measured on vertical samples taken from the front or back panel of the bottles. Two samples per bottle were evaluated by measuring stress vs. strain curves.

Further, the side mold seam near the bottom of the bottle and the bottom weld line were evaluated since these locations could potentially be initiation sites for failure. Two side seam samples were obtained from each bottle (one from each side), and one bottom weld line sample located near the middle of the bottom. These samples were evaluated by determining the load at yield point, as opposed to determining the stress, since it was not possible to accurately determine the dimensions of these samples. Because of the

presence of the mold seam and weld line, the thickness varied substantially depending on where the thickness measurement was performed. Therefore, the load at yield point (lb) is reported as the strength of the side and bottom seams.

Figure 2 displays a typical stress vs. strain curve obtained for a sample from the front panel of a control bottle. Samples taken from failed product/package systems, as described in Chapter 3.E.1., exhibited similar curves. From this plot, the yield stress could be determined from the maximum stress on the curve and the tensile modulus was obtained by determining the slope of the best fit line up to a strain of 0.05 in/in. Figure 3 shows typical results obtained for the modulus of elasticity determination. This particular sample has a yield stress and modulus of elasticity of 2,800 and 26,100 psi, respectively.

Other approaches, including the secant and tangent modulus methods [20], are often used to determine tensile modulus from typical nonlinear stress-strain curves. However, since the stress vs. strain curves obtained for all samples, such as that shown in Figure 3, were nearly linear up to a strain of approximately 0.05 in/in, the linear-fit method was utilized. This approach allowed the systematic comparison of tensile modulus for several different samples. Since pre-load forces were used to remove slack from the samples, the initial data at a strain of 0 in/in were not used for the regression analyses. Therefore, the linear fits did not intersect the abscissa at a strain of 0 in/in.

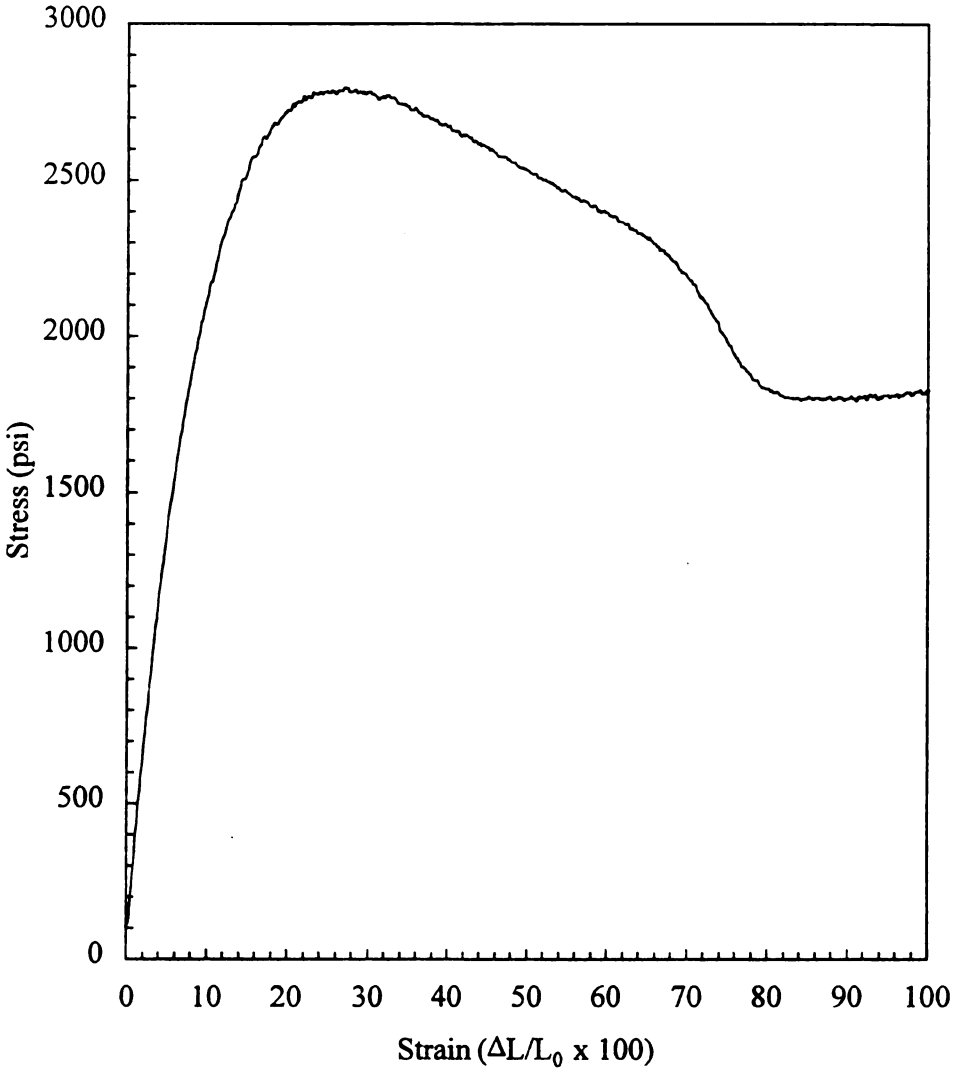

Figure 2. Stress vs. strain plot for empty control bottle panel sample.

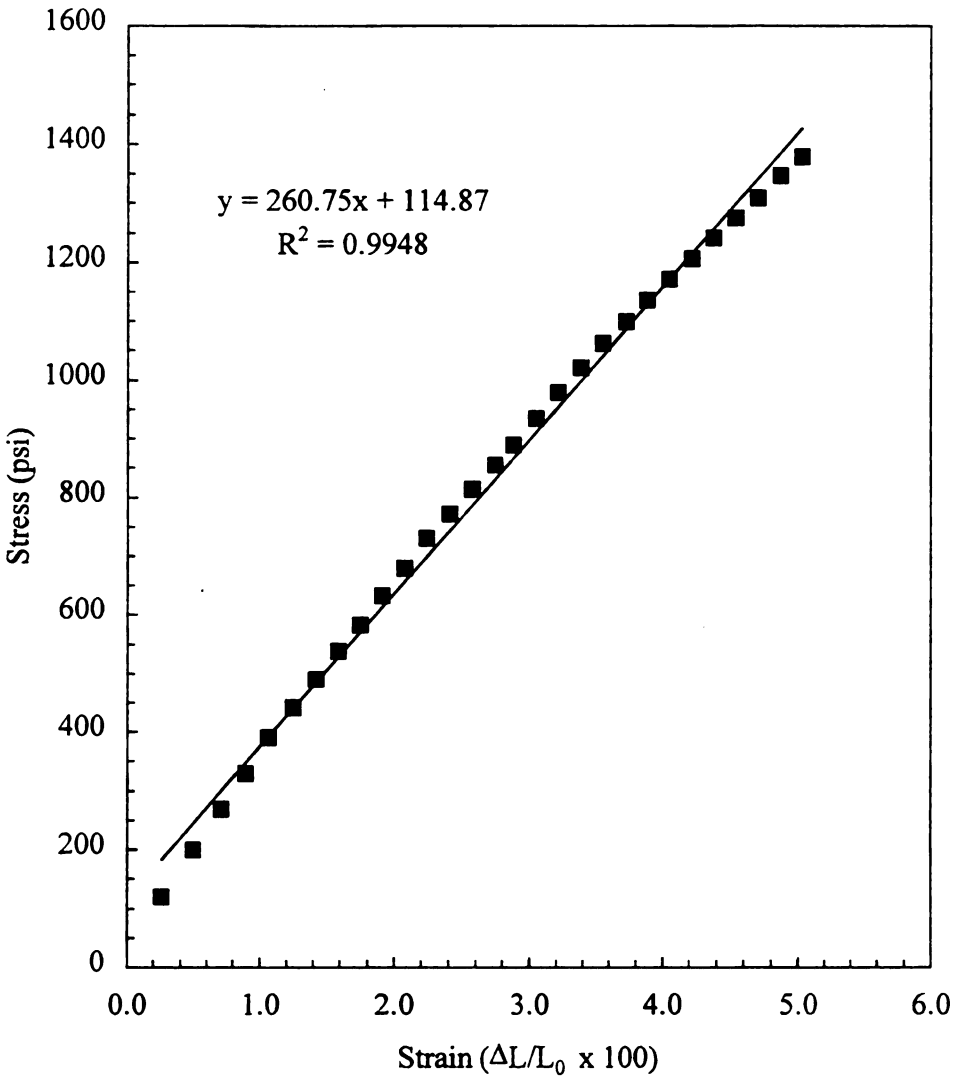

Figure 3. Modulus of elasticity determination for empty control bottle panel sample.

3. Dynamic Mechanical Properties

Dynamic mechanical tests, over a wide temperature range, are typically sensitive to the chemical and physical structure of plastics. This type of mechanical analysis is often the most sensitive test for studying secondary transitions in polymers, as well as the morphology of crystalline polymers [21]. For this reason, dynamic mechanical analysis (DMA) was also used as a performance criterion to investigate the relationship of this property to package integrity during storage.

The DMA test measures the response of a material to a sinusoidal stress applied to the sample. Since the stress and strain are normally out-of-phase, the two quantities obtained from such a test are a modulus and a phase angle (sometimes called a damping term). Results are normally given in terms of the storage modulus (G'), loss modulus (G"), and tan δ, where tan δ = G"/G' and δ is the angle that represents the time lag between the applied stress and resulting strain. Tan δ is a measure of the ratio of energy dissipated as heat to the maximum energy stored in the material during one cycle of oscillation. G' is the same as shear modulus measured by other techniques at comparable time scales, if there is small to medium amounts of damping, and G" is directly proportional to the heat dissipated per cycle [21].

The dynamic mechanical properties are very sensitive to various types of transitions, relaxation processes, and morphology in multiphase systems. In particular, the damping, which is directly related to tan δ, is extremely sensitive to these types of processes. Therefore, any dramatic changes that may occur in the tan δ peak as product/package systems age could be related to changes in polymer morphology.

Figure 4 displays the DMA plot for an empty control bottle front panel sample. The temperature dependence of G', G", and tan δ are typical of polyethylene-based polymers [21, 22]. The transition at approximately -10 to 0 °C corresponds to a pre-melting effect in which the polymer is becoming softer as it approaches the melting point and the beginning of the melting point is observed at approximately 120 to 130 °C. The results for this control bottle are presented in Chapter 3.E.2. for comparison to the DMA results obtained from bottles of failed product/package systems.

4. Percent Crystallinity

Percent crystallinity is a key physical property in determining the performance of many plastic packaging materials, including high density polyethylene bottles such as those evaluated in this study. It can influence the permeability, mechanical properties, and appearance. Therefore, changes in the percent crystallinity are expected if significant changes in mechanical properties are observed. For these reasons, percent crystallinity was determined for failed package systems and the results compared to the control samples.

Percent crystallinity was determined from DSC data as described in Chapter 2.B.7. Figure 5 shows a typical DSC plot for a sample taken from the front panel of a control HDPE bottle. The enthalpy of crystallization for this sample was 167 J/g, which gave a percent crystallinity of 57% using eq 2. The onset of the melt endotherm at ~120 °C and the peak at 132 °C are typical of a HDPE polymer.

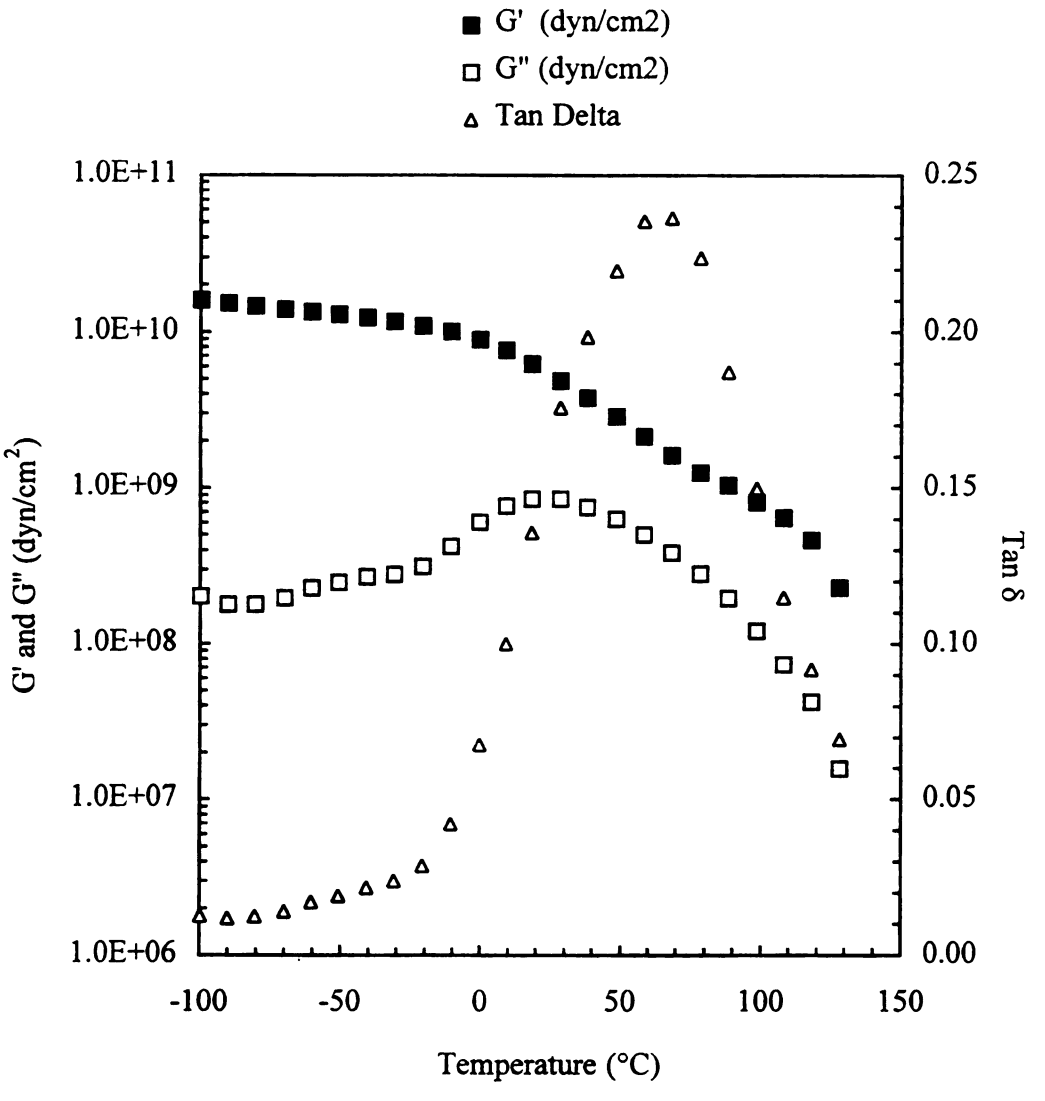

Figure 4. DMA plot for empty control bottle front panel sample.

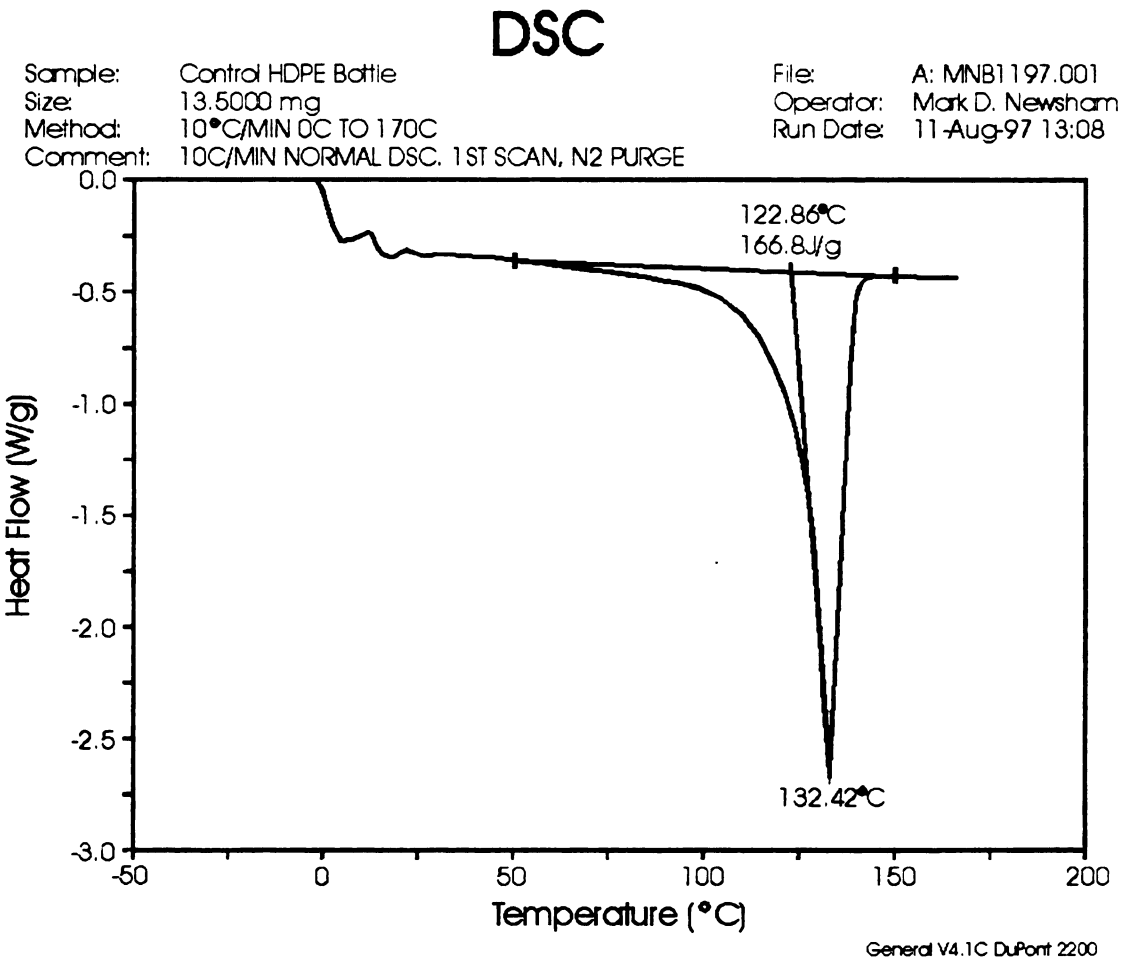

Figure 5. Typical DSC plot for empty control bottle front panel sample.

5. Yellowness Index

Uniform yellowness scales have been developed to enable the systematic comparison of the degree of yellowness of different materials. The most common yellowness scale used is based on the CIE color coordinates, which permits the determination of the yellowness index based on the CIE X, Y, and Z coordinates. The index is designed such that yellow- and blue-appearing materials possess negative and positive yellowness indices, respectively. The yellowness index can provide a useful tool in describing color changes of plastic packaging materials as they discolor due to aging over time.

While the color of a packaging system may not impact the overall performance of the product/package system, it can influence how a consumer views the product and its quality. For example, if a container slowly changes color, a consumer may perceive that the product or package system may be defective or unsafe for some reason. These factors may cause a consumer to purchase a different brand. For this reason, the yellowness index of the exterior bottle surface was monitored as an indication of package system acceptability. Because the product is in contact with the inside surface of the packaging system, it is expected that the interior surface may change color more rapidly than the exterior surface of the package. Therefore, the interior bottle surface yellowness index was monitored for comparison to the exterior surface yellowness index.

6. Sorption of d-Limonene for Anti-Bacterial Surface Cleaner

d-Limonene, a well-known component of many products, can sorb into plastic packaging materials and affect the mechanical properties and permeability. Since the anti-bacterial surface cleaner contained d-limonene as one of its components, the sorption of d-limonene into the HDPE bottle for samples of this product was determined for failed product/package systems. d-Limonene was not expected to be present in the control bottles and indeed was not detected.

7. Summary of Empty Control Bottle Properties

Table 3 summarizes the properties measured for the control bottles. The yield stress, modulus of elasticity, and percent crystallinity are all typical values associated

Table 3. Properties of empty HDPE control bottles.

Property	**Value**
Yield Stress (psi)	2880 ± 50
Modulus of Elasticity (psi)	26,100 ± 800
Strength of Side Mold Seam (lb)	8.1 ± 0.8
Strength of Bottom Weld Line (lb)	7.9 ± 0.9
Yellowness Index (exterior surface)	-2.31 ± 0.95
Yellowness Index (interior surface)	0.66 ± 0.75
% Crystallinity	59 ± 3
d-Limonene concentration (ppm)	none detected

with high density polyethylene. The yellowness index determined for both the exterior and interior bottle surface indicated a nearly white color. Although the bottles were visually white, the negative value measured for the exterior surface of the bottle (-2.31) suggests a somewhat yellow appearance, while the positive value for the interior surface (0.66) suggests a bluish color. The strength of both the side mold seam and bottom weld line was determined to be approximately 8 lb. As expected, d-limonene was not detected in the control bottles.

B. Effect of Simulated Distribution Testing

1. Introduction

The effect of the physical environment on the integrity of most product/package systems is often an extremely important packaging issue to consider, and one that the typical consumer does not often think of. In order for a packaging system to perform as intended, it must survive the transportation and storage environment that most products are exposed to in order to successfully distribute the product. Although the exact nature of the physical environment can vary depending on the mode of transportation utilized, the overall effect on an otherwise well-packaged product can be very detrimental if the shock and vibration forces associated with the distribution environment are not understood and accounted for by the packaging system design.

The effect of shock and vibration forces on a product/package system can impact the integrity of the system in three ways. First, defects due to the distribution process can result in damage to the packaging system, but not result in damage to the product. These

types of defects can be serious from an economic standpoint since many consumers will not purchase products in which the packaging system appears damaged or defective. Second, the defect can result in immediate damage to the product. This is clearly an undesirable situation since damaged products often cannot be sold and the supplier must take a loss. Third, the defect could cause failure of the product/package system during storage. This is the area that will be focused on in the present study.

Simulated Distribution Testing using the ISTA standard for domestic shipments [10] was used to expose the packaged products to the shock and vibration forces associated with the distribution environment. Details of the test are described in Chapter 2.B.2., but the methodology used to determine the details are presented here. Two independent procedures are described in this standard. Procedure 1 is for packaged-products weighing 100 lb or more, and Procedure 1A is for packaged-products weighing under 100 lb. Since the corrugated shipping containers with the product/package systems used in this study weighed less than 100 lb (~20 lb - see Table 2, page 16) Procedure 1A of the ISTA standard was utilized for the Simulated Distribution Testing.

The test sequence of the standard calls for the vibration test to be conducted first, followed by impacts, and finally an optional compression test. Compression testing was not performed because the product/package systems investigated were not designed to support any load during long-term storage. This necessitates that the corrugated shipping container supports the maximum load requirement. Method B of the vibration test section of the standard was followed since this method uses a hydraulic vibration system. According to the standard, a random truck/air vibration spectrum was used that provided

an overall G_{rms} acceleration level of 1.15 G. The breakpoints of the Power Density Spectrum are summarized in Table 4. For the impact test, Procedure 1A required a free-fall drop height of 30 inches for packages weighing 1 to 20.99 lb, along with the drop sequence described in Chapter 2.B.2. The vibration and drop tests represent the Simulated Distribution Testing.

Table 4. Breakpoints of truck/air vibration spectrum.

Frequency (Hz)	PSD Level (G^2/Hz)
1.0	0.0001
4.0	0.01
100.0	0.01
200.0	0.001

One of the goals of this research was to develop a better understanding of the effect of the physical environment on product/package interaction and how such an environment can influence the integrity of stored product/package systems. In an effort to evaluate the influence of the physical environment, three product/package systems were investigated and the effect of Simulated Distribution Testing on their integrity during long-term storage was observed. To this end, the storage stability of two different sets of product/package systems, that were exposed to each of the four storage environments (i.e., ambient, 100, 120, and 140 °F), was studied. The first set of product/package samples was subjected to Simulated Distribution Testing. Following exposure to simulated shock and vibration forces, the physical defects present in the packaging systems were characterized by determining and quantifying the various types

of defects. The second set of test samples, which were not exposed to Simulated Distribution Testing, comprised bottles that were simply filled with product, sealed, and stored in the four climatic environments.

An additional goal of this study is to initiate studies that will result in a fundamental understanding of product/package interaction or compatibility, and allow the use of accelerated aging to predict integrity of product/package systems under expected environmental conditions. Therefore, after characterization of defects resulting from Simulated Distribution Testing, all product/package systems were placed in the respective storage environments and inspected periodically until failure occurred, as described in Chapter 3.D.

2. Package System Defects Caused by Simulated Distribution Testing

Inspection of the product/package systems following Simulated Distribution Testing showed that several types of defects were caused by the shock and vibration forces associated with the testing. These defects were classified as either being present in the bottle or closure component of the packaging system. Bottle defects were classified as dents, abrasions, and creases. Dents were the most severe type of bottle defect and appeared as significant indentations in the bottle geometry, typically observed in the shoulder or bottom corner of the bottle. Figures 6 - 10 show bottles with typical shoulder dents and Figure 11 displays a bottle representing a typical bottom dent. These photographs were taken after product/package system failure occurred, thus in select cases a stress crack is observed. However, the overall shape and location of the dents did

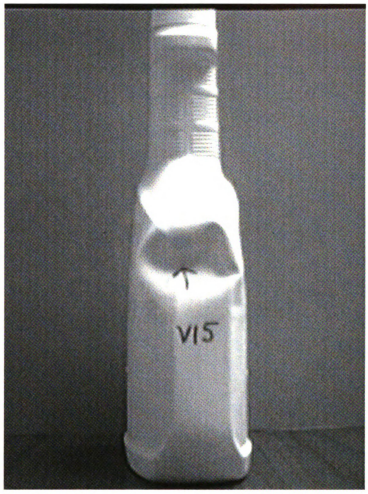

Figure 6. Shoulder dent in laundry additive bottle placed in storage at 140 °F.

Figure 7. Shoulder dent in anti-bacterial cleaner bottle placed in storage at 140 °F.

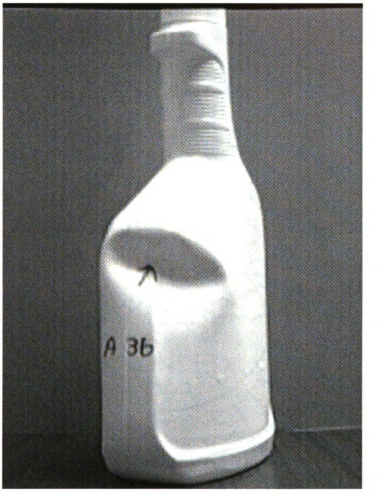

Figure 8. Shoulder dent in anti-bacterial cleaner bottle placed in storage at 120 °F.

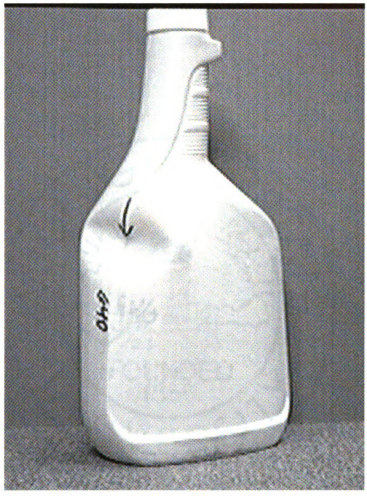

Figure 9. Shoulder dent in glass surface cleaner bottle placed in storage at 120 °F.

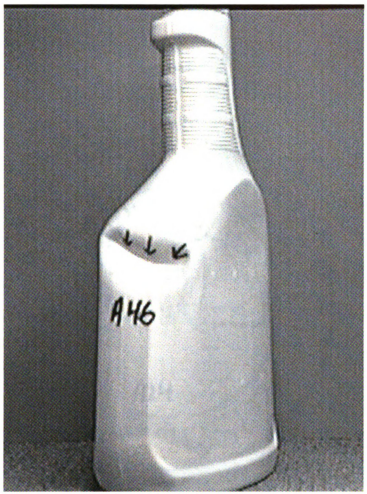

Figure 10. Shoulder dent in anti-bacterial cleaner bottle placed in storage at 100 °F.

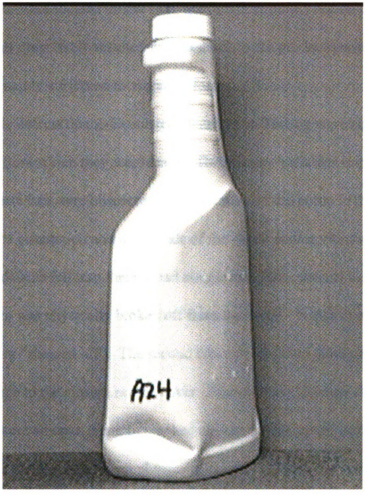

Figure 11. Bottom dent in anti-bacterial cleaner bottle placed in storage at 120 °F.

not change during the aging process. Abrasion defects appeared as "scuffed" areas of the bottle and showed no sign of actual bottle deformation. These types of defects clearly are not as severe as bottle dents. Defects that resulted in a change in bottle surface integrity, but were also not as severe as dents, were classified as creases. Creases often appeared in the bottle neck, or were located on the side, bottom, or shoulder region of the bottle. Dents and creases most likely resulted from a shock to the product/package system, while abrasions were mainly attributed to vibration forces.

The bottle defects due to Simulated Distribution Testing were not dependent on the body cavity from which they were made. The primary variables impacting the distribution defects that were observed are the location of the bottle in the shipping container, and the orientation and magnitude of the shock and/or vibration forces.

Closure defects fell into three broad categories. First, defects were observed in which the closure was physically broken off from the bottle. In this case the closure was classified as being "sheared off". The second type of simulated distribution defect resulted in damage to the closure nozzle cover. Four types of damage observed in this broad category were an open, bent, or cracked closure nozzle cover, or the more serious damage in which the cover had been physically broken off from the rest of the closure body. The last classification of a package system defect was a cracked closure body. All of the closure defects were most likely caused by a shock from the distribution testing drop sequence, although it is possible that open nozzle covers could result from vibration forces.

Table 5 shows the total number of each defect type found in the respective product/package systems after Simulated Distribution Testing, along with the percent of the total bottle population. The data for bottle defects is also shown graphically in Figure 12. The most prevalent type of defect observed were creases (approximately 85% of all bottles had a crease in the bottom and neck region of the bottle). The bottom creases probably resulted from the shipping containers being impacted in bottom down orientation, while the neck creases most likely occurred from a top down orientation impact. Panel and shoulder creases were also observed, with approximately half of all bottles exhibiting these types of defects. Shoulder creases probably resulted in the same manner as the neck creases, and the panel creases most likely occurred from impacts to

Table 5. Characteristic package system defects from Simulated Distribution Testing.

Component	Defect	Total Number	% of Total Population[1]
Bottle	Shoulder Dent	86	15.9
	Bottom Dent	50	9.3
	Panel Abrasion	63	11.7
	Bottom Abrasion	20	3.7
	Shoulder Abrasion	15	2.8
	Neck Crease	461	85.4
	Bottom Crease	459	85.0
	Shoulder Crease	304	56.3
	Panel Crease	258	47.8
Closure	Sheared Off	15	2.8
	Nozzle Cover Off	23	4.3
	Nozzle Cover Open	3	0.6
	Crack in Nozzle Cover	2	0.4
	Nozzle Cover Bent	1	0.2
	Crack in Body	3	0.6

[1] Total number of product/package systems examined was 540.

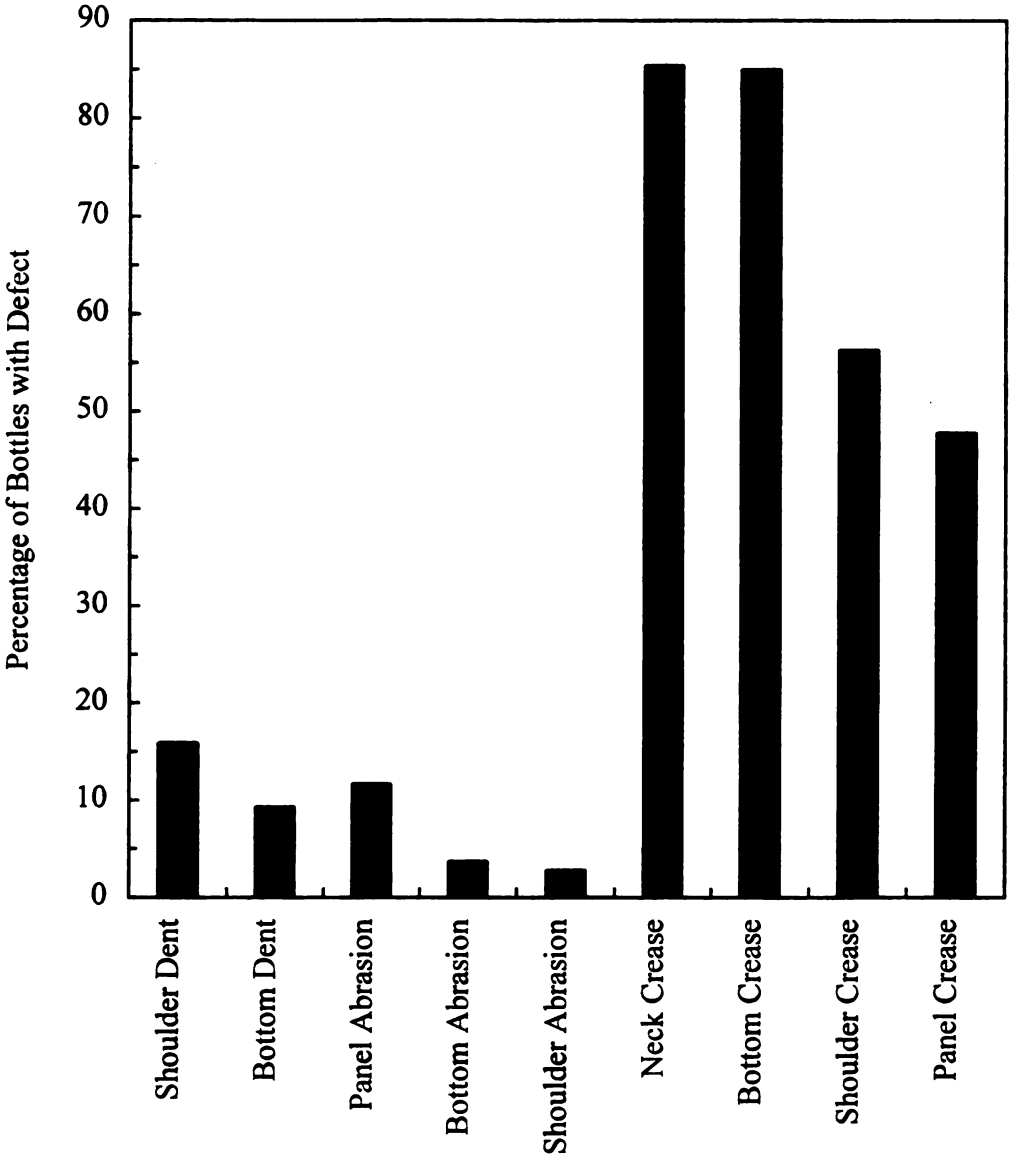

Figure 12. Bottle defects in product/package systems from distribution testing.

the shipping container sides.

Table 5 shows that a significant number of product/package systems exhibited the most severe type of defect, a shoulder or bottom dent, from the Simulated Distribution Testing. Approximately 16% of the bottles had a dent in the shoulder region, while 9.3% had a dent located near the bottom of the bottle.

Abrasion defects were also observed in many of the product/package systems, although they were not as prevalent as other types of defects. The most prevalent location for abrasions was on the ridge located near the bottom of the bottle panel, with 11.7% of the bottles exhibiting these panel abrasions. A smaller percentage of bottles had abrasions on the bottom (3.7%) and shoulder (2.8%) region of the bottle.

In general, closure defects occurred less frequently than bottle defects as Table 5 and the corresponding Figure 13 show. However, Simulated Distribution Testing caused 2.8% of the packaging systems to have the closure sheared off, clearly resulting in a non-functional package. A higher percentage (4.3%) had the nozzle cover broken off which is also considered a serious defect. A relatively minor number of packaging systems had other types of closure defects. Less than 1% of all product/package systems tested exhibited a crack in the nozzle cover or closure body, or an opened or bent nozzle cover. From a packaging standpoint, this may not be a type of defect that warrants additional packaging cost to prevent for these types of products. However, other types of defects that occur at higher frequency, such as dents and abrasions, may justify additional packaging cost to reduce the total number of damaged packages.

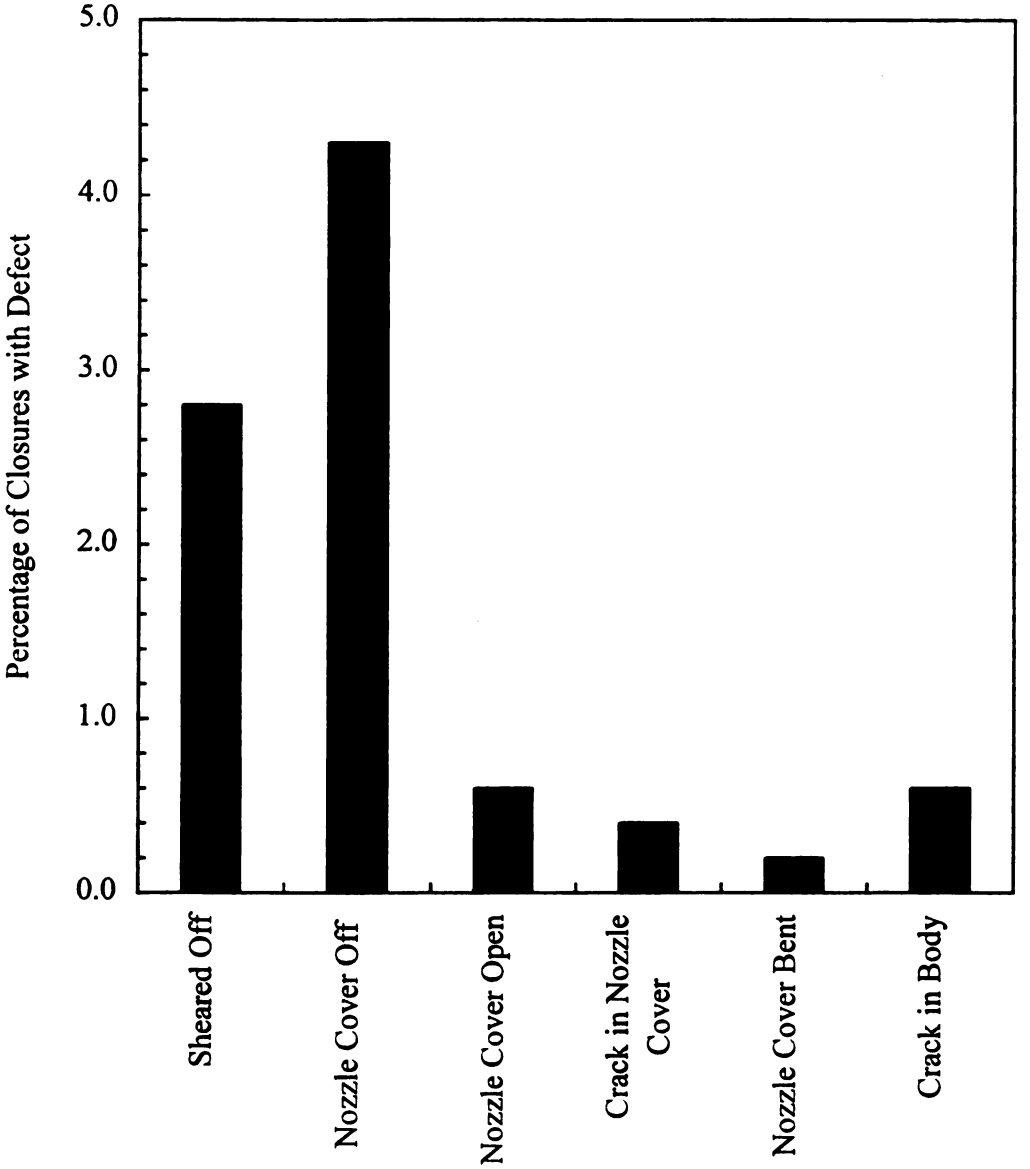

Figure 13. Closure defects in product/package systems from distribution testing.

Table 6 presents summary data for the overall number and percentage of dents, abrasions, creases, and closure damage. Out of the 540 product/package systems subjected to Simulated Distribution Testing, only two exhibited no observable damage. Of the defects listed in Table 6, dents and closure damage were found to be the most detrimental to performance. Clearly, closure damage can result in an improperly working packaging system. The dents initially only affect the product appearance, however, as described in Chapter 3.D., dents were usually initial sites for leakage during long-term storage. Of the total number of bottles examined, 24.1% showed either a shoulder or bottom dent, and 8.7% exhibited some form of closure damage. Abrasions were observed in 17.0% of the bottles examined, but were never observed to be an initiation site for leakage.

Table 6. Number of package systems with characteristic defects.

Defect	Total Number	% of Total Population
Crease	532	98.5
Dent	130	24.1
Abrasion	92	17.0
Closure Damage	47	8.7
No Defect Found	2	0.4

C. Package System Weight Loss During Storage

1. Introduction

Weight loss was monitored as a function of time to indicate potential detrimental interaction between product and package system. Excessive weight loss could indicate

poor product/package integrity. On the other hand, if weight loss falls within acceptable limits, the product/package system is most likely performing as intended. In addition, comparison of weight loss for the two sets of product/package systems provides an understanding of the effect of Simulated Distribution Testing on this property. Finally, weight loss measurements could allow a correlation between package system weight loss at the elevated temperatures and weight loss under ambient storage conditions, although this is not a primary issue for the research presented here. Acceptable weight loss limits will vary depending on supplier and product, but are typically about 1%.

2. Percent Weight Loss Results

Product/package systems were removed from storage chambers and weighed approximately monthly during the six month study. Before weight measurements were made, the samples were allowed to equilibrate to ambient conditions for at least 12 hours. Typically, twenty replicate measurements were made since twenty samples per set were placed in storage. However, as packaging systems failed they could not be used for weight measurements, and therefore, less than twenty replicate measurements may have been obtained. For complete sets of samples that did not fail, the storage time was approximately 180 days. For the sets that did fail, data could only be collected during the time when the product/package system integrity was maintained.

The weight measurement results are presented in Figures 14, 15, and 16 for the bleach alternative laundry additive, anti-bacterial surface cleaner, and glass surface cleaner systems, respectively, which plot the data as % weight loss vs. time for each

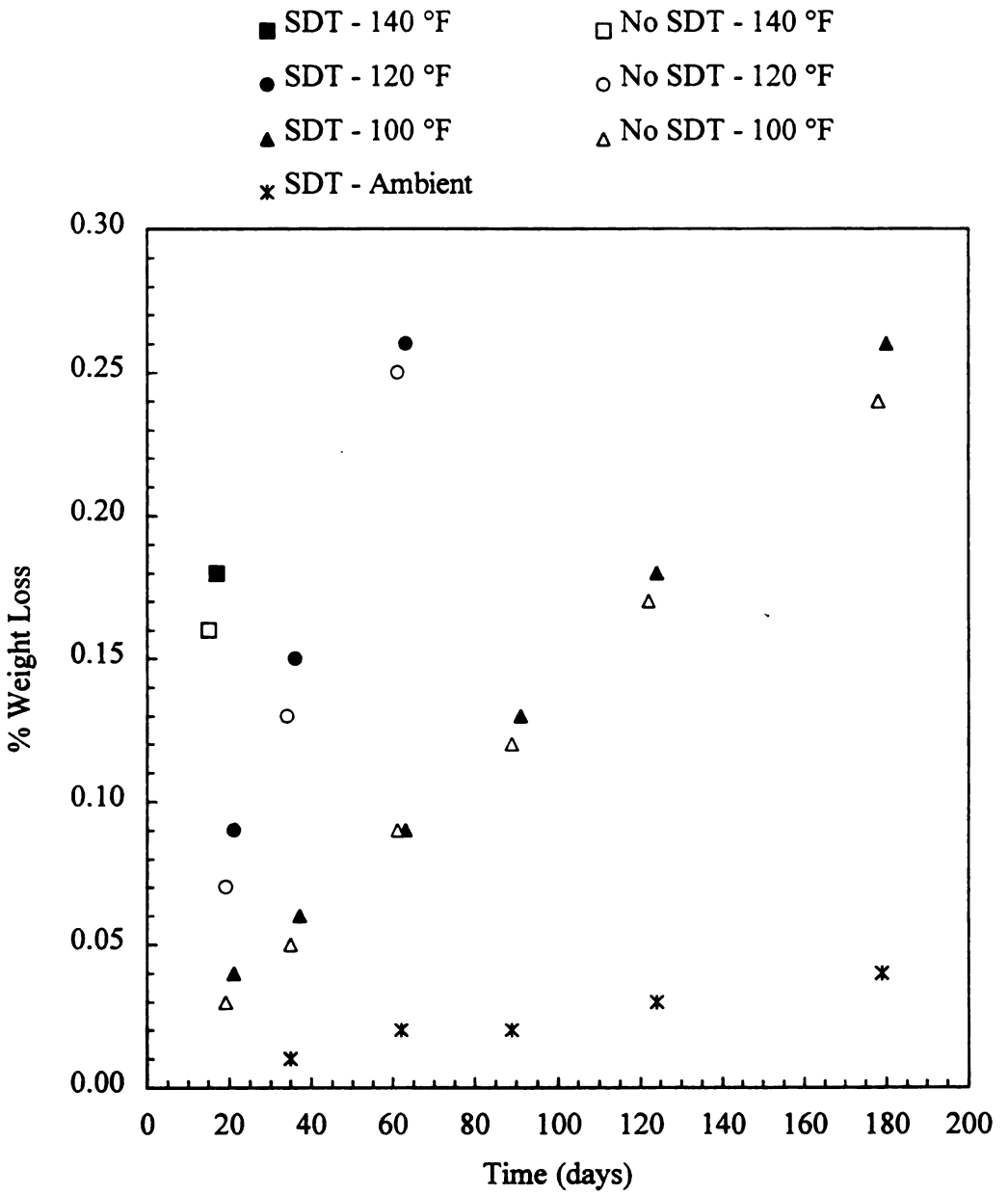

Figure 14. % weight loss vs. time for laundry additive.

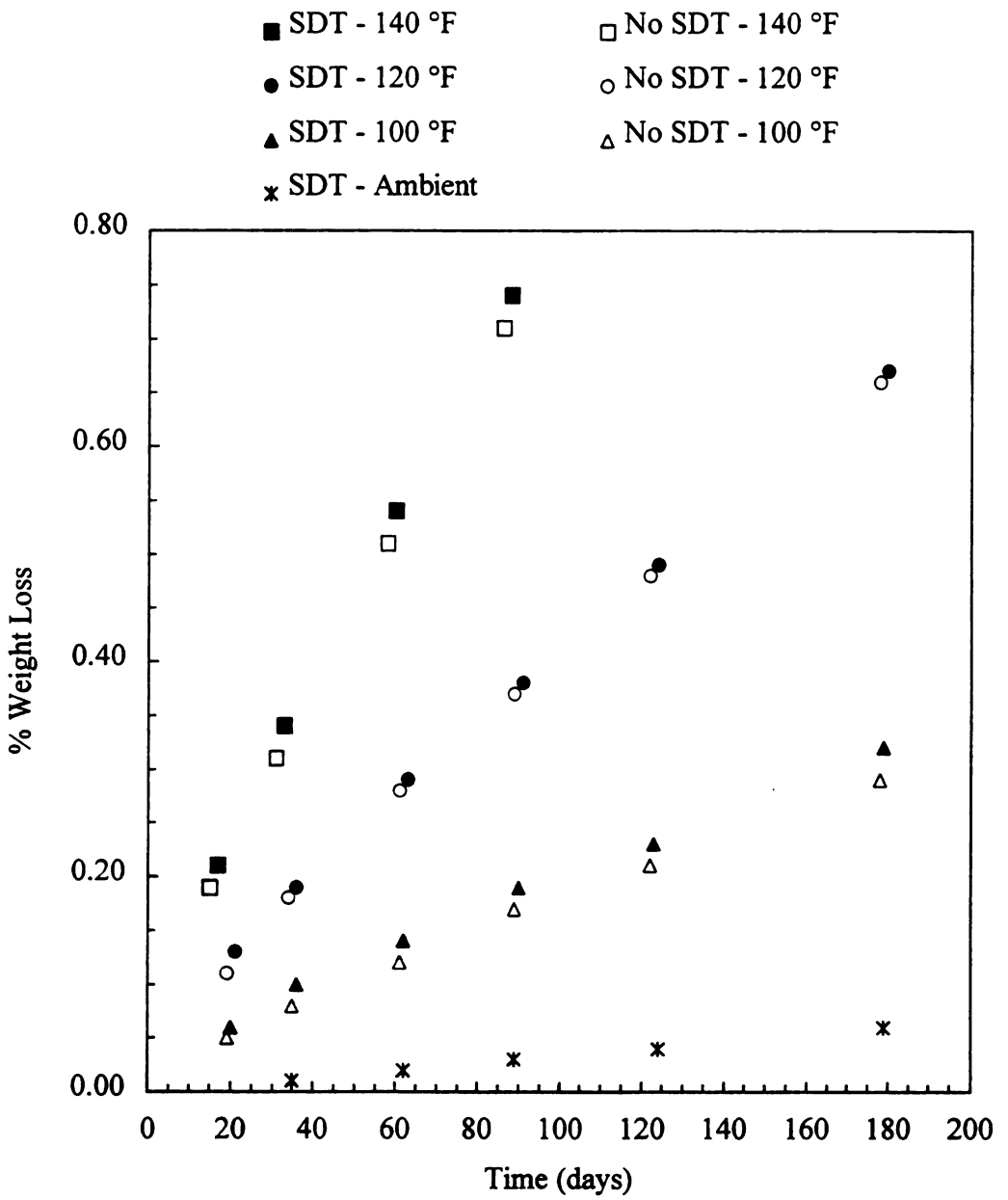

Figure 15. % weight loss vs. time for anti-bacterial cleaner.

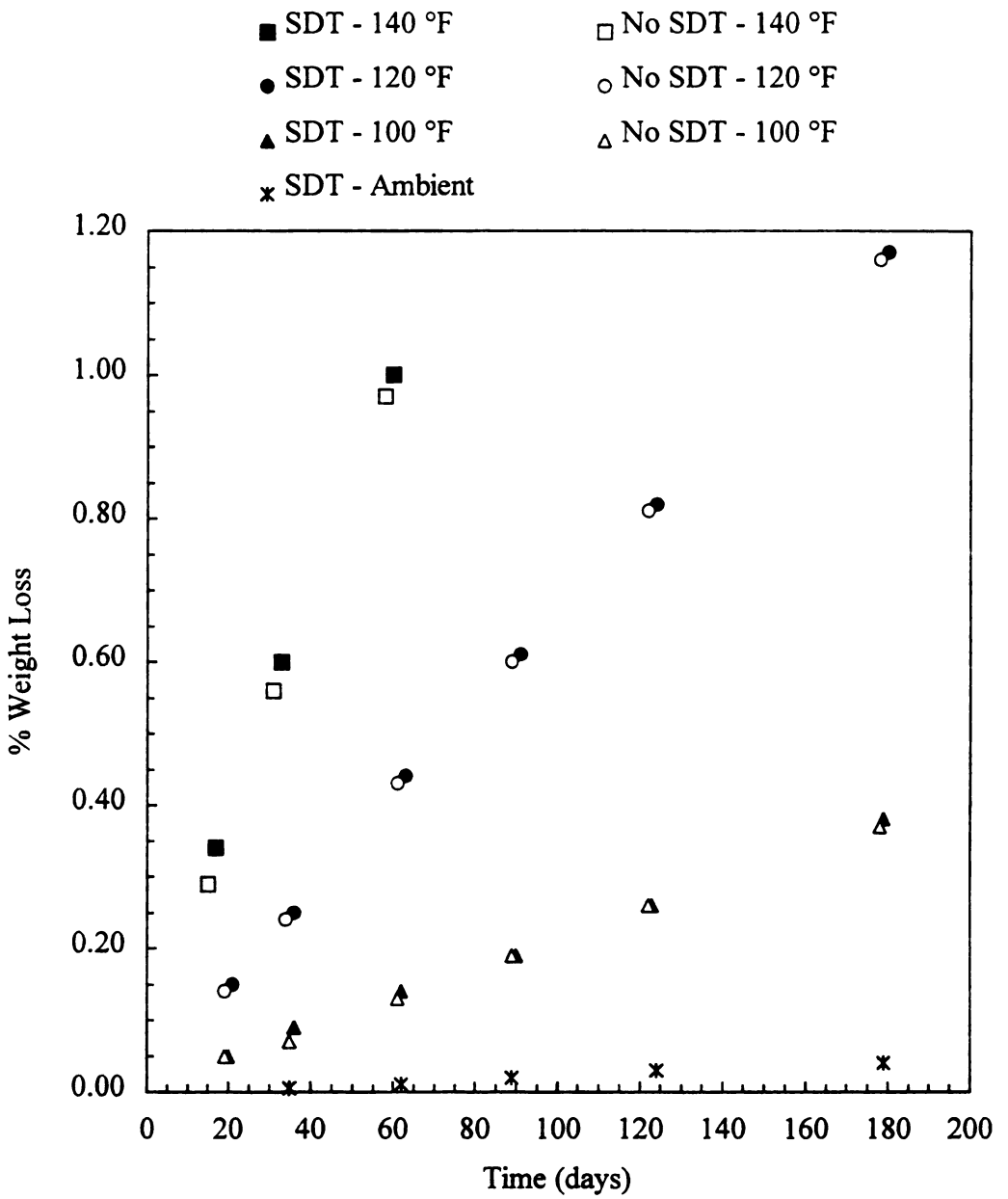

Figure 16. % weight loss vs. time for glass surface cleaner.

storage condition. The standard deviation for all data points is ± 0.01. The data for each product/package system exhibit the expected relationship, in that the percent weight loss is higher at a given time as the storage temperature is increased. As the temperature is increased, volatile components in the product will exhibit higher vapor pressure, and the permeability of the HDPE packaging material will increase. These two factors will allow more volatile components to exit the packaging system, and hence result in greater weight loss with increased temperature. Further, inspection of the data presented in Figures 14 - 16 shows that the weight loss results are not dependent on Simulated Distribution Testing for any of the product/package systems.

Table 7 summarizes the overall percent weight loss at the end of storage for all product/package systems investigated. The glass surface cleaner is the only product that exhibited a weight change of greater than 1% during the study, which occurred under the 120 °F storage condition. However, the weight loss of less than 1.2% for both sets of product/package systems is still minimal, and these product/package systems did not fail during the course of the study. Both the bleach alternative laundry additive and anti-bacterial surface cleaner systems remained at a weight loss of well below 1% under all storage conditions during the study. Therefore, for all three product/package systems the results clearly indicate that the package systems performed as intended until failure occurred or until the end of the study.

Table 7. Percent weight loss at the end of storage.

		Percent Weight Loss	
Product	**Temperature (°F)**	**SDT (# days)**	**No SDT (# days)**
Bleach Alternative Laundry Additive	Ambient	0.04 (179)	-
	100	0.26 (180)	0.24 (178)
	120	0.26 (63)	0.25 (61)
	140	0.18 (17)	0.16 (15)
Anti-Bacterial Surface Cleaner	Ambient	0.06 (179)	-
	100	0.32 (179)	0.29 (178)
	120	0.67 (180)	0.66 (178)
	140	0.74 (88)	0.71 (86)
Glass Surface Cleaner	Ambient	0.04 (179)	-
	100	0.38 (179)	0.37 (178)
	120	1.17 (180)	1.16 (178)
	140	1.00 (60)	0.97 (58)

3. Weight Loss Rates

Figures 14 - 16 show that the weight loss for all three product/package systems, under all storage conditions, increases nearly linearly with time. This allows the use of linear fits to determine weight loss rates for each product, under each storage condition. The results from these linear fits are summarized in Table 8. The glass surface cleaner exhibited the highest weight loss rate under elevated storage conditions. The bleach alternative laundry additive showed the lowest weight loss rate under ambient and 100 °F conditions, while the anti-bacterial surface cleaner gave the lowest rate at 120 and 140 °F.

Table 8. Weight loss rates during aging.

		Wt. Loss Rate (%/day)	
Product	**Temperature (°F)**	**SDT**	**No SDT**
Bleach Alternative Laundry Additive	Ambient	0.00020	-
	100	0.0014	0.0013
	120	0.0041	0.0043
	140	0.0106	0.0107
Anti-Bacterial Surface Cleaner	Ambient	0.00034	-
	100	0.0016	0.0015
	120	0.0034	0.0034
	140	0.0074	0.0073
Glass Surface Cleaner	Ambient	0.00025	-
	100	0.0020	0.0021
	120	0.0064	0.0064
	140	0.0153	0.0158

It is difficult to give a full analysis of the weight loss rate results without understanding the chemical composition of the products (this information is classified as proprietary and therefore is not available). However, a number of factors can influence the weight loss of product/package systems such as those investigated.

Assuming the closure provides a hermetic seal, the overall mechanism of weight loss is one of permeation of components in the contact phase through the packaging material [23]. The permeation process involves three steps, the first of which is the sorption of permeant into the packaging material. This sorption process is dictated by the solubility of permeant in the polymer comprising the packaging material. Once sorption takes place the permeant must then diffuse through the bulk phase of the medium, which is controlled by the diffusion coefficient. Finally, after the permeant diffuses through the medium it must desorb or evaporate from the external surface of the packaging material.

Thus, the permeability constant (P) is determined by the diffusion (D) and solubility (S) coefficients of the permeant in the medium, as shown by eq 4.

$$P = D \times S \tag{4}$$

This relationship is only applicable for product components that do not strongly interact with the plastic packaging material they are in contact with, since D and S will be independent of permeant concentration. However, for a highly interactive system, such as for d-limonene and HDPE, the diffusion process is more complicated because the diffusion and solubility coefficients may vary as a function of permeant concentration. Nevertheless, the diffusion and solubility coefficients will be dependent on the particular permeant and plastic packaging material, and therefore, eq 4 shows that permeation through a packaging material will depend on the packaging material composition, and the composition and size of the permeant molecule.

In addition to chemical composition, the percent crystallinity of the packaging material will strongly influence the rate of permeation through a plastic packaging material. Since permeation occurs in the amorphous region of a polymer, greater weight loss would be expected for less crystalline materials of the same generic family (i.e., HDPE). Since all bottles were the same in this study, and the percent crystallinity did not change (see Chapter 3.E.4.), percent crystallinity should not have been a factor.

Product composition is important because it is the volatile components of the product that will sorb into and diffuse through the package, resulting in the loss of weight

by the product/package system. Components with high vapor pressure and/or volatile components present in high concentration would be expected to result in an increase in the weight loss rate by affecting the driving force for permeation, since an increase in driving force will increase the permeation rate through a material. In addition, more volatile components will tend to cause an increase in pressure build-up inside the package, which leads to an increased driving force for permeation through the packaging material. Pressure could also cause the packaging material to weaken over time.

Although pressure was not measured during this study, it was qualitatively observed that the glass surface cleaner exhibited the greatest pressure build-up. This observation is supported quantitatively by the weight loss rate data at 100 °F. The glass surface cleaner exhibited the highest rate and percent weight loss at the end of the study. Clearly other factors will impact the rate and weight loss, as described above, but the relatively high pressure build-up is most likely a significant factor.

D. Characterization of Package System Failure During Storage

1. Introduction

All product/package systems exposed to the storage conditions were inspected frequently to identify samples that failed. For this study, failure was defined as any leakage of product from the packaging system, as determined by visual inspection. The frequency of inspection was dependent on the status of all product/package systems. During time periods when large numbers of samples were failing, inspection was

performed almost daily. However, when systems were not failing at a high rate, only weekly inspections were conducted.

Throughout the course of the inspection process, the product/package systems visually appeared to go through three different stages before failure occurred. The first stage was characterized by slight bulging (swelling) of the bottom section of the bottle. Although pressure measurements were not made during this study, it visually appeared that the pressure inside the packaging system was increasing during this stage. While a slight bulging of the bottle bottoms was observed, the bottles would still sit upright on a surface and would retain their original shape when cooled to ambient conditions (as observed during the weight measurements). During the second stage, severe bulging of the bottom occurred, as the internal pressure appeared to increase significantly. This build-up of pressure was qualitatively observed by the fact that it took considerably more force to compress the bottles by hand than when they were first placed in storage. During this stage, the bottles would rock on a flat surface and therefore were described as having "rocker bottoms". Further, the bottles did not return to their original shape when cooled to room temperature, as they would not sit upright on a surface. The final stage that was often visually observed was characterized by a stress crack in the region of the bottle where failure eventually occurred. During this stage, the bottle integrity was already severely reduced, however, the product/package systems were left in storage until visual leakage occurred. When a product/package system failed it was removed from storage, analyzed for failure mode as described below, and evaluated for performance criteria (see Chapter 3.E.).

During the six month study, four sets of product/package systems failed. These were: 1) bleach alternative laundry additive stored at 140 °F, 2) anti-bacterial surface cleaner stored at 140 °F, 3) glass surface cleaner stored at 140 °F, and 4) bleach alternative laundry additive stored at 120 °F. The remaining sets did not fail, except for select product/package systems that were exposed to Simulated Distribution Testing.

2. Characterization of Failure Modes

All observed product/package system failures were due to environmental stress cracking which resulted in product leaking from the bottle. The vast majority of product/package systems failed in locations that did not have an obvious defect that could be associated with Simulated Distribution Testing. These types of failures were independent of whether or not the system experienced the shock and vibration forces of distribution testing. Product/package systems that had shoulder or bottom dents from the testing were prone to fail prematurely, as described below.

Tables 9 and 10 tabulate the total number of failures observed for each mode for the product/package systems stored at 140 and 120 °F, respectively. The data for failure modes not associated with Simulated Distribution Testing are also shown graphically in Figures 17 and 18. Figure 17 displays the data by separating the results for all three product/package systems stored at 140 °F into each failure mode category. Figure 18 shows the results in similar format for the laundry additive system stored at 120 °F. The predominant mode of failure for all product/package systems was a stress crack located near the center of the bottle bottom edge, horizontal to the edge. Figure 1 (page 11)

Table 9. Failure modes observed at 140 °F.

	Bleach Alternative Laundry Additive		Anti-Bacterial Surface Cleaner		Glass Surface Cleaner	
Failure Mode	**SDT**	**No SDT**	**SDT**	**No SDT**	**SDT**	**No SDT**
Front/Bottom Horizontal	11	11	6	13	7	11
Back/Bottom Horizontal	5	8	8	5	7	8
Front/Bottom Vertical	0	1	0	0	5	1
Back/Bottom Vertical	0	0	0	0	1	0
Neck Seam	0	0	3	2	0	0
Shoulder Dent	4	-	3	-	0	-
Bottom Dent	0	-	0	-	0	-

Table 10. Failure modes observed at 120 °F and totals.

	Bleach Alternative Laundry Additive		Total from Tables 9 and 10	
Failure Mode	**SDT**	**No SDT**	**SDT**	**No SDT**
Front/Bottom Horizontal	8	15	32	50
Back/Bottom Horizontal	10	5	30	26
Front/Bottom Vertical	1	0	6	2
Back/Bottom Vertical	0	0	1	
Neck Seam	0	0	3	2
Shoulder Dent	0	-	7	-
Bottom Dent	1	-	1	-

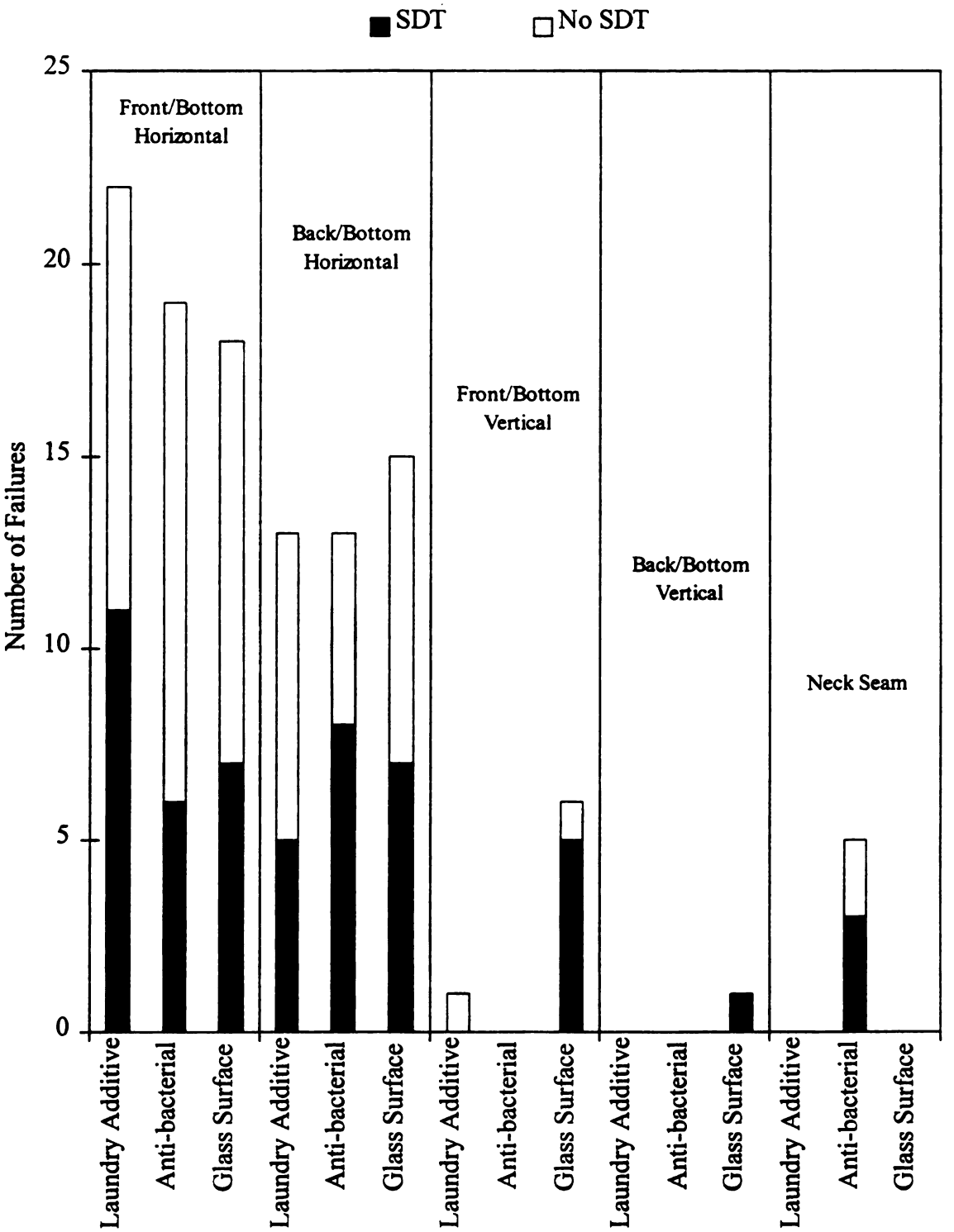

Figure 17. Number of failures for product/package systems stored at 140 °F.

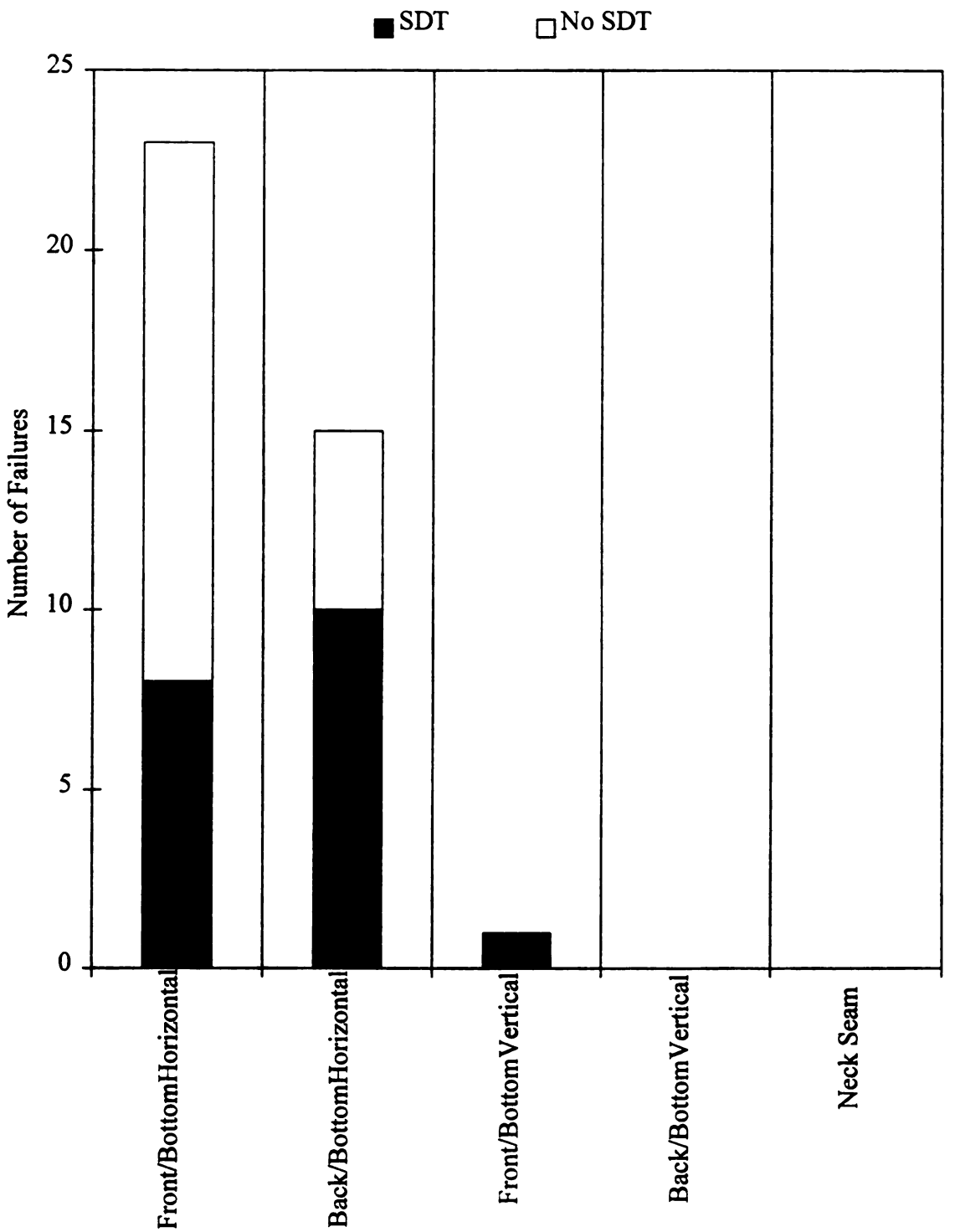

Figure 18. Number of failures for laundry additive system stored at 120 °F.

depicts this type of failure for one of the bleach alternative laundry additive samples that failed at 140 °F. The arrow points to the area where the crack is located, which is approximately 7 mm long and runs horizontal to the bottom edge of the bottle. The figure shows this failure in the front of the bottle for this particular sample, but a similar type of failure was observed in the back of other bottles as well.

The data in Tables 9 and 10, along with the corresponding figures, show that only two other failure modes were observed that were not associated with Simulated Distribution Testing. The first type was a stress crack located along the bottom edge of the bottle similar to that described above, except it was oriented vertical with respect to the bottom edge. This failure also occurred either in the front or back of the bottle. Figure 19 displays an example of a product/package system that failed by this mode for one of the laundry additive samples that failed at 140 °F. The arrow in the figure points to the location of the stress crack. Figure 20 depicts the same bottle in detailed view and clearly shows the vertical stress crack. The second failure mode involved stress cracks which caused product/package system failure that were located in the bottle mold seam in the neck region of the bottle. This failure mode only occurred for the anti-bacterial surface cleaner product/package system, stored under the 140 °F environmental condition. However, out of the forty samples there were only five of these types of failures.

It is difficult to assess the impact of Simulated Distribution Testing on product/package system failure by simply visualizing the data in tabular or graphical format. Therefore, a two-tailed Fisher's Exact Test statistical analysis was performed

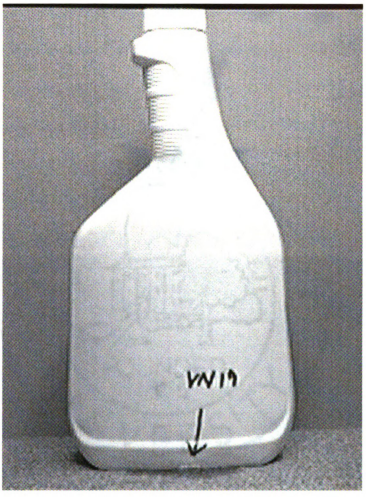

Figure 19. View of bottle with vertically oriented stress crack.

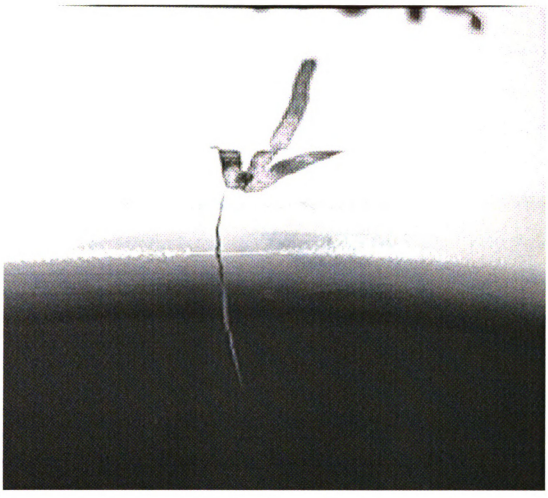

Figure 20. Detailed view of bottle with vertically oriented stress crack.

using SAS [24] to compare failure mechanisms for product/package systems experiencing Simulated Distribution Testing to those that did not. This test is similar to the chi-square test in that it returns the probability of getting a difference greater than that observed, assuming that the two sets of data are equal. Typical convention is that a probability value less than ~0.05 provides evidence that the two sets of data being analyzed are different, while a value less than ~0.001 strongly indicates a difference in the two sets of data.

The results of Fisher's Exact Test are presented in Table 11. All results obtained

Table 11. Fisher's Exact Test results for failure mode analysis.

		Fisher's Exact Test Probability
Product	**Temp. (°F)**	**SDT vs. No SDT**
Laundry Additive	140	0.85
	120	0.07
Surface Cleaner	140	0.20
Glass Surface Cleaner	140	0.19

at 140 °F indicate that the failure mechanism was not a direct result of the physical distribution environment, as the results are statistically similar whether the product/package system was exposed to Simulated Distribution Testing or not (i.e., probability values are greater than 0.05). The laundry additive product/package system stored at 120 °F does not provide as easily interpreted results, since the probability value is closer to 0.05. This suggests that there is a greater probability that there is a difference between the "SDT" and "No SDT" results. The data presented in Table 10 shows that

both sets of samples failed predominantly by a stress crack oriented horizontally. Systems that experienced Simulated Distribution Testing were fairly evenly distributed between front and back failure, while the "No SDT" data is skewed towards failure in the front of the bottle. Whether this difference is statistically significant can only be determined by performing the experiment with a larger sample size.

In an effort to determine the cause of the typical type of failure mode located near the bottom of the bottle, two factors were investigated. First, comparison of failure with the body cavity of each bottle was investigated. The bottles were obtained from a extrusion blow molding process that had 16 different cavities. A defect in one of the molds for a particular body cavity can cause defects in the bottles that are produced in that cavity. These defective bottles will often result in premature failure when compared to bottles from other non-defective cavities. However, in this study, body cavity did not influence product/package system integrity during storage, as there was a random distribution of body cavities for the failed product/package systems.

In addition to investigating the effect of body cavity on product/package system integrity, the thickness of the bottle was measured in several regions in an effort to identify areas of the bottle with uneven material distribution, since this would be a likely source of stress-induced failure. The regions were selected to include the areas where stress cracks were experimentally observed. To this end, the bottom edge of the bottle (front and back) was of particular interest due to the high frequency of failures that were a result of a stress crack in this region of the bottle. In addition, the neck region was a site for a small number (5) of anti-bacterial failures (see Table 9, page 63) and therefore was

an area of interest. The thickness measurements in this region were made opposite the gripped section of the neck. Thickness measurements were performed at numerous different bottle regions as shown below.

1. A 3x3 grid (9 locations) on the front panel of the bottle
2. A 3x3 grid (9 locations) on the back panel of the bottle
3. 5 locations running from left to right along the bottom front edge
4. 5 locations running from left to right along the bottom back edge
5. 5 locations running down the neck mold seam

The results from the thickness measurements are summarized in Table 12. There did not appear to be an obvious thickness trend for the front or back panel of the bottle, as it varied from approximately 18 - 36 mil and 24 - 39 mil, respectively. The thickness of the back panel (30.1 ± 3.8 mil) on average was thicker than the front panel (25.1 ± 3.2 mil). However, the thickness in each of these regions does not impact integrity of product/package systems, since no failures were found in these regions. Since these were the regions in which samples were taken for yield stress and modulus of elasticity measurements, the thickness was measured for each individual sample for these measurements.

In contrast to the bottle panels, there is a clear thickness trend along each bottom edge of the bottle. The thickness is greater near the sides of the bottle than near the center, as shown in Table 12. The minimum thickness of 15.6 mil is located near the center of each bottom edge. This result gives an indication of the reason for the

Table 12. Thickness measurements of bottles used for the product/package systems.

Region of Bottle	Location #	Thickness (mil)
Front Panel	1	20.9 ± 1.3
	2	24.5 ± 0.8
	3	18.2 ± 0.3
	4	24.2 ± 1.4
	5	28.8 ± 1.0
	6	21.1 ± 0.5
	7	27.1 ± 1.6
	8	35.9 ± 1.4
	9	25.1 ± 0.4
	Average	25.1 ± 3.2
Back Panel	1	24.0 ± 0.5
	2	28.8 ± 1.1
	3	25.6 ± 1.4
	4	27.1 ± 0.6
	5	33.8 ± 1.4
	6	28.8 ± 1.3
	7	31.1 ± 1.0
	8	38.8 ± 1.7
	9	32.5 ± 1.7
	Average	30.1 ± 3.8
Bottom Front Edge	1	18.7 ± 1.1
	2	18.9 ± 0.8
	3	15.6 ± 0.5
	4	15.9 ± 0.5
	5	20.3 ± 0.6
Bottom Back Edge	1	22.8 ± 0.5
	2	17.0 ± 0.6
	3	15.6 ± 0.6
	4	19.5 ± 1.0
	5	24.7 ± 0.6
Neck Mold Seam	1	47.6 ± 1.3
	2	51.2 ± 3.7
	3	62.0 ± 7.0
	4	60.6 ± 4.3
	5	52.9 ± 3.6

predominant product/package system failures observed (as shown in Tables 9 and 10, page 63) in this thin section of the bottle.

The neck mold seam region of the bottle also follows a distinct thickness trend as shown in Table 12. There is a maximum thickness of about 62 mil, which corresponds to the approximate location of the five neck seam failures that were observed for the anti-bacterial surface cleaner product/package system. This thickness variation could result in additional residual stress during molding which, for the five failures described, could have been the weak section in the bottle.

Dents in the bottle were the only type of distribution defect that appeared to influence the storage stability of the product/package systems. There were no failures observed that were caused by abrasions or creases. Tables 9 and 10 (page 63) show that there were a total of eight failures associated with shoulder (7) and bottom (1) dents. These types of failure modes always resulted in a stress crack located in the dent. Figures 6 and 7 (pages 40 and 41, respectively) display the bottles from laundry additive and anti-bacterial surface cleaner product/package systems, respectively, that failed at 140 °F by this mode. Each of these systems failed due to a shoulder dent. The stress crack is readily obvious in the detailed views shown in Figures 21 and 22 for these laundry additive and surface cleaner systems, respectively. The environmental stress crack is different for each of these examples, indicating that the actual failure is dependent on the shape and location of the dent.

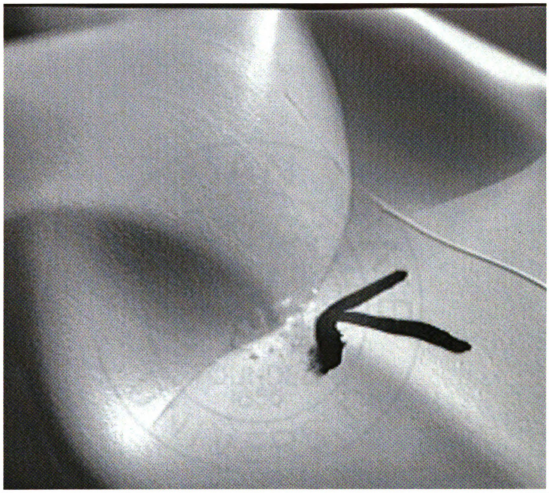

Figure 21. Detailed view of laundry additive bottle shoulder dent of Figure 6.

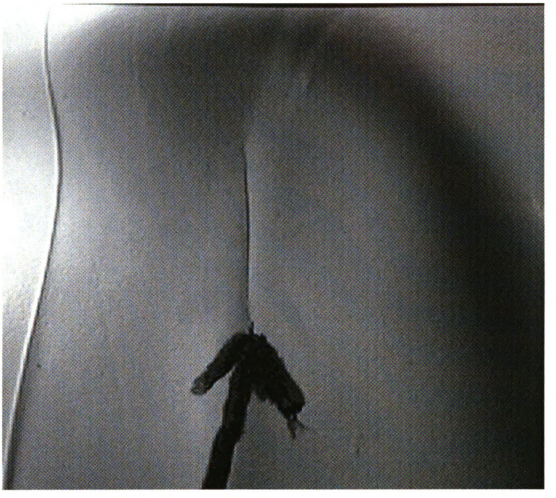

Figure 22. Detailed view of anti-bacterial cleaner bottle shoulder dent of Figure 7.

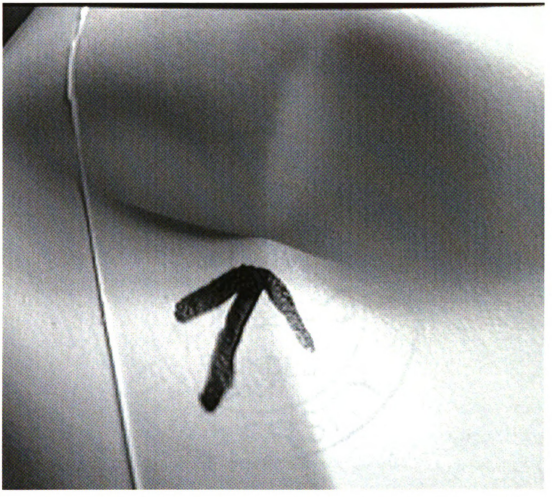

Figure 23. Detailed view of anti-bacterial cleaner bottle shoulder dent of Figure 8.

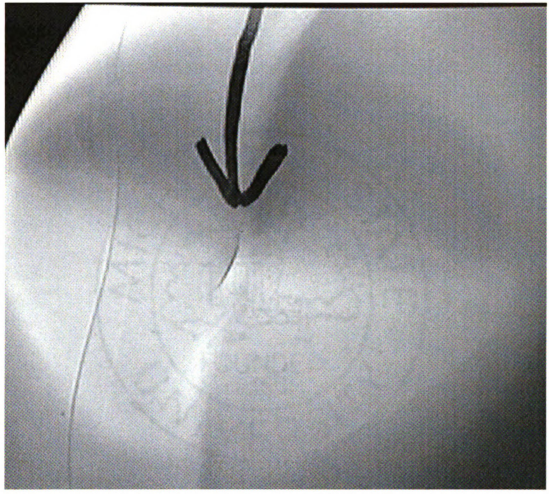

Figure 24. Detailed view of glass surface cleaner bottle shoulder dent of Figure 9.

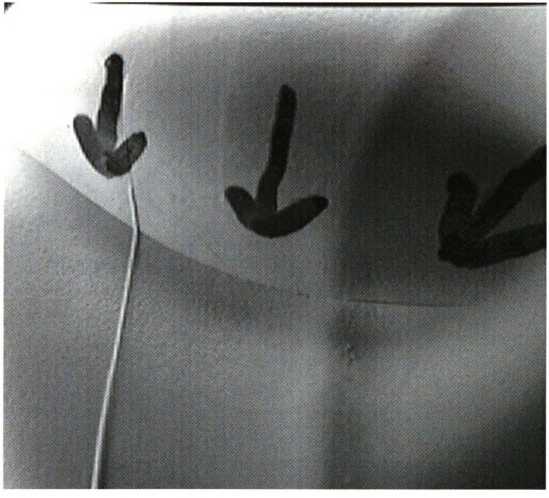

Figure 25. Detailed view of anti-bacterial cleaner bottle shoulder dent of Figure 10.

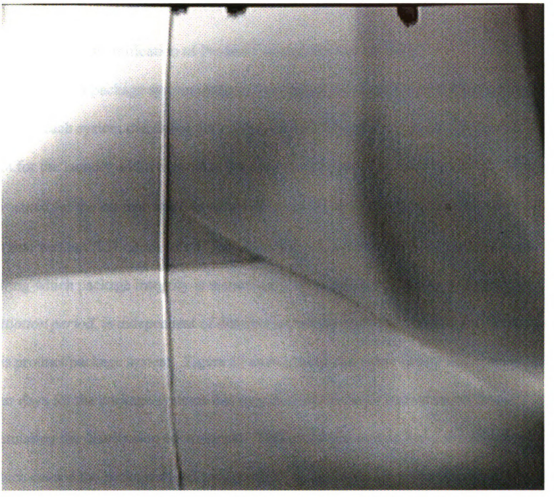

Figure 26. Detailed view of anti-bacterial cleaner bottle bottom dent of Figure 11.

Figures 8 - 11 (pages 42 - 45) show photographs of several other examples of product/package systems that failed due to shoulder or bottom dents. In all cases, the stress crack located in the dent is clearly observed in the detailed views associated with each bottle (Figures 23 - 26).

3. Quantification of Product/Package System Integrity

Product/package system integrity was quantified by plotting cumulative failure vs. time for each system that failed during the course of this study. Figure 27 displays this plot for the laundry additive product/package system that was stored at 140 °F. Data is presented for the set that was exposed to Simulated Distribution Testing (■) and for the set that was not (□). Both sets of data show that, in general, there is a period of time during which package integrity is maintained. This period, which will be called the *initiation period*, is independent of distribution testing and is approximately 23 days for this product/package system. Figure 27 shows that there is one failure that occurred after four days for the package systems that experienced the shock and vibration forces simulating the distribution environment. This particular sample had a shoulder dent which caused the package to fail prematurely. Samples for all product/package systems that failed during the *initiation period* had a shoulder or bottom dent that were caused by the Simulated Distribution Testing.

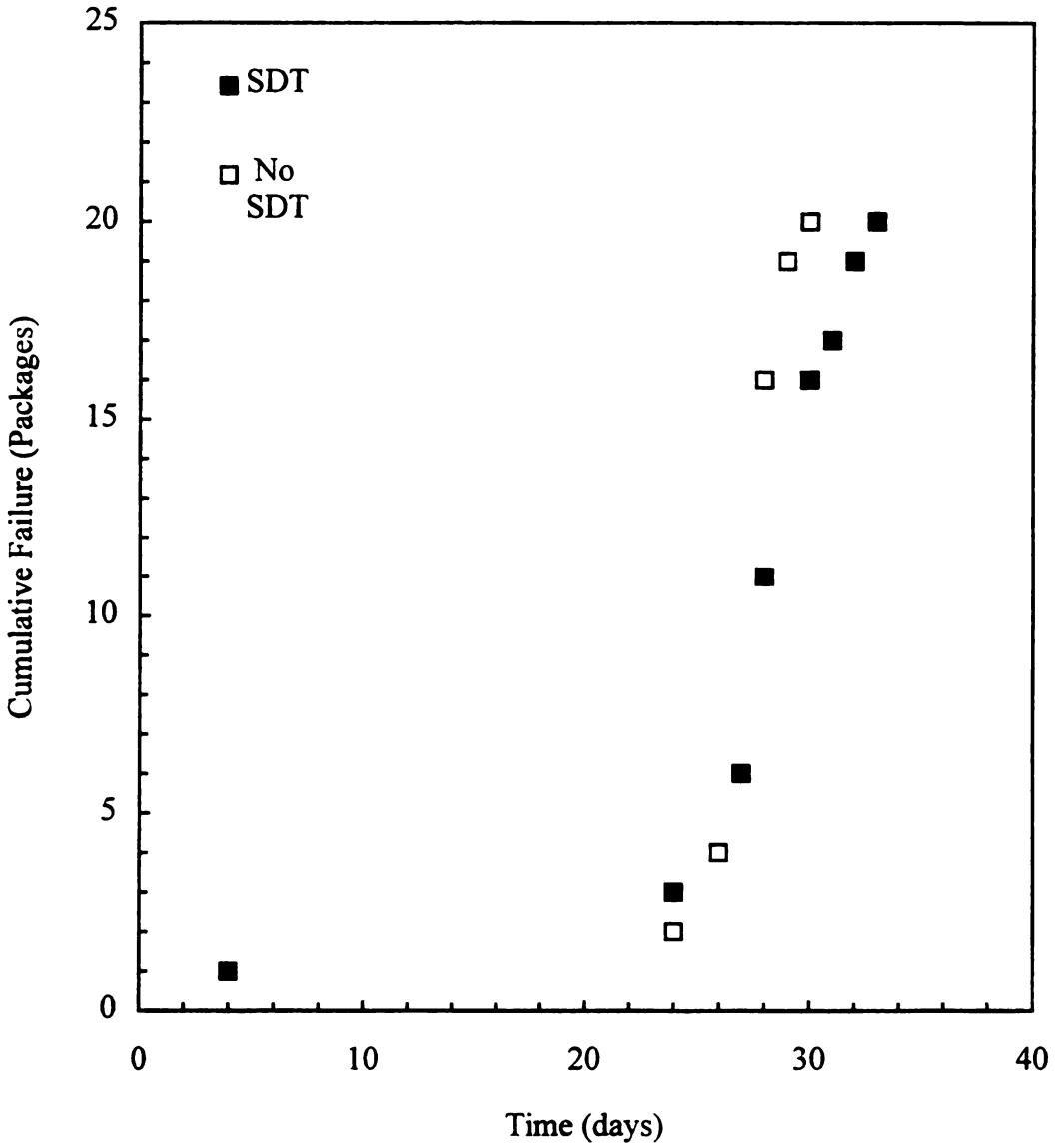

Figure 27. Cumulative failure vs. time for laundry additive at 140 °F.

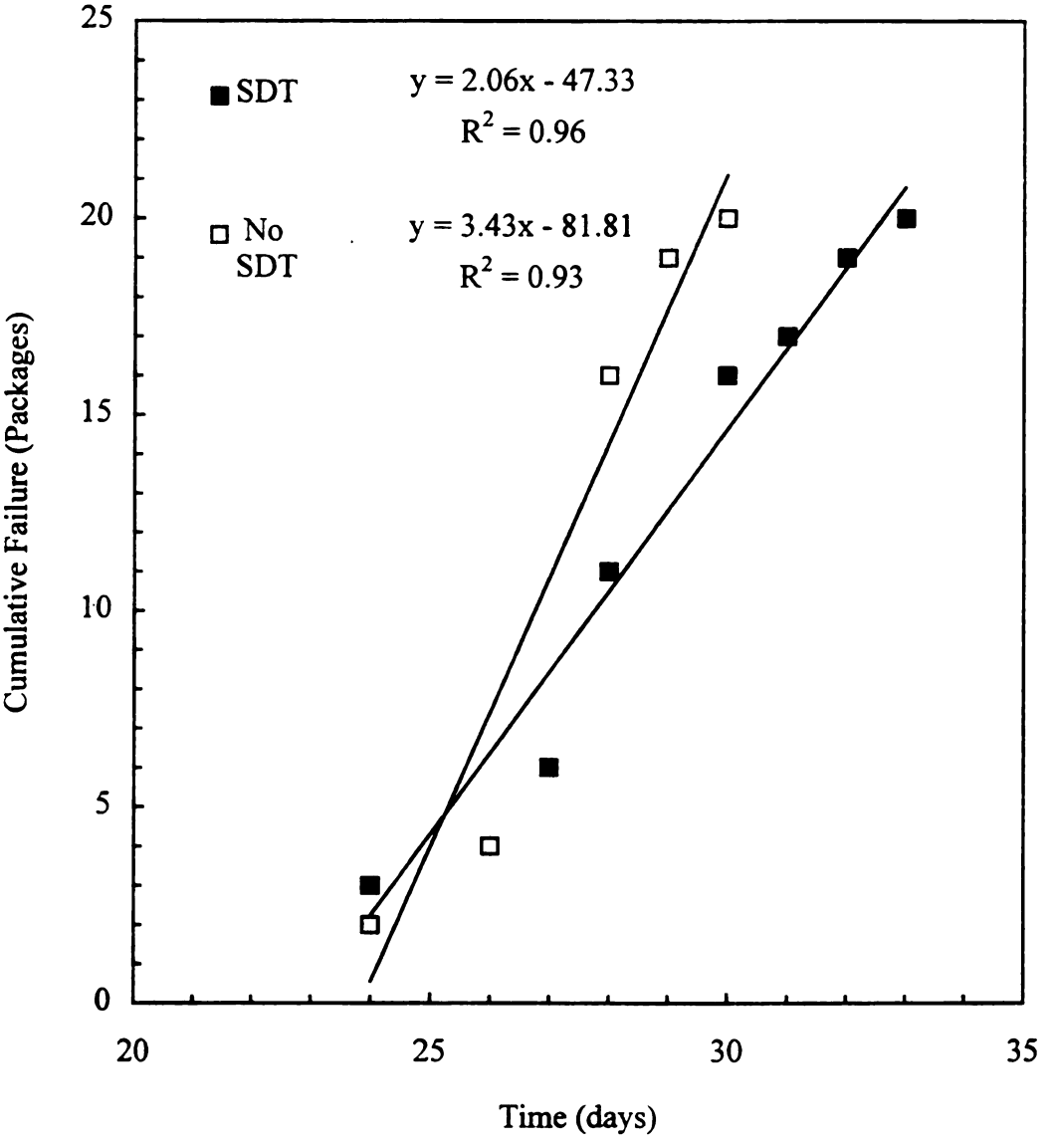

Figure 28. Expanded cumulative failure vs. time for laundry additive at 140 °F.

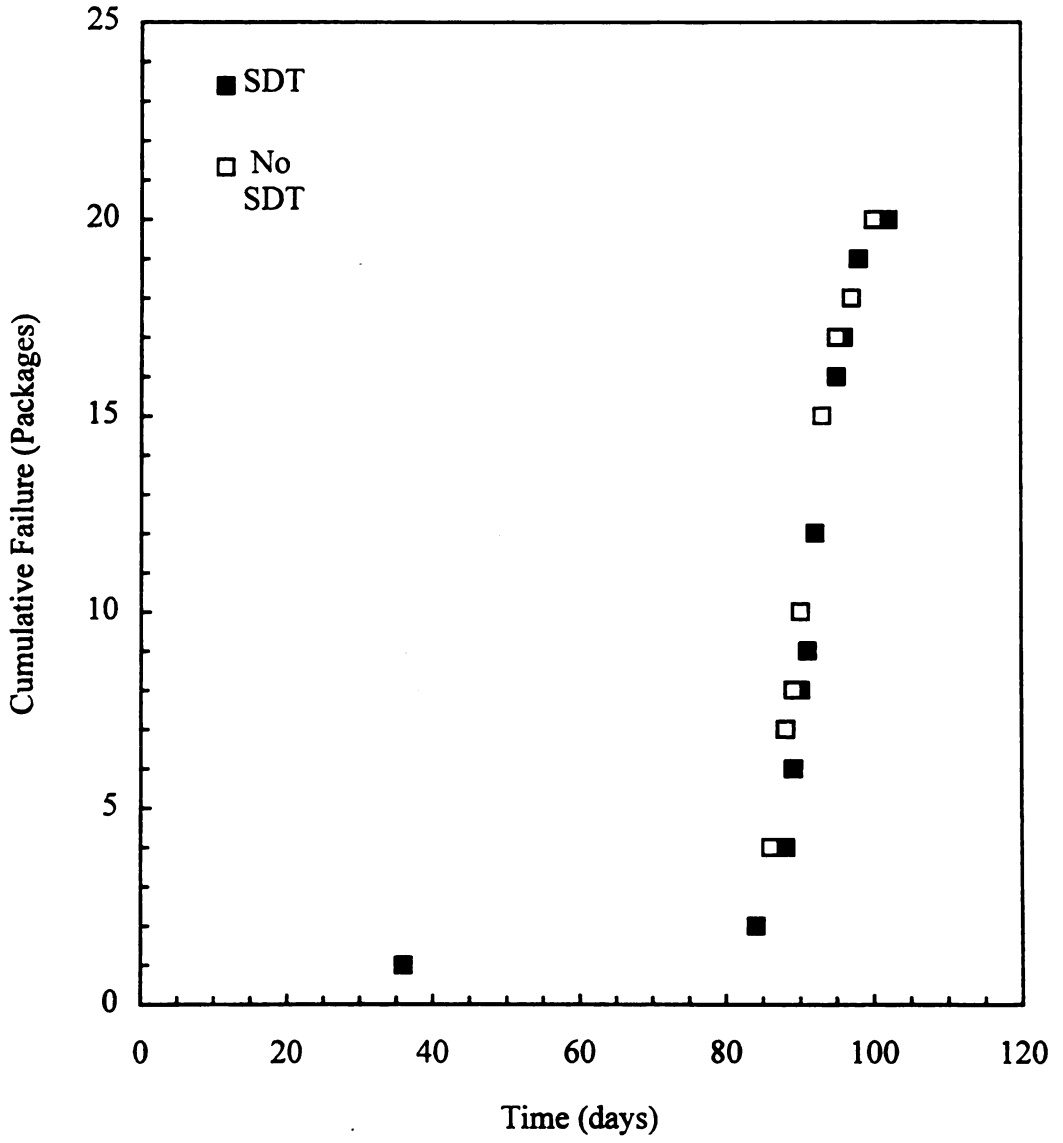

Figure 29. Cumulative failure vs. time for laundry additive at 120 °F.

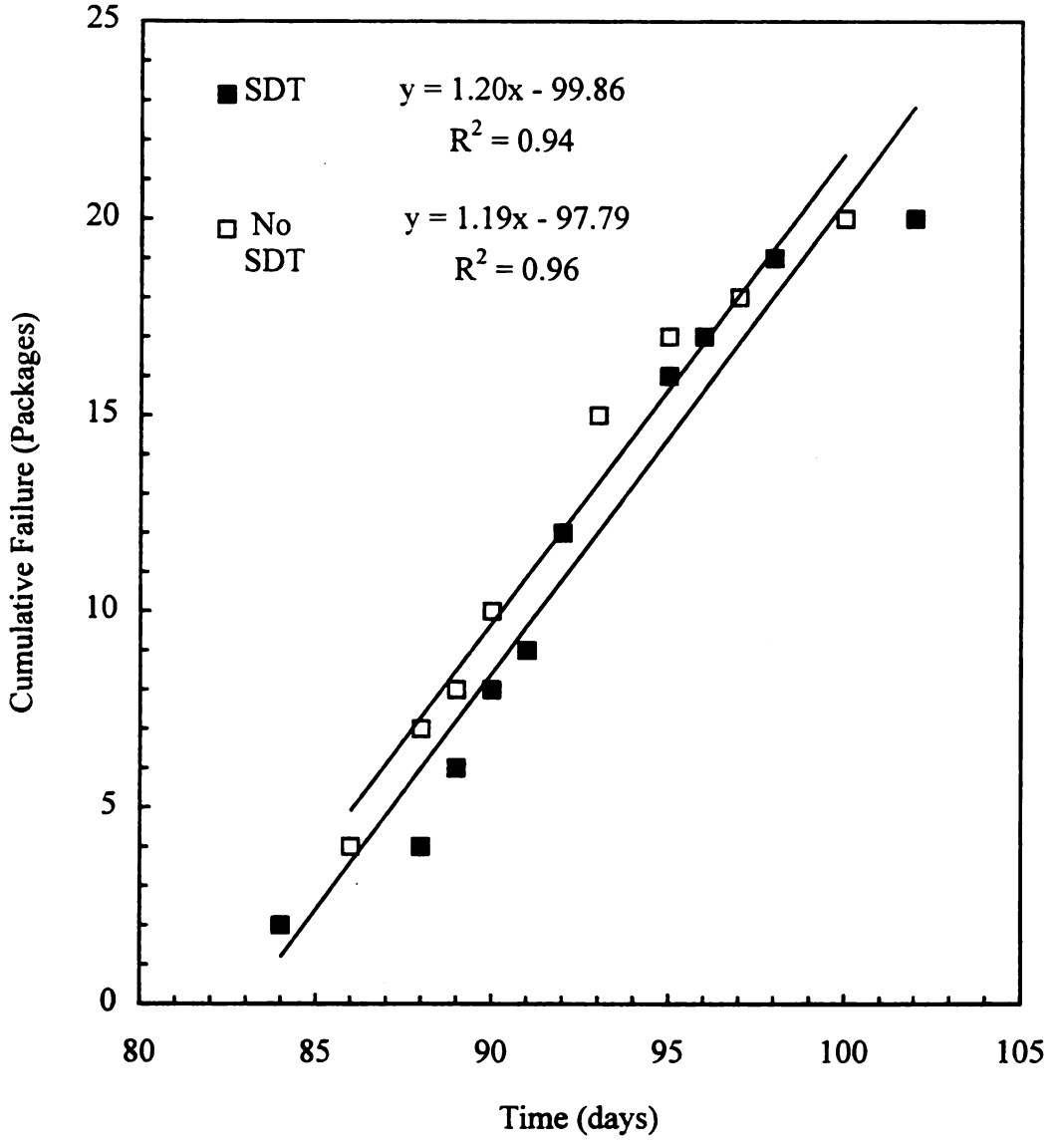

Figure 30. Expanded cumulative failure vs. time for laundry additive at 120 °F.

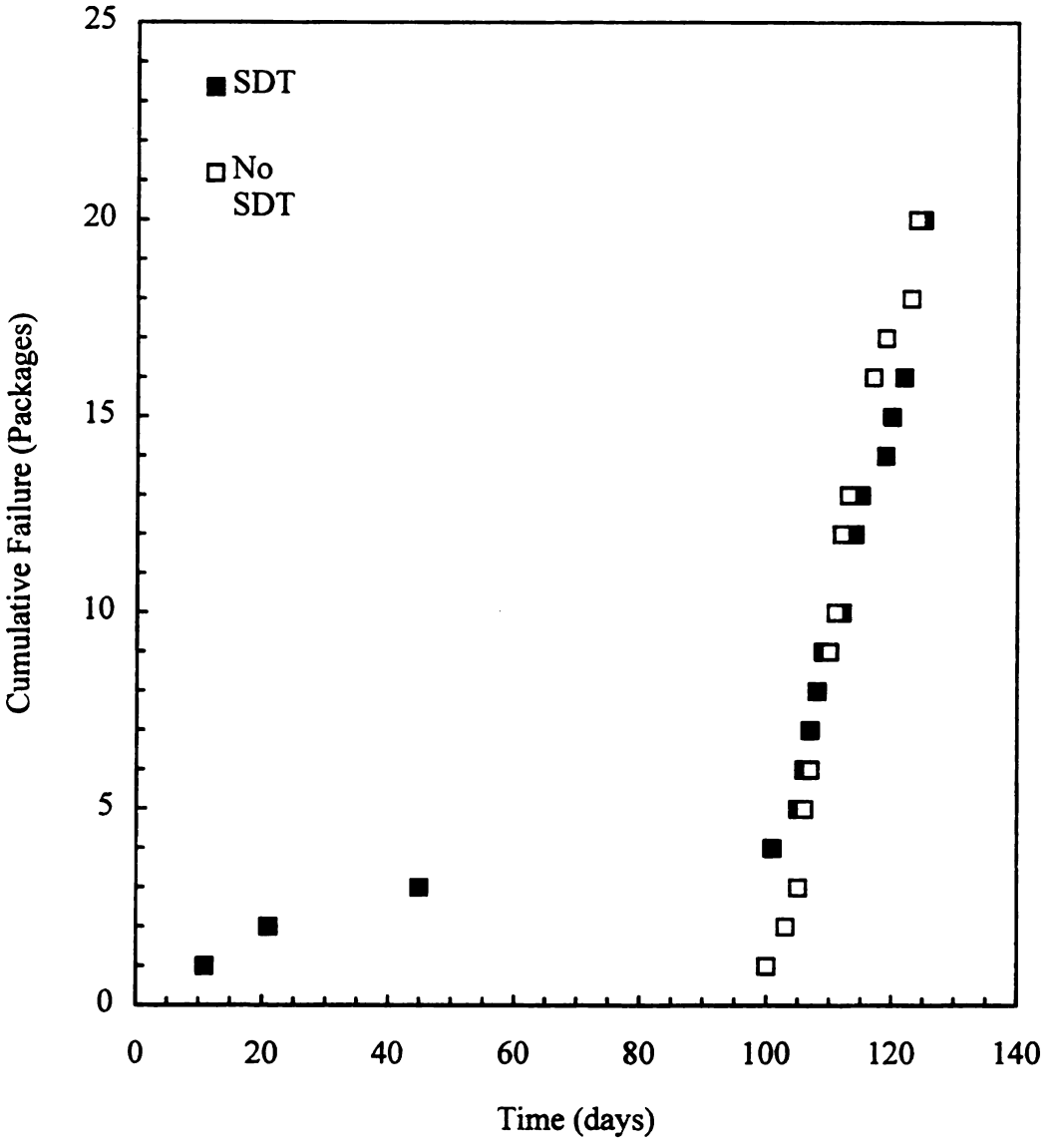

Figure 31. Cumulative failure vs. time for anti-bacterial cleaner at 140 °F.

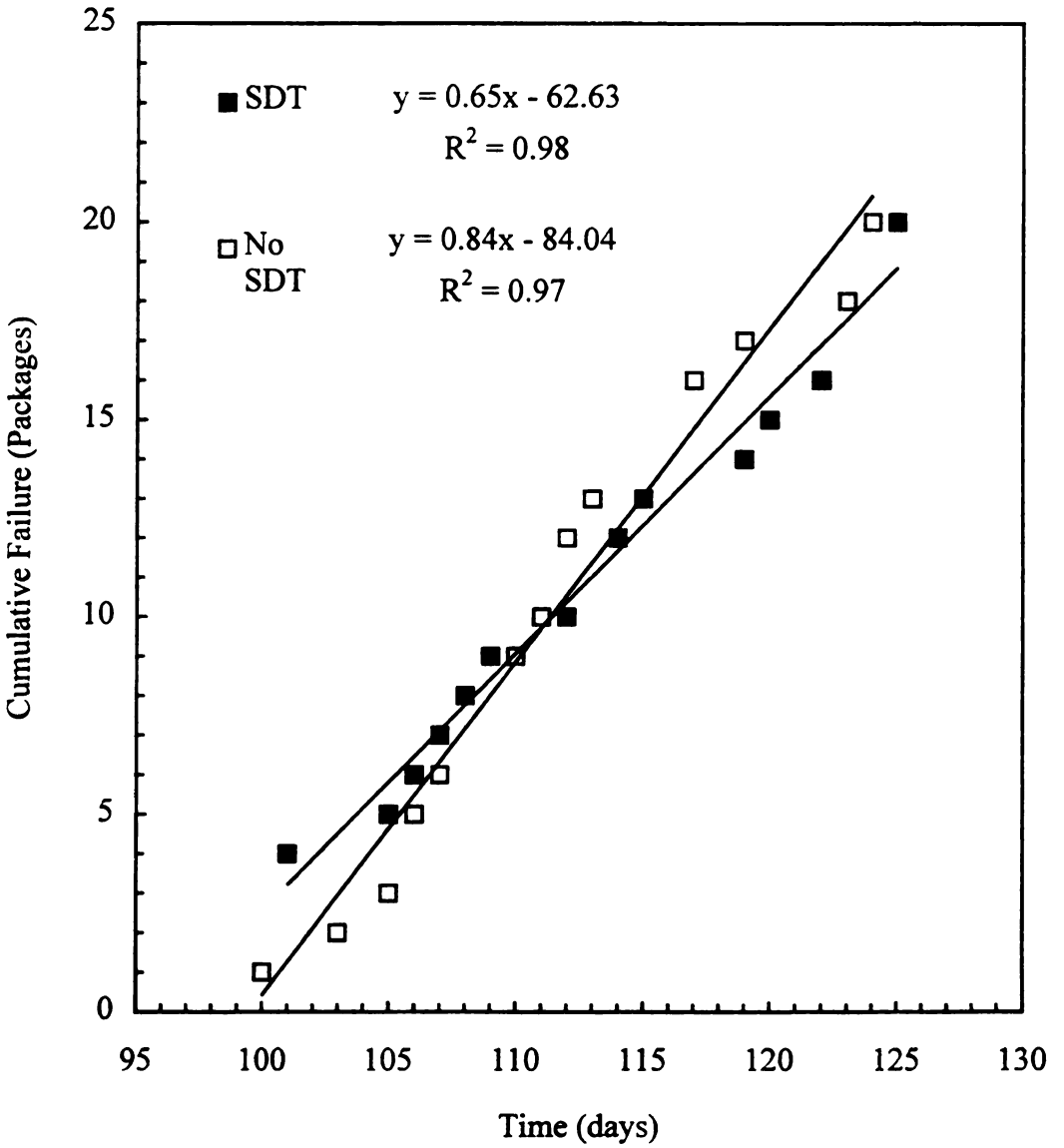

Figure 32. Expanded cumulative failure vs. time for anti-bacterial cleaner at 140 °F.

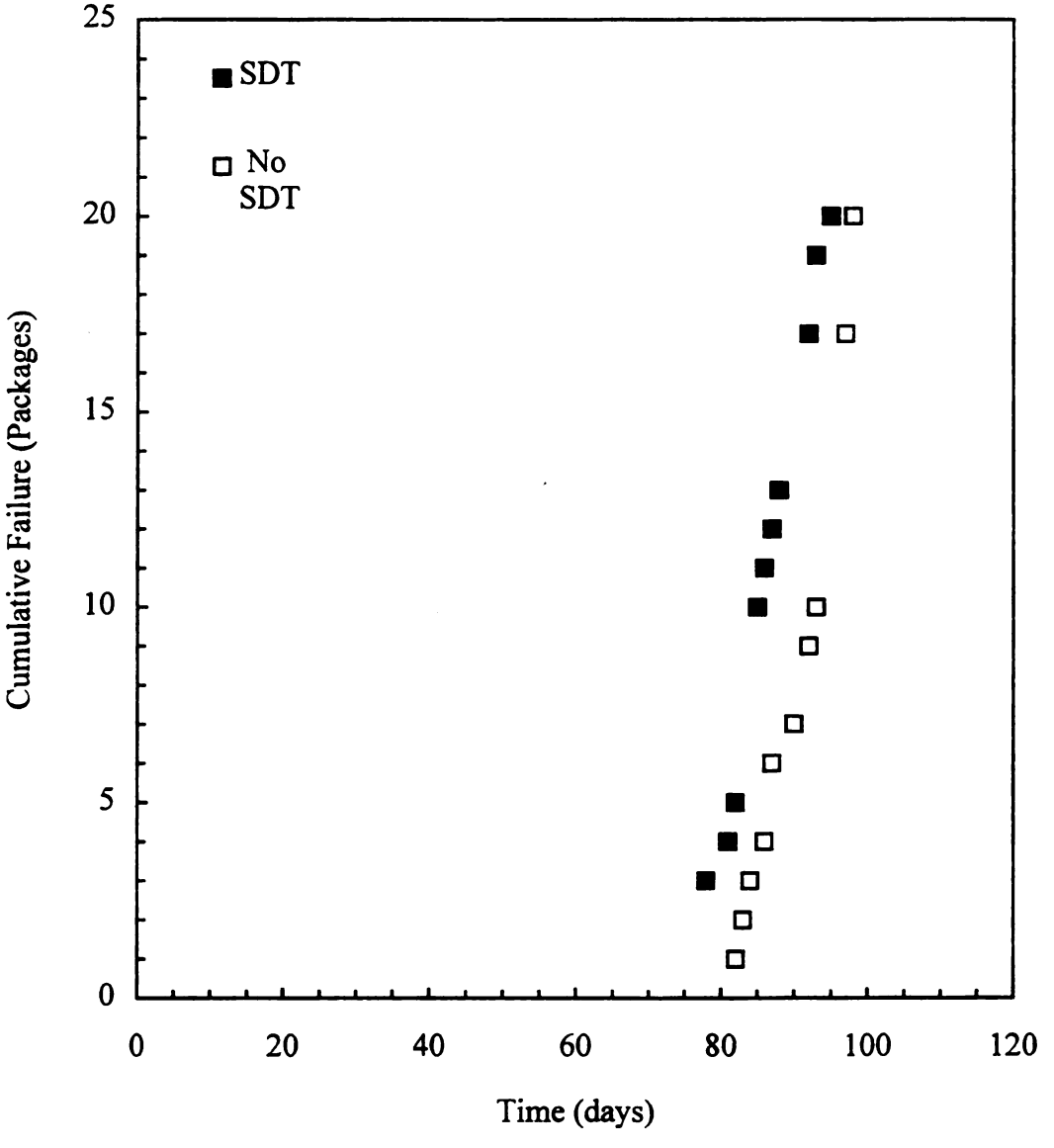

Figure 33. Cumulative failure vs. time for glass surface cleaner at 140 °F.

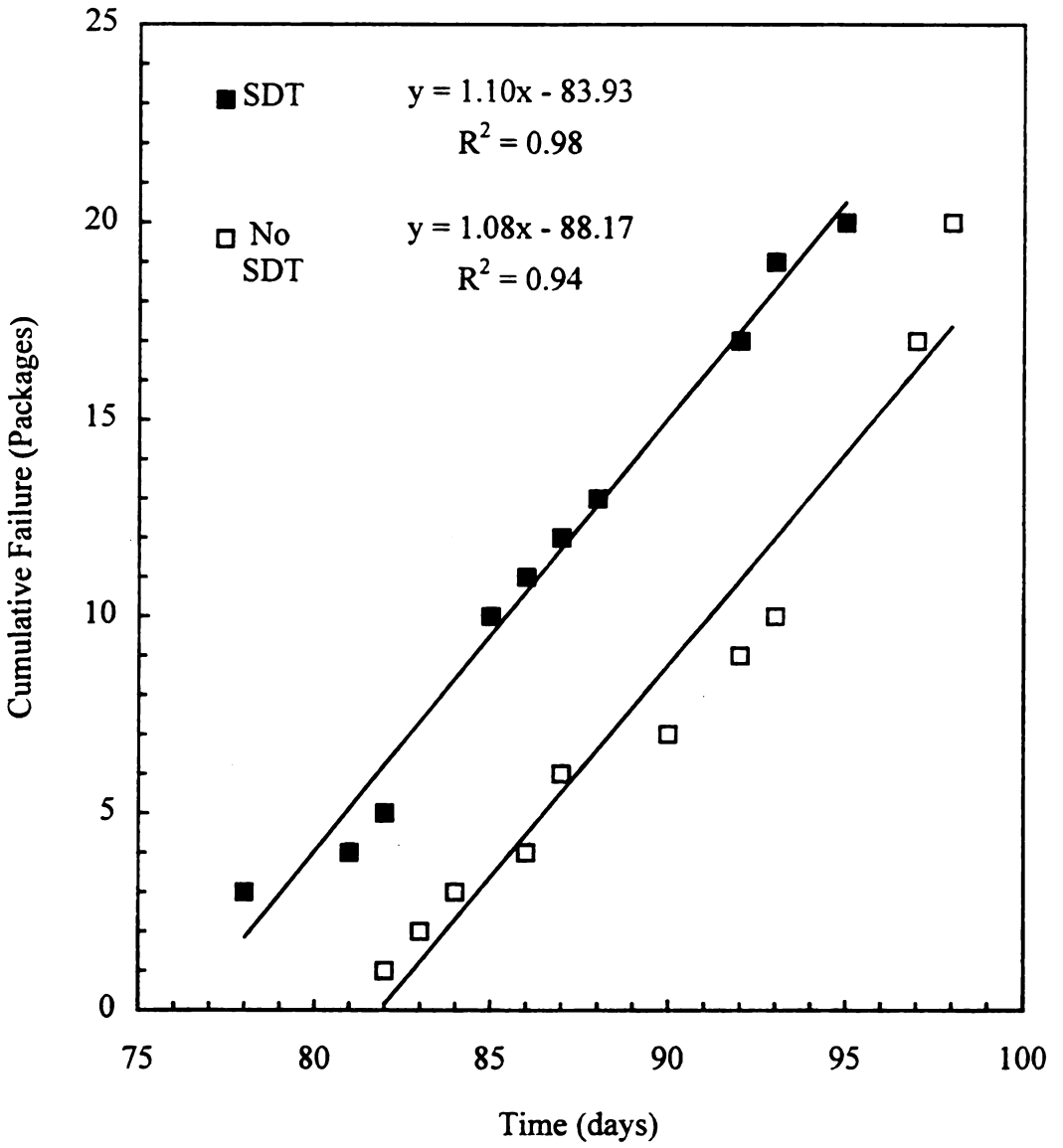

Figure 34. Expanded cumulative failure vs. time for glass surface cleaner at 140 °F.

Failure rates were determined from the cumulative failure vs. time plots by analyzing the data that occurred after the *initiation period.* Samples that failed during the *initiation period* were not used because these samples obviously failed due to a different mechanism than those that failed after the *initiation period.* The data was fit using a linear regression and the resulting slope provided the failure rate (packages/day) and the *initiation period* was determined from the x-axis intercept. This procedure allowed a comparison of the two sets of data to determine the effect of Simulated Distribution Testing on product/package system integrity.

Figure 28 shows an expanded view of the cumulative failure vs. time plot for the laundry additive system, along with the results of the linear relationships for each data set. The failure rates are 2.1 and 3.4 packages/day for the "SDT" and "No SDT" data, respectively. *Initiation periods* are 23.0 and 23.8 days for each set of data.

Figures 29 - 34 display the corresponding cumulative failure vs. time and expanded plots for the laundry additive system stored at 120 °F and the two surface cleaner products stored at 140 °F. All these plots show the same general behavior as that described above for the 140 °F laundry additive system. There is a characteristic *initiation period* during which only systems that received a dent from Simulated Distribution Testing failed, and then the majority of package systems begin to lose integrity. The failure rates and *initiation periods* determined by fitting a linear equation to each set of data are summarized in Tables 13 and 14, respectively.

Table 13. *Initiation periods* during storage.

		Initiation Period (Days)	
Product	**Temperature (°F)**	**SDT**	**No SDT**
Laundry Additive	140	23.0	23.8
	120	83.2	82.2
Surface Cleaner	140	96.4	100.0
Glass Surface Cleaner	140	76.3	81.6

Table 14. Failure rates during storage.

		Failure Rate (Packages/day)	
Product	**Temperature (°F)**	**SDT**	**No SDT**
Laundry Additive	140	2.1	3.4
	120	1.2	1.2
Surface Cleaner	140	0.65	0.84
Glass Surface Cleaner	140	1.1	1.1

The slopes of the regression lines used to obtain failure rates for each set of "SDT" vs. "No SDT" data were compared by analysis of covariance to determine if the observed differences are statistically significant. The results of this statistical analysis are displayed in Table 15. The covariance probabilities significantly greater than 0.05 for the

Table 15. Analysis of covariance results for cumulative failure vs. time plots.

		Covariance Probability
Product	**Temperature (°F)**	**SDT vs. No SDT**
Laundry Additive	140	0.019
	120	0.95
Surface Cleaner	140	9.0×10^{-4}
Glass Surface Cleaner	140	0.83

laundry additive and glass surface cleaner product/package systems stored at 120 and 140 °F, respectively, provide compelling evidence that Simulated Distribution Testing does not impact the long-term storage stability. In contrast, the probabilities less than 0.05 for the laundry additive and anti-bacterial surface cleaner stored at 140 °F suggest that there is a statistical difference between the "SDT" and "No SDT" data. However, inspection of the cumulative failure vs. time plots shown in Figures 28 and 32 for the laundry additive and anti-bacterial cleaner systems, respectively, show that these package systems exposed to Simulated Distribution Testing appear to fail at a slightly slower rate than those that were not exposed to the testing. Since this behavior is not likely, the most probable conclusion is that Simulated Distribution Testing also does not impact the results for these product/package systems. Therefore, all results suggest that the distribution environment does not impact storage stability as long as the shock and vibration forces do not cause a severe dent in the product/package system.

All three product/package systems stored at 140 °F failed during the six month study. Although the chemical composition of each product is not known, the failure rate and *initiation period* results follow the expected trend based on the known chemical aggressiveness of each product. The bleach alternative laundry additive was expected to be the most aggressive, and indeed this product/package system exhibits the shortest *initiation period* and highest failure rate. The two surface cleaners have similar *initiation periods* and failure rates, although the glass surface cleaner has a slightly shorter *initiation period* and higher failure rate. This result can qualitatively be explained by the fact that the internal pressure appeared to be greater for the glass cleaner than for the anti-

bacterial cleaner. This would cause higher stress, and therefore, would result in accelerated failure due to environmental stress cracking.

Another important conclusion is that if the distribution environment causes a shoulder or bottom dent, the product/package system integrity will most likely be seriously compromised. Although there were only eight occurrences of product/package systems stored at 120 and 140 °F that failed from dents resulting from distribution testing, this result clearly shows the importance of defects that can occur due to the distribution of the product. Product/package systems that received serious shoulder or bottom dents in the bottle due to the shock and vibration forces from the physical environment are likely to fail prematurely. In fact, these are the only types of defects associated with the Simulated Distribution Testing that appeared to initiate failure of the product/package systems. Every product/package system exposed to the elevated temperature environmental conditions, including 100 °F, that had a shoulder or bottom dent either failed or exhibited a stress crack at the end of the study. As an example, Figures 10 and 25 (pages 44 and 78, respectively) depict an anti-bacterial cleaner system that failed after 47 days during 100 °F storage. Further, select product/package systems with distribution dents which were stored under ambient conditions also failed during the course of the study, and several had visual signs of environmental stress cracks at the end of the study.

As stated previously, one of the goals of this research is to develop techniques that allow the use of accelerated aging data to predict the long-term storage stability under actual storage conditions. In order to accomplish this, failure rate data at several different

temperatures would be required to determine the functional dependence on temperature. However, during this study the only product/package system that failed at more than one temperature was the bleach alternative laundry additive system stored at 140 and 120 °F. Since failure occurred at only two temperatures, the exact temperature dependence cannot be determined. However, general concepts using the *initiation period* and failure rate data shown in Tables 13 and 14 (page 90), respectively, can be developed.

The *initiation period* and failure rate data for the laundry additive system show the expected temperature dependent trends. The *initiation period* increases with a decrease in temperature. This trend is not surprising since it should take longer for failure to begin when a product/package system is stored at a lower temperature. Further, the failure rates decrease with a decrease in temperature, which is anticipated because most temperature dependent reactions will decrease in rate as the temperature is decreased. Unfortunately, as stated previously, the functional form of these dependencies cannot be determined because data for only two temperature conditions is available.

Data was acquired at 140 and 120 °F because these are typical temperatures used in the industry for accelerated aging studies. The results presented here indicate that if a temperature greater than 140 °F were used, the *initiation period* would be less than 24 days and the failure rate would be greater than 2 - 3 packages/day. This prediction could help determine an experimental design strategy for an accelerated aging study at a higher temperature. Similarly, at temperatures lower than 120 °F, the *initiation period* would be greater than 83 days and the failure rate would be less than 1.2 packages/day.

In order to predict values, assumptions are required since data is available at only two temperatures. It is difficult to predict what the relationship between *initiation period* and temperature will be, but the failure rates will be assumed to follow Arrhenius behavior described by the Arrhenius equation,

$$k = A_0 e^{-E_a/RT} \tag{5}$$

where k is the rate constant, A_0 is the pre-exponential factor, E_a is the activation energy, R is the gas constant (1.987 $cal \cdot K^{-1} \cdot mol^{-1}$), and T is temperature (K). The Arrhenius expression shows that a plot of ln(k) vs. 1/T will be linear with a slope of $-E_a/R$. Plotting the ln(failure rate) vs. 1/T for the bleach alternative laundry additive data yields an activation energy of 10.7 $kcal \cdot mol^{-1}$ (slope = -5398.6 K^{-1}).

It is difficult to draw any conclusions from the magnitude of the activation energy because rate data regarding the environmental stress cracking mechanism is not available. However, for the purpose of this research, the assumption of Arrhenius behavior and calculation of the activation energy allows the prediction of the rate constant at any temperature, assuming the failure mechanism is the same under each condition. This approach could be used to predict the failure rate under actual storage conditions once the *initiation period* has expired. For example, the failure rates under the two other storage conditions used in this study of 100 °F and an ambient condition of 70 °F are predicted to be 0.66 and 0.25 packages/day, respectively, based on this type of Arrhenius analysis.

4. General Cumulative Failure vs. Time Behavior

The general time dependent behavior of failure for product/package systems such as those investigated is indicated by the results described above. Generic cumulative failure vs. time plots are shown in Figure 35 for a product/package system exposed to three different storage temperatures (T1 > T2 > T3). This is the type of behavior expected if the failure mechanism is the same under each storage condition. During the *initiation period*, which increases with a decrease in temperature, failure is only observed for package systems that experience dents from distribution forces. The slope during the *initiation period* will be dependent on the number of product/package systems with dents. After this time period, cumulative failure will increase in a linear fashion with time and, as shown in Figure 35, the failure rate will decrease as the temperature is decreased.

If data were available at a minimum of three different temperatures, such as shown in Figure 35, the functional form of the *initiation period* and failure rate temperature dependence could be determined. As described above for the laundry additive product/package system, this would permit estimation of *initiation period* and failure rate for any storage temperature, as long as the failure mechanism was the same.

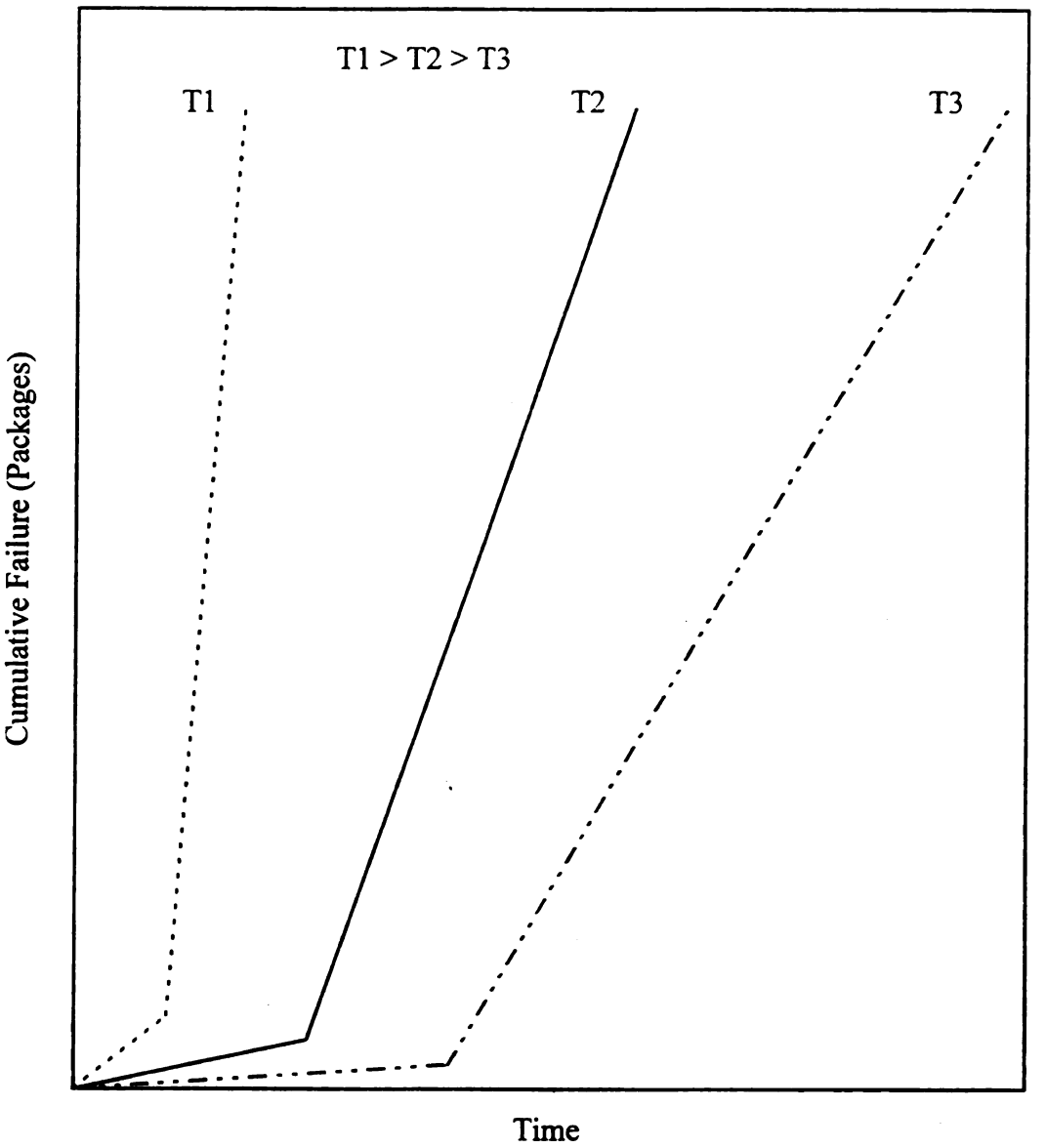

Figure 35. General cumulative failure vs. time plot as a function of temperature.

E. Environmental Effects on Package System Properties

1. Mechanical Properties

Figure 36 displays the change in yield stress of samples taken from bottle panels as a function of time for the bleach alternative laundry additive product/package system stored at 140 °F. The data is separated into two categories. The solid squares (■) represent data obtained on bottles from package systems that were exposed to Simulated Distribution Testing and the open squares (□) are for data collected on samples that were not exposed to the shock and vibration forces associated with the distribution environment. The value obtained for the control bottle is shown at time = 0 days, along with the standard deviation error bars associated with the measurement (10 bottles were measured for the control bottle data). The rest of the data were obtained by measuring the yield stress on bottle samples taken from product/package systems that failed, and therefore, the approach often only allowed the measurement of a single bottle. For this reason, there are no error bars associated with these measurements and the data shown is the average of two samples obtained from the front or back panel of each bottle. This type of approach allows the observation of general trends for this preliminary study and will be used for most of the performance criteria data.

The yield stress data shown in Figure 36 was analyzed by performing a t-test to compare the "SDT" to "No SDT" data, and to compare the control data to the "SDT" and

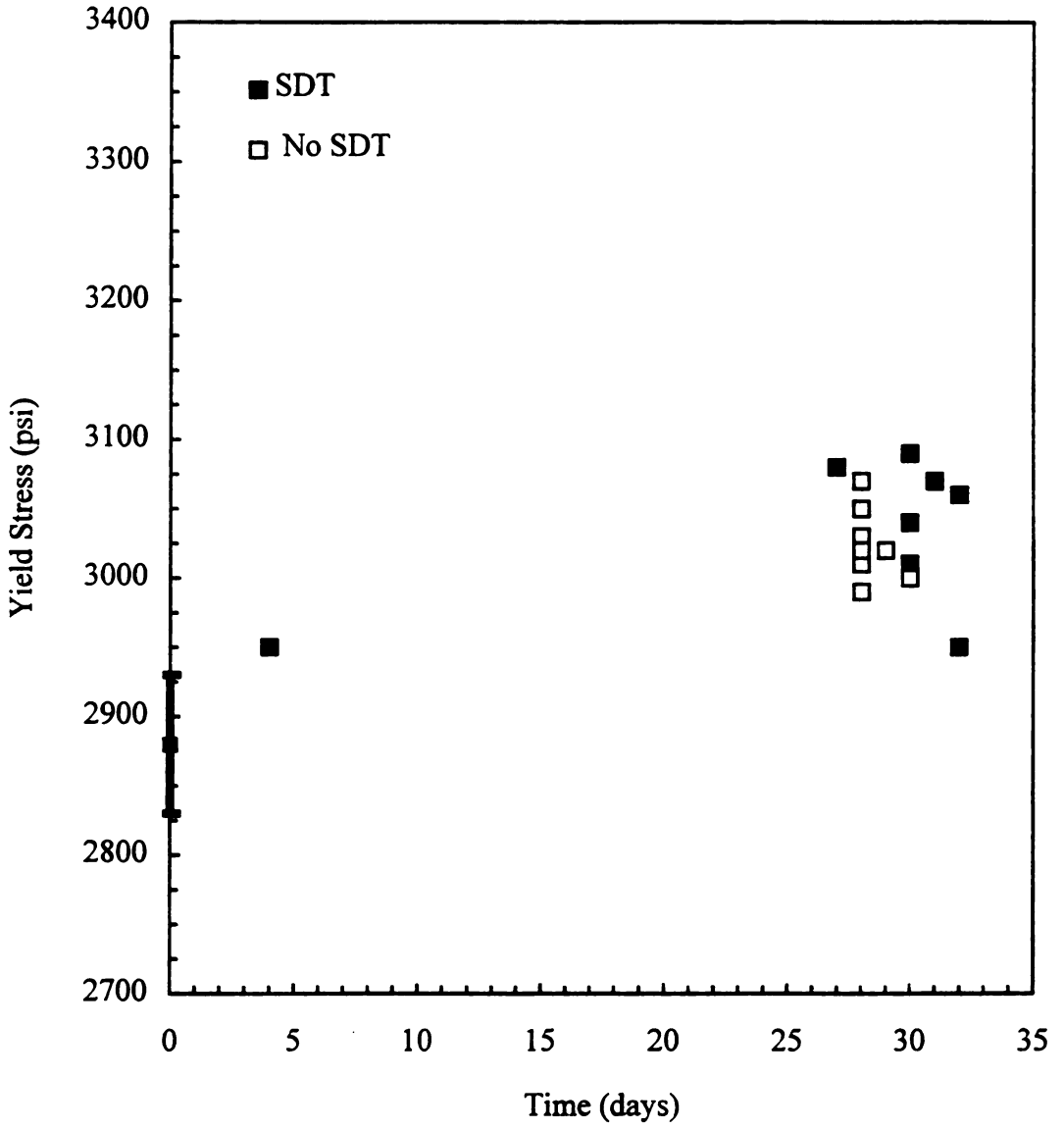

Figure 36. Yield stress vs. time for laundry additive bottle panels stored at 140 °F.

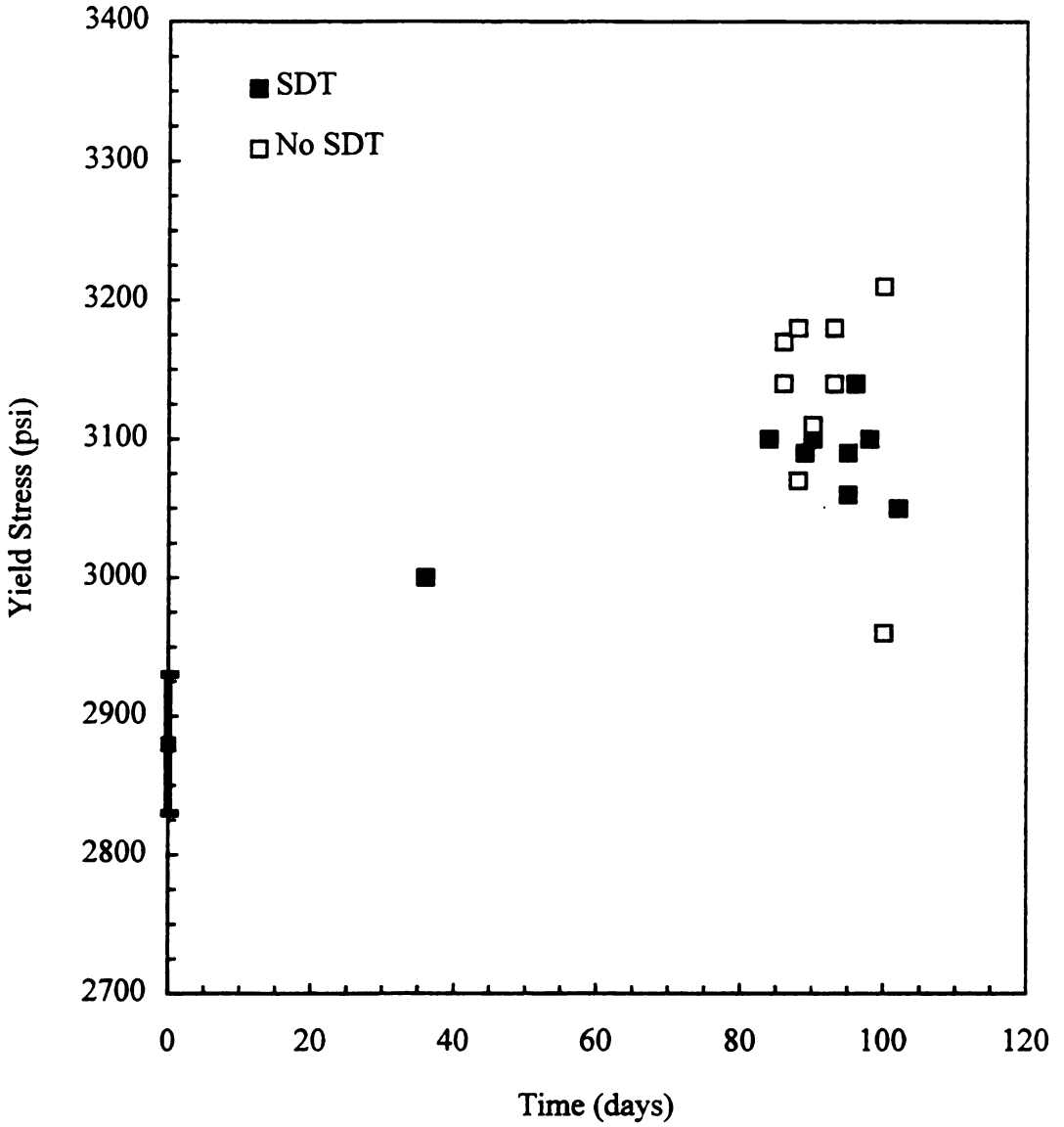

Figure 37. Yield stress vs. time for laundry additive bottle panels stored at 120 °F.

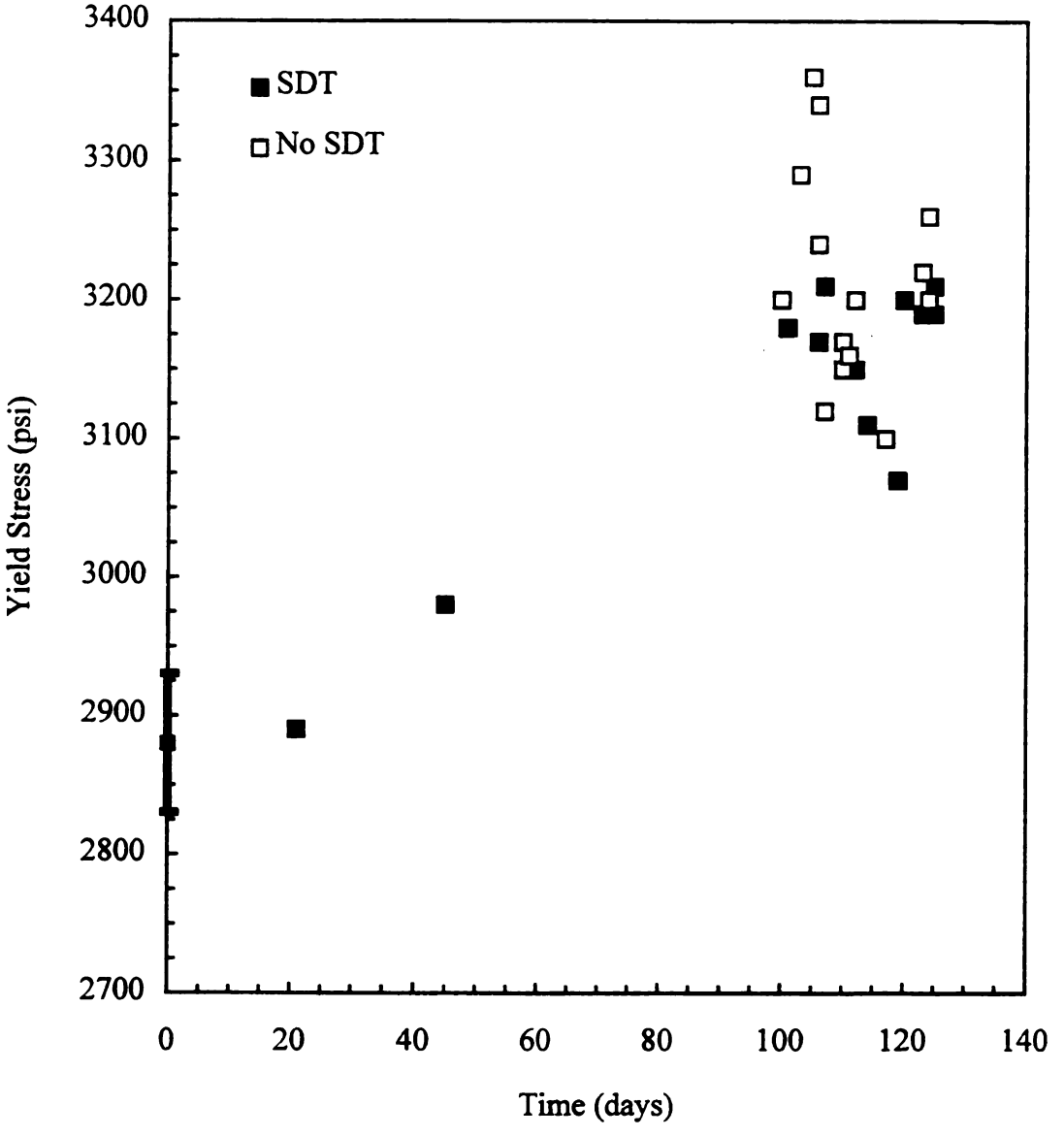

Figure 38. Yield stress vs. time for anti-bacterial cleaner bottle panels stored at 140 °F.

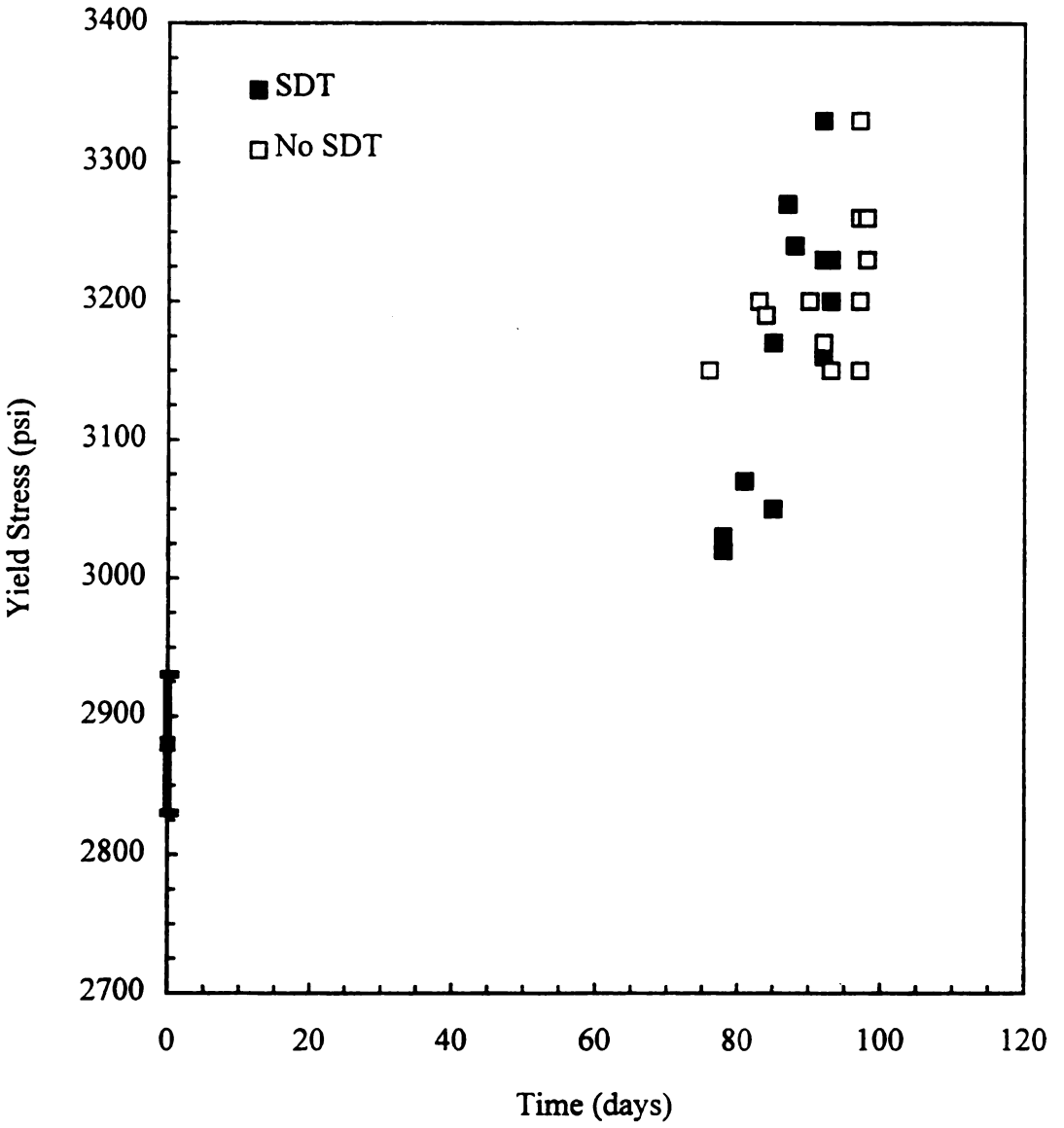

Figure 39. Yield stress vs. time for glass surface cleaner bottle panels stored at 140 °F.

"No SDT" data for failed product/package systems. The former will indicate if the Simulated Distribution Testing has an effect on yield stress and the later will indicate if the yield stress for failed systems differs from the control bottle result. A two-tailed t-test was performed using the "TTEST" statistical function included in the Microsoft Excel© spreadsheet program. As with Fisher's Exact Test, a probability of less than about 0.05 suggests that there is a statistical difference between the two sets of data being analyzed, while a value less than about 0.001 provides compelling evidence that there is a difference. Results obtained for bottles that failed due to shoulder or bottom dents were not used in the t-test calculation because these samples failed by a different mechanism than those measured towards the end of the storage time.

The t-test statistical analysis results for the yield stress data are shown in Table 16. The results for the laundry additive system stored at 140 °F show two main points.

Table 16. t-Test results for tensile yield stress.

		t-Test Probability		
Product	**Temp. (°F)**	**Control vs. SDT**	**Control vs. No SDT**	**SDT vs. No SDT**
Laundry Additive	140	1.2×10^{-6}	3.8×10^{-7}	0.36
	120	8.6×10^{-9}	1.2×10^{-7}	0.21
Surface Cleaner	140	6.7×10^{-11}	1.6×10^{-11}	0.13
Glass Surface Cleaner	140	8.2×10^{-8}	3.5×10^{-10}	0.24

First, the t-test probability of 0.36 for the "SDT" vs. "No SDT" comparison indicates that yield stress of failed systems is not dependent on whether Simulated Distribution Testing was performed. Second, there is a statistically significant difference between the control

bottle yield stress and the yield stress measured for failed systems (t-test probability = $1.2x10^{-6}$ and $3.8x10^{-7}$ for "SDT" and "No SDT", respectively). The modest increase in the yield stress is estimated to be approximately 7% from the data in Figure 36. The corresponding data for the bleach alternative laundry additive system stored at 120 °F is shown in Figure 37. t-Test results at this lower storage temperature indicate similar trends to the 140 °F data, in that the data is not dependent on Simulated Distribution Testing and there is a modest increase in yield stress.

The two surface cleaner product/package systems exposed to the 140 °F storage condition showed similar yield stress results as the bleach alternative laundry additive at 140 °F. The yield stress vs. time plots are shown in Figures 38 and 39 for the anti-bacterial and glass surface cleaners, respectively, and the t-test results are summarized in Table 16. Again, the yield stress is not dependent on the physical environment the product/package system was exposed to, and there is a modest increase in the yield stress. However, in contrast to the bleach alternative laundry additive data shown in Figure 36, both surface cleaner product/package systems appear to exhibit a slightly higher increase in yield stress (estimated to be approximately 10%).

The fact that the yield stress is not dependent on the physical environment associated with product distribution is an important conclusion. From a theoretical consideration, the result implies that the amorphous domain of the packaging material is not impacted by shock and vibration forces, since the stress vs. strain measurement up to yield point samples the elastic regime of a material [25]. The elastic regime is dictated by the amorphous domains of a semi-crystalline material such as HDPE. From a practical

standpoint, this suggests that the strength of the packaging material is not affected by the shock and vibration forces associated with the transportation environment. This result is not surprising, since these forces resulting from product distribution would be expected to affect overall package characteristics (i.e., dents, abrasions, creases, etc.), but not alter the polymer morphology which influences properties such as yield stress.

The modest increase in yield stress, however, is an interesting and surprising result, even though the practical implication is most likely minimal. The result is surprising because long-term aging is normally associated with a decrease in material properties as fatigue occurs, especially for plastic packaging materials. The modest increase in yield stress is even more surprising for the anti-bacterial surface cleaner product/package system. This product contains d-limonene which was shown to sorb into the HDPE packaging material during the course of the study (see Chapter 3.E.5.). Since prior work [13] has shown that the mechanical properties of low density polyethylene are reduced by the sorption of d-limonene into the material, it is expected that such a decrease in mechanical properties would occur for HDPE. However, this was not observed.

A possible explanation for the increase in yield stress is that the bottles are undergoing an annealing process during storage at elevated temperatures. The thermal and mechanical history during polymer processing are known to affect mechanical properties by impacting the morphology of the polymer. Any subsequent process which affects this morphological structure would also be expected to impact the mechanical properties. Annealing is a well-known process that causes a polymer to relax towards a

more thermodynamically favorable structure. Indeed, yield stress and tensile modulus of polypropylene have been shown to increase at annealing temperatures as low as 100 °C [25]. For these reasons, the minimal increase observed in yield stress could be related to annealing.

Another possible explanation for the increase in yield stress is that a chemical reaction such as crosslinking is causing an increase in molecular weight, and thus an increase in yield stress. HDPE is known to become more brittle during long-term aging due to crosslinking. However, significant crosslinking would most likely be required to increase the yield stress by the amounts observed and therefore is probably not as likely the cause of the increased yield stress as annealing. Furthermore, yield strength of polyethylene is not extremely sensitive to molecular weight [4].

In an effort to determine if product/package system integrity can be related to the changes in yield stress, the final mechanical properties of samples that had not failed by the end of the study were measured and compared to the values obtained for failed samples. These mechanical property results are shown in Table 17. The t-test was used again as a statistical analysis tool to compare the different sets of data. The 100 °F data for product/package systems at the end of the study were used for comparison purposes for all sets of data. As an example, the yield stress results for failed laundry additive product/package systems stored at 140 and 120 °F were compared to the final results for the laundry additive stored at 100 °F. Similar comparisons were made for the anti-bacterial and glass surface cleaner product/package systems.

Table 17. Mechanical properties of product/package systems at the end of the study.

Product	Temperature (°F)	Yield Stress (psi)	Tensile Modulus (psi)
Laundry Additive	100	3030 ± 50	26,000 ± 900
	Ambient	2960 ± 40	25,900 ± 700
Anti-bacterial Surface Cleaner	120	3100 ± 40	26,500 ± 600
	100	3010 ± 50	25,600 ± 800
	Ambient	2910 ± 30	24,500 ± 600
Glass Surface Cleaner	120	3060 ± 30	25,500 ± 500
	100	3010 ± 40	25,600 ± 700
	Ambient	2930 ± 40	25,600 ± 700

Table 18 displays the t-test results, where the tensile yield stress of failed product/package systems is compared to the final results obtained on samples stored at 100 °F. The t-test probabilities shown for bleach alternative laundry additive panel samples stored at 140 °F indicate that there is no statistical difference between the failed and final bottle panel yield stress values (for both "SDT" and "No SDT"), suggesting that for this product/package system yield stress is not directly related to package integrity during storage. In contrast, the t-test results for the same product/package system stored at 120 °F give a different conclusion. The probability values for the two different

Table 18. t-Test results for yield stress at the end of the study.

		t-Test Probability	
Product	Temp. (°F)	Final (100 °F) vs. SDT	Final (100°F) vs. No SDT
Laundry Additive	140	0.79	0.58
	120	0.012	4.9×10^{-3}
Surface Cleaner	140	8.8×10^{-7}	1.5×10^{-6}
Glass Surface Cleaner	140	2.5×10^{-4}	9.9×10^{-9}

physical environments are both less than 0.05 indicating that there is a statistical difference between the final yield stress obtained and that for the failed systems. In addition, comparing the data for failed product/package systems at 140 to 120 °F shows a statistically significant difference between the two (t-test probability for "SDT" and "No SDT" are 0.017 and 1.1×10^{-3}, respectively).

Statistical analysis performed for the two surface cleaner product/package systems gives a similar conclusion as the 120 °F laundry additive system, except the t-test probabilities being much less than 0.001 provide strong evidence of a difference in properties. Clearly for these product/package systems, the yield stress measured for the failed system panels is greater than that for systems sampled at the end of the study that did not fail.

The practical importance of the observed differences in yield stress when comparing final package systems to those that failed during the study is not readily understood. While not fully understood, the results suggest that there is a correlation between package system integrity and yield stress, even though the observed increases are relatively small (i.e., the largest increase is about 10%). However, it is difficult to rationalize why package failure would be related to an increase in tensile yield stress. If anything, this result would tend to imply that the packages are becoming stronger, and hence, would become more resistant to failure. Further work would be required to understand if product/package system failure can be directly related to tensile yield stress.

Data for the change in the modulus of elasticity are presented in a similar fashion as the yield stress data described above. That is, modulus of control samples is displayed

at time = 0 days, along with the standard deviation error bars associated with the measurement. The rest of the data points are for panel samples taken from individual bottles and therefore there are no error bars for these measurements. Each data point represents an average of two measurements taken for the same bottle. In addition, the data was analyzed using the t-test in a similar fashion as described above.

Figures 40 and 41 display the bottle panel tensile modulus as a function of time for the bleach alternative laundry additive system stored at 140 and 120 °F, respectively. The results of the t-test analysis are shown in Table 19. As with the yield stress data, Simulated Distribution Testing does not impact the modulus results, as the t-test probabilities of 0.32 and 0.26 for the 140 and 120 °F data, respectively, strongly suggest. Using the t-test to compare the control modulus to the "SDT" and "No SDT" 140 °F data provides conflicting results. The t-test probabilities of 0.10 and 6.1×10^{-3} indicate that there is no statistical difference between "Control" and "SDT" while there is a difference between "Control" and "No SDT". However, the value of 0.10 is approaching 0.05 and therefore does not provide strong evidence that the "Control" data is similar to the "SDT' data. Clearly, it is not expected that the different physical environments should impact

Table 19. t-Test results for modulus of elasticity.

		t-Test Probability		
Product	**Temp. (°F)**	**Control vs. SDT**	**Control vs. No SDT**	**SDT vs. No SDT**
Laundry Additive	140	0.10	6.1×10^{-3}	0.32
	120	0.072	0.019	0.26
Surface Cleaner	140	0.075	0.010	0.34
Glass Surface Cleaner	140	6.9×10^{-4}	1.3×10^{-6}	0.059

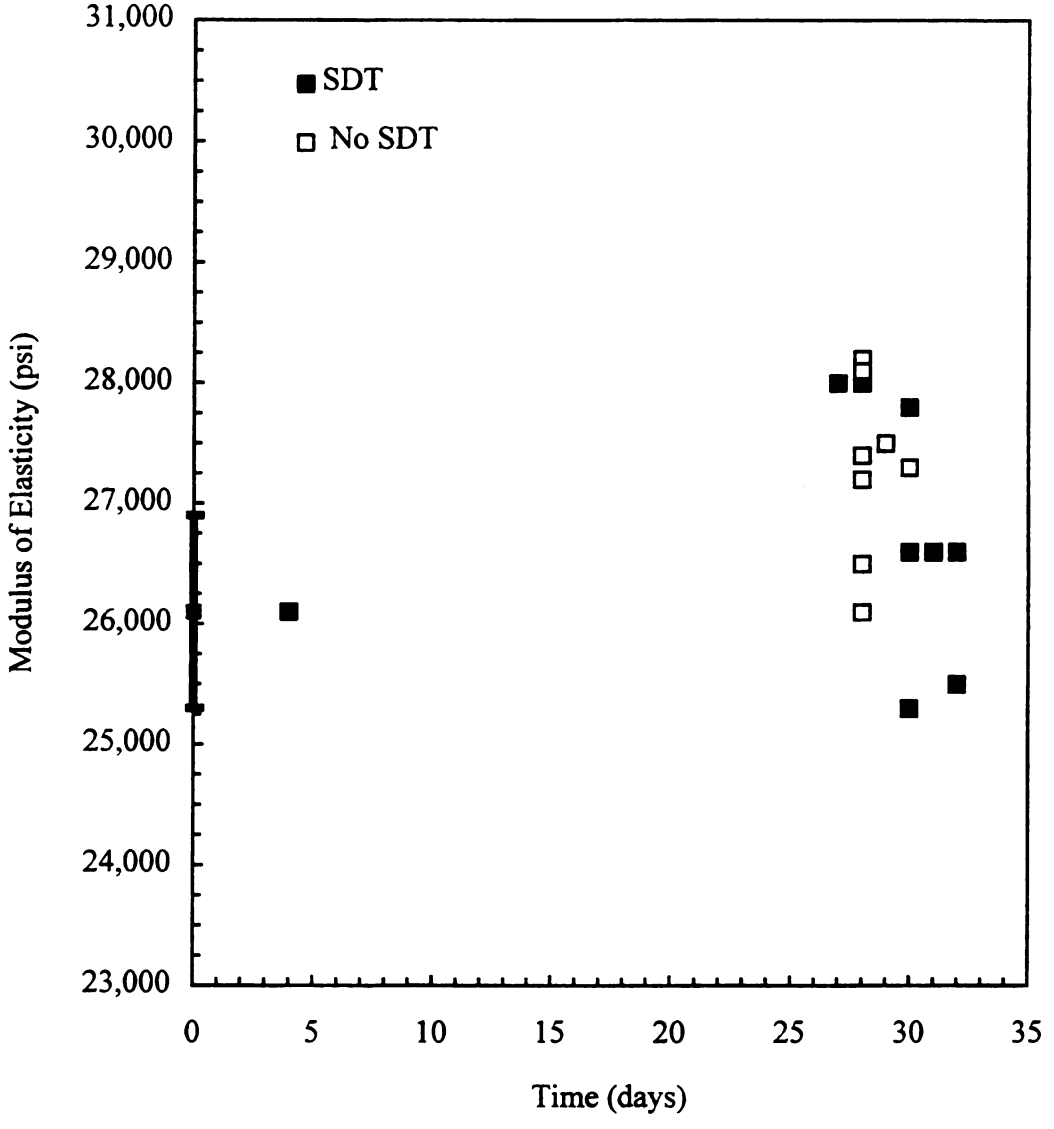

Figure 40. Modulus of elasticity vs. time for laundry additive bottle panels stored at 140 °F.

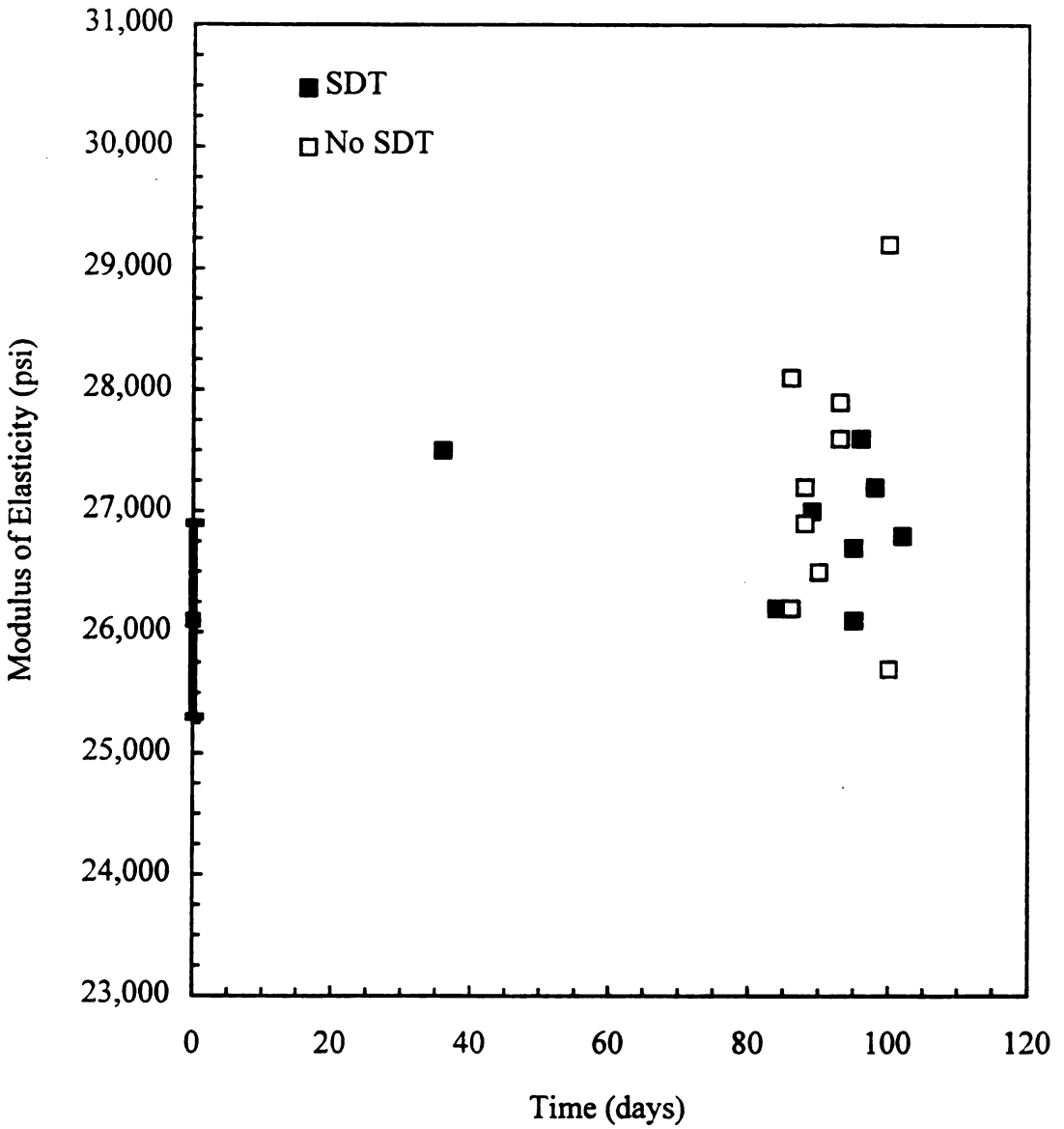

Figure 41. Modulus of elasticity vs. time for laundry additive bottle panels stored at 120 °F.

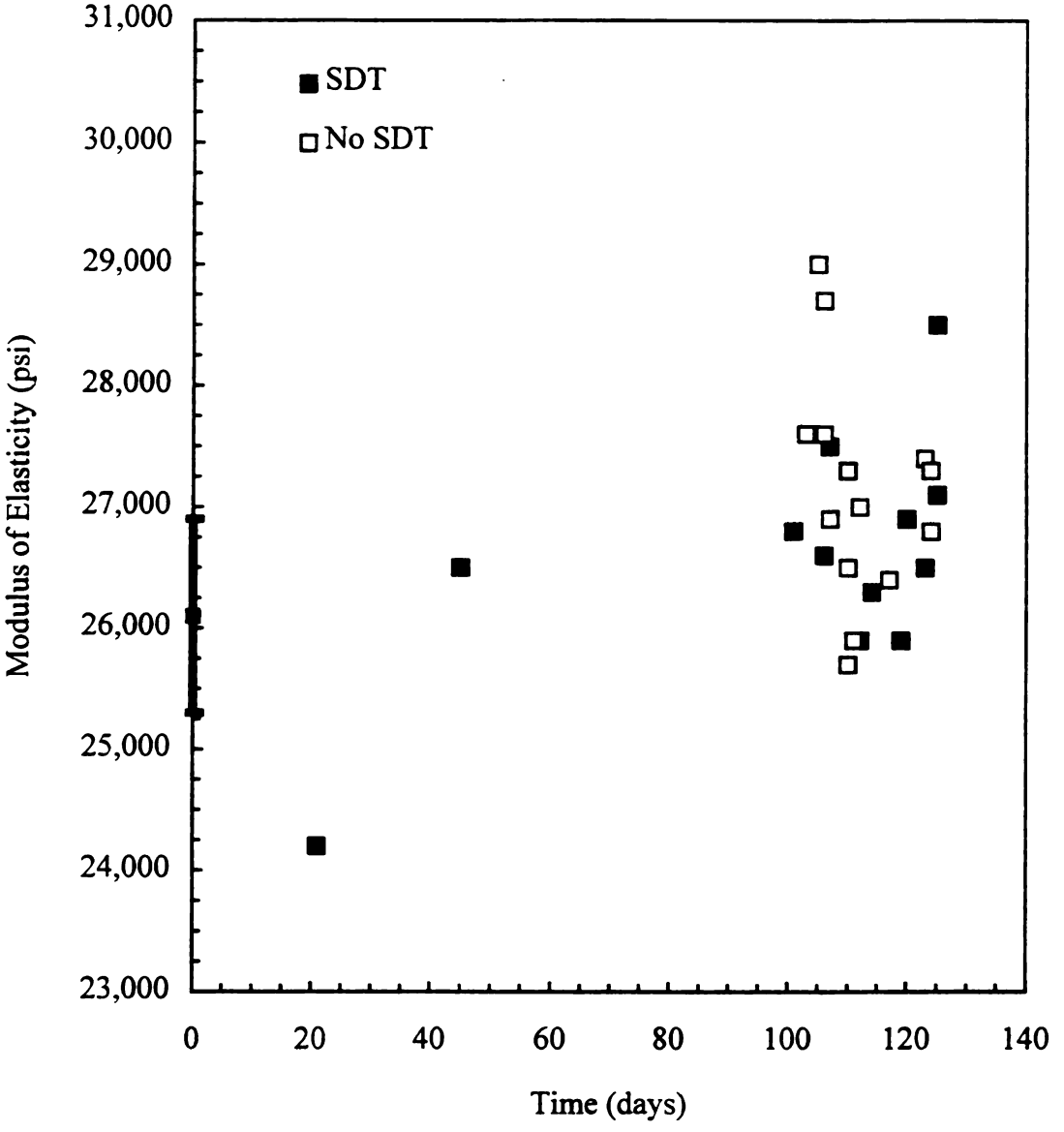

Figure 42. Modulus of elasticity vs. time for anti-bacterial cleaner bottle panels stored at 140 °F.

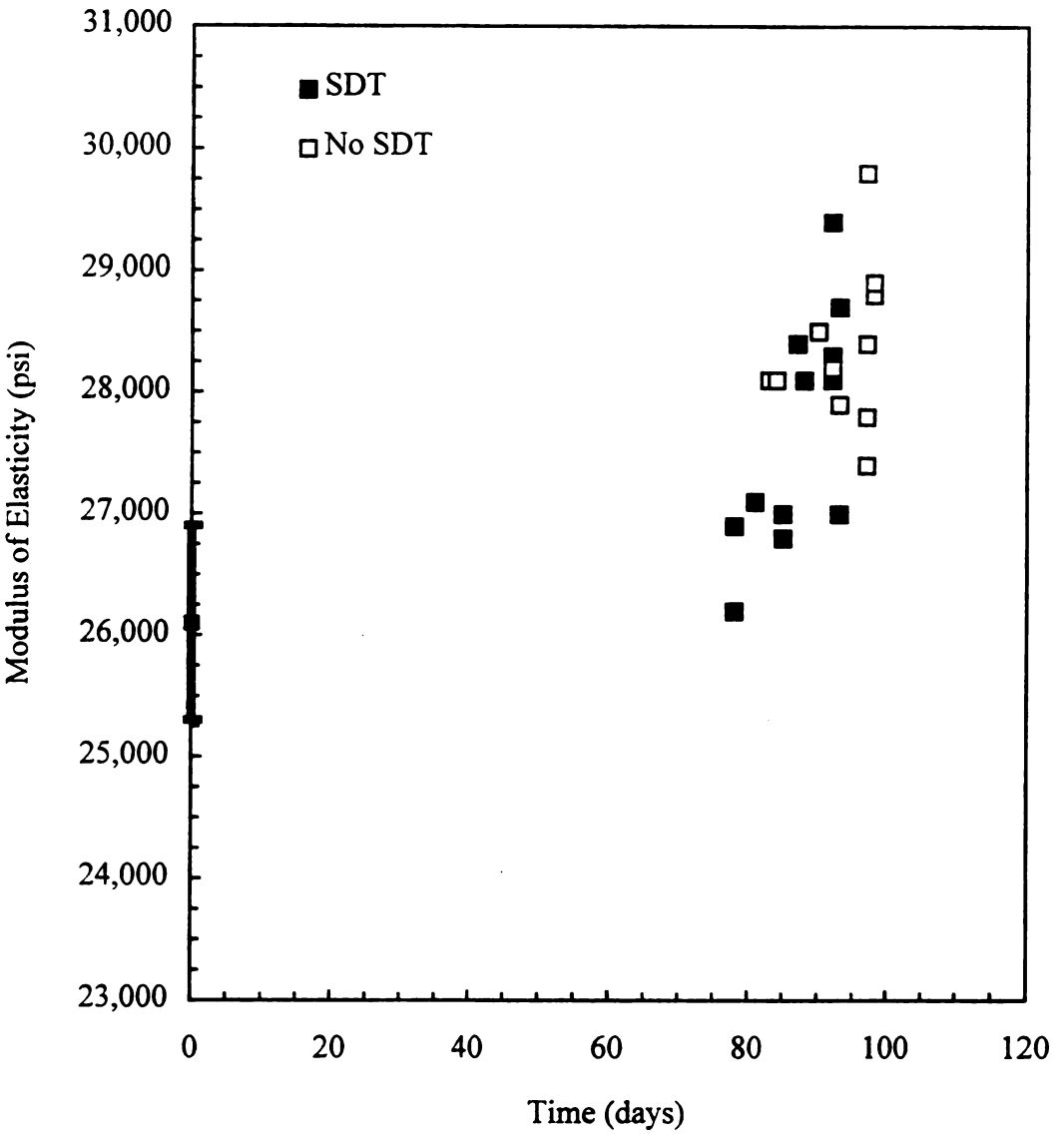

Figure 43. Modulus of elasticity vs. time for glass surface cleaner bottle panels stored at 140 °F.

these results. The same type of results were obtained for the 120 °F laundry additive modulus data, as shown in Table 19 and Figure 41. In this case, the t-test probability of 0.072 for the "Control" vs. "SDT" data is quite close to 0.05, the probability value below which there is a statistically significant difference between the two test values.

The modulus of elasticity results obtained for the anti-bacterial surface cleaner product/package system stored at 140 °F, shown graphically in Figure 42 and summarized in Table 19, are also similar to the laundry additive system results described above. The data strongly suggests that there is no statistical difference between the "SDT" and "No SDT" results, and the comparison to the control modulus is contradictory. However, visual observation of the data shown in Figure 42 indicates that the "SDT" and "No SDT" data are slightly higher than the control bottle measurement.

In contrast to the laundry additive and anti-bacterial surface cleaner modulus data, the results presented in Figure 43 for the glass surface cleaner product/package system exposed to the 140 °F storage environment clearly show a moderate increase in tensile modulus as a function of time. This conclusion is further supported by the t-test probabilities shown in Table 19. While there is no statistical difference between the "SDT" and "No SDT" data, probabilities significantly less than 0.05 when compared to the values for the control bottles provide compelling evidence of a statistically significant difference in the modulus of elasticity for the failed product/package systems. The observed increase in the modulus for failed systems was approximately 10% when compared to the control samples.

t-Test results comparing the final modulus of elasticity data shown in Table 17 (page 106) with the values obtained for failed product/package systems are shown in Table 20. All t-test probabilities shown in this table, with the exception of that for the "SDT" laundry additive stored at 140 °F, are significantly less than 0.05. This result indicates that there is a statistical difference between the modulus obtained for package systems that did not fail by the end of the study and failed systems. All figures associated with this data show that there is a modest increase in the modulus of elasticity.

Table 20. t-Test results for modulus of elasticity at the end of the study.

		t-Test Probability	
Product	**Temp. (°F)**	**Final (100 °F) vs. SDT**	**Final (100 °F) vs. No SDT**
Laundry Additive	140	0.077	4.5×10^{-3}
	120	6.9×10^{-4}	6.9×10^{-4}
Surface Cleaner	140	2.7×10^{-3}	2.7×10^{-4}
Glass Surface Cleaner	140	1.3×10^{-5}	1.0×10^{-8}

The observed increase in modulus of elasticity is certainly an interesting result. Unlike the tensile yield stress results in which it is difficult to conclude that an increase in yield stress could impact package system integrity, it is possible to rationalize a correlation between tensile modulus and package failure. An increase in modulus of elasticity implies that the plastic comprising the bottle is becoming more brittle. Certainly a more brittle packaging material would be more susceptible to failure when exposed to shock and vibration forces. However, in this case, the increase in modulus occurs while the product/package systems are stationary in storage. Nevertheless, this

could potentially lead to additional stresses that would ultimately result in environmental stress cracking. This hypothesis would clearly require additional research to verify.

In addition to determining the yield stress and modulus of elasticity for bottle panels sampled from failed product/package systems, the strength of the side seam and bottom weld line were also evaluated. For this determination, two side seam samples and one bottom weld line sample were analyzed from each sampled bottle and the results compared to control bottle values of 8.1 ± 0.8 and 7.9 ± 0.9 lb for the side and bottom seams, respectively. All of the data obtained for each of these properties fell within one standard deviation of the mean, and therefore, did not change during storage. This result is consistent with the observation that none of the failure modes were located at either of these bottle locations. The data clearly indicate that this property is not directly related to package integrity for the respective product/package systems investigated. In addition, the results where independent of Simulated Distribution Testing, suggesting that product distribution does not affect the strength of the side mold seam or bottom weld line.

2. Dynamic Mechanical Properties

The last type of mechanical property evaluation performed was dynamic mechanical analysis. Bottle sampling from product/package systems was somewhat different for dynamic mechanical analysis than for those previously described for yield stress and modulus of elasticity. In contrast to the previously described mechanical testing in which several samples were evaluated throughout the study, only one DMA panel sample was evaluated for select test conditions. Therefore, the DMA plot was

obtained for the control bottle (see Chapter 3.A.3.), and for single bottles that were sampled towards the end of the test time for each product/package system, under the storage conditions of 140 and 120 °F. Further, only systems that experienced Simulated Distribution Testing were evaluated. The purpose of this approach was to determine if the DMA properties changed in any way after long-term storage and to provide an indication if there is a need for further research in this area.

Figures 44 and 45 display the DMA plots obtained from panel samples of failed bottles containing the bleach alternative laundry additive product at 140 and 120 °F, respectively. The overall shape and location of the thermal transitions are similar for each of these two plots and they are very similar to the DMA plot for the control bottle (see Figure 4, page 32). This indicates little, if any, change in the storage and loss modulus as a function of temperature.

Similar conclusions are drawn for the two surface cleaner product/package systems. The DMA plots for the anti-bacterial surface cleaner at 140 and 120 °F are shown in Figures 46 and 47, respectively. For this system, the 140 °F data was obtained for a failed product/package system and the 120 °F data was obtained on a sample that had not failed by the end of the study. Figures 48 and 49 show the corresponding 140 and 120 °F DMA plots for the glass surface cleaner product/package system.

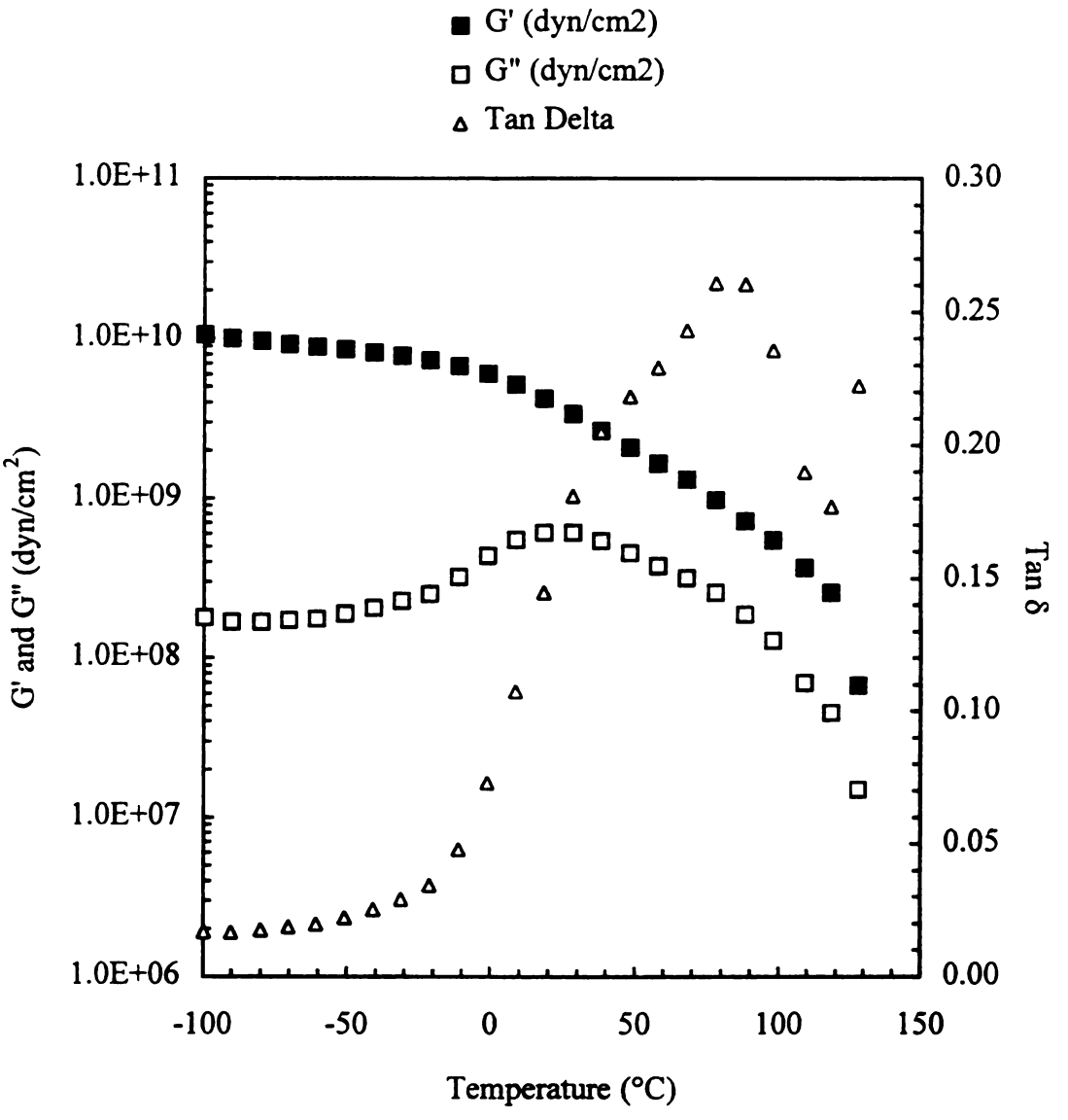

Figure 44. DMA plot for failed laundry additive bottle panel after 27 days at 140 °F.

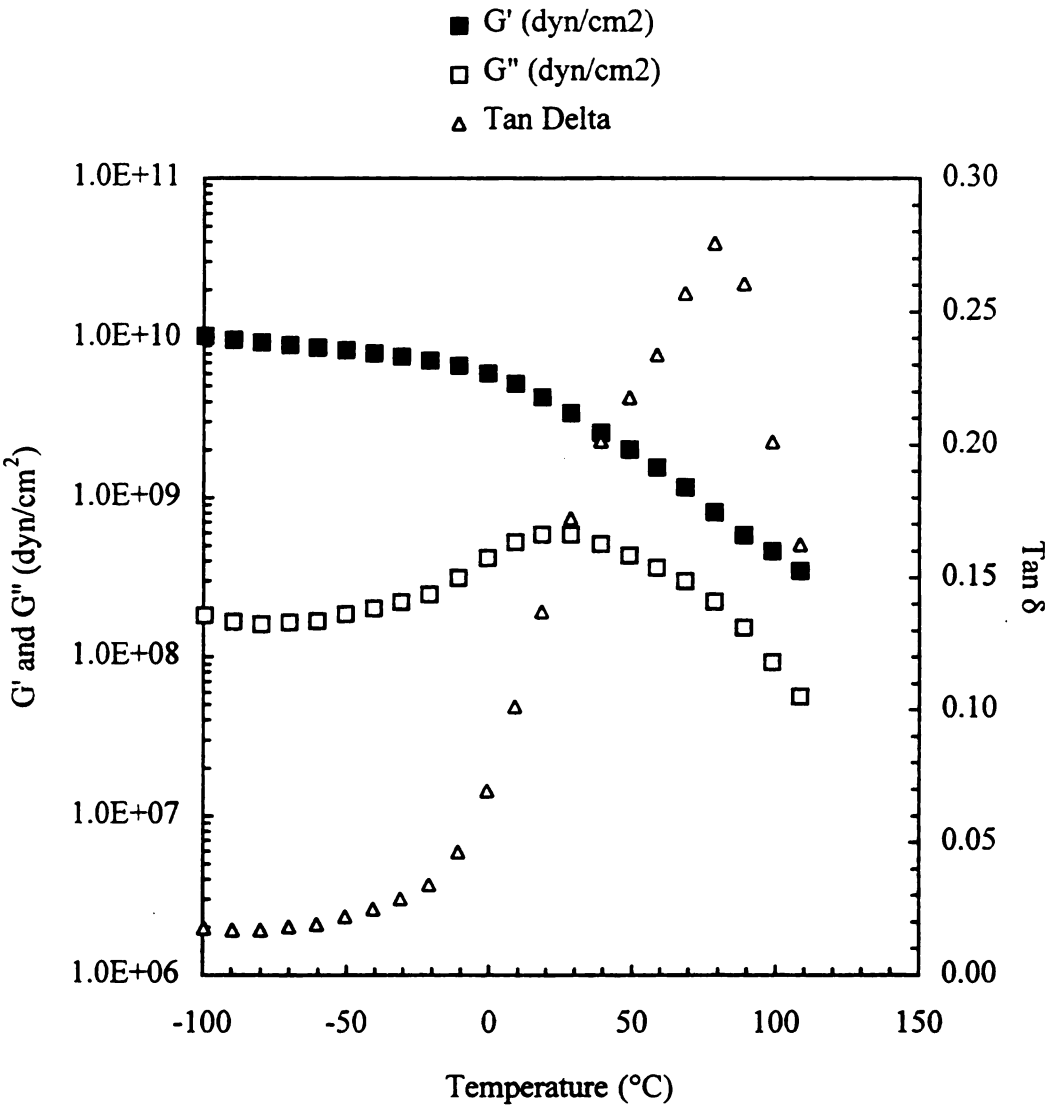

Figure 45. DMA plot for failed laundry additive bottle panel after 90 days at 120 °F.

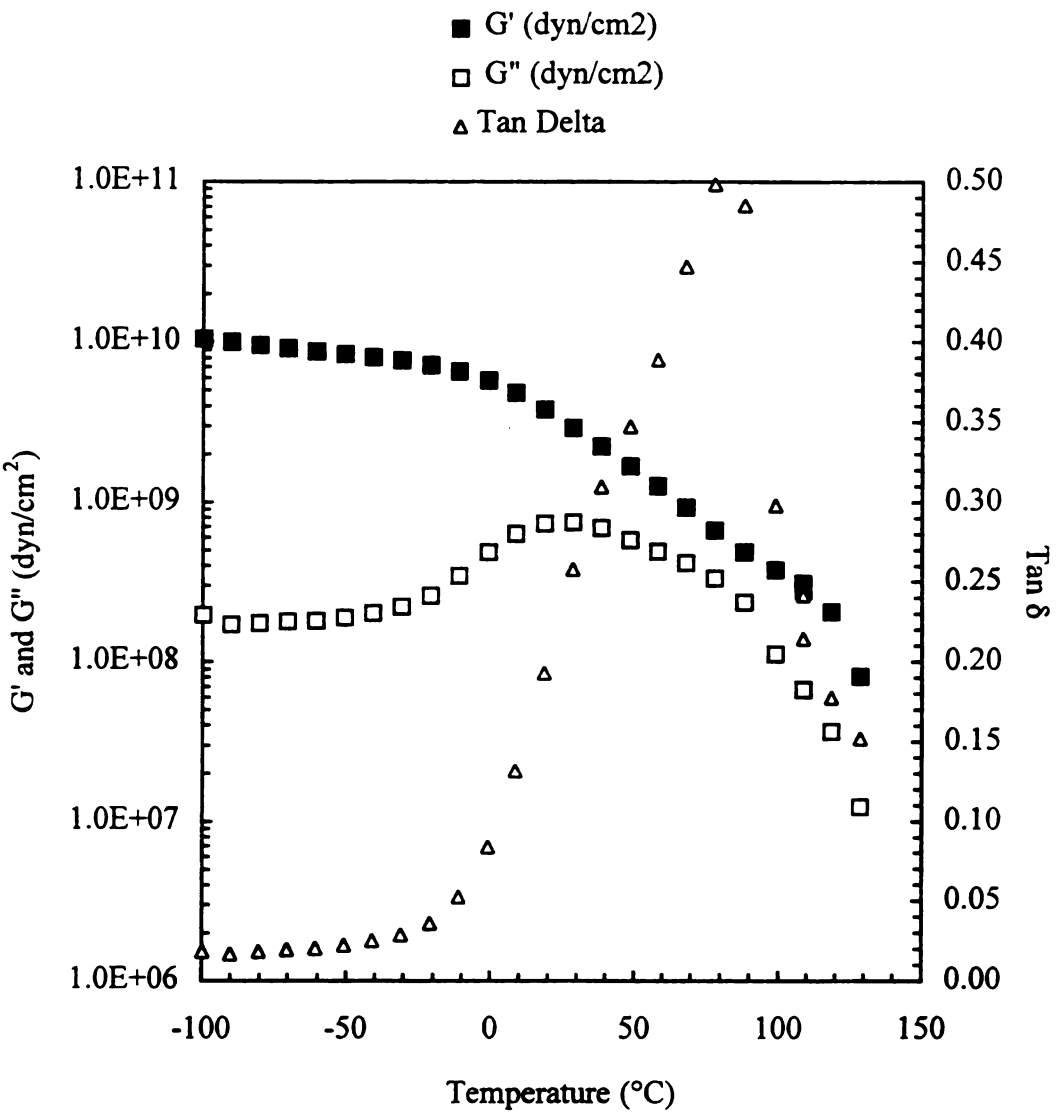

Figure 46. DMA plot for failed anti-bacterial cleaner bottle panel after 109 days at 140 °F.

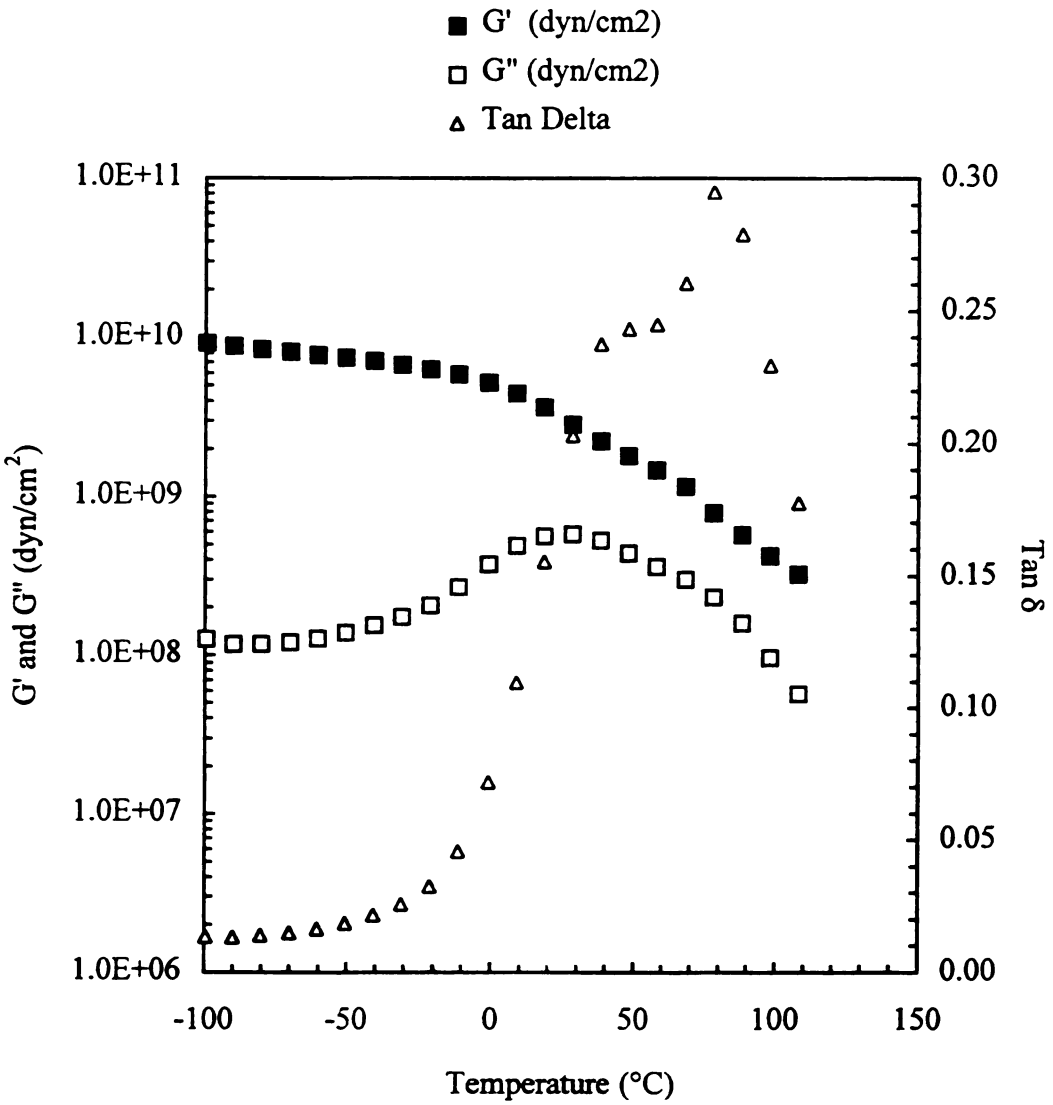

Figure 47. DMA plot for anti-bacterial cleaner bottle panel after 180 days at 120 °F.

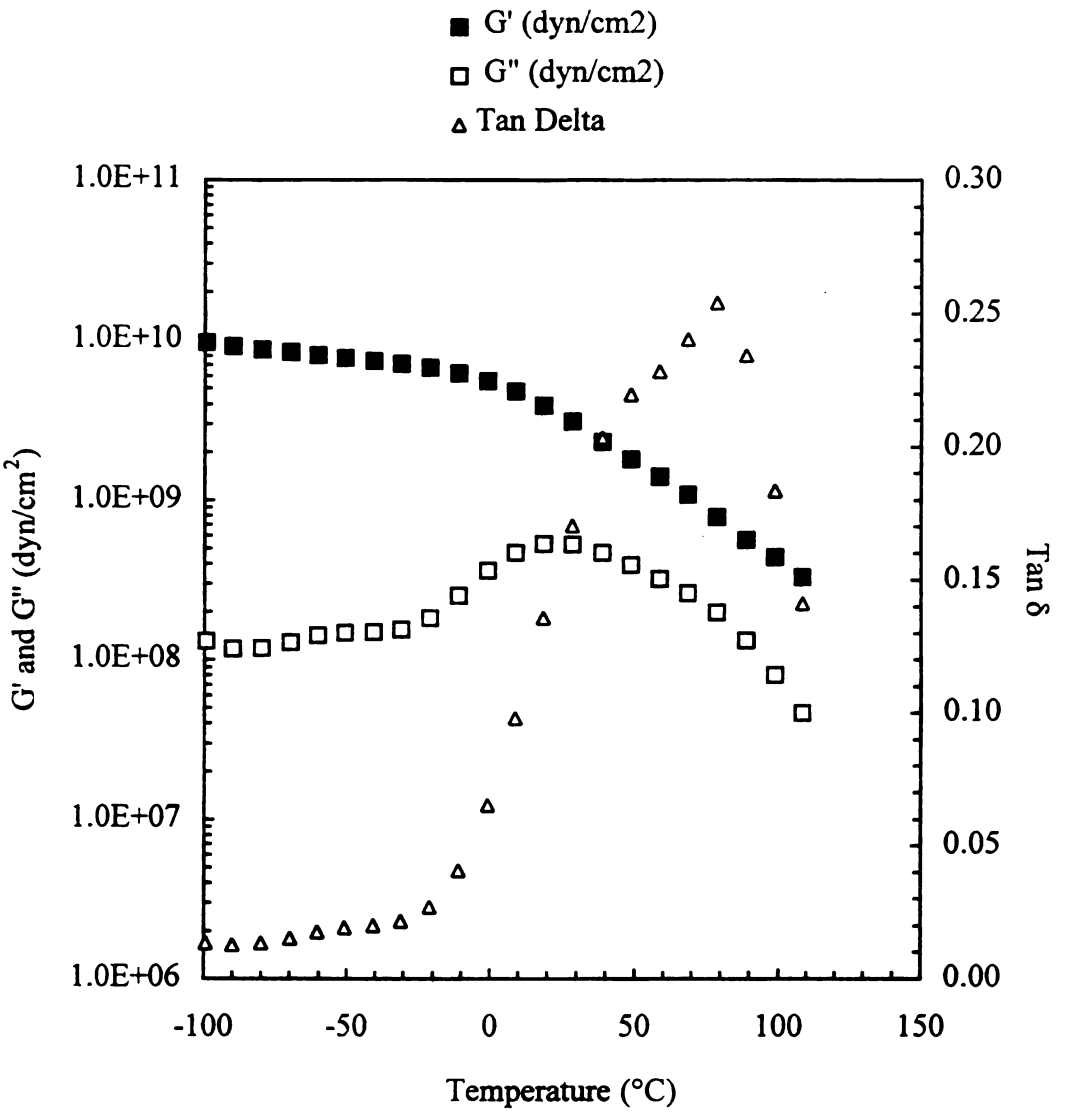

Figure 48. DMA plot for failed glass surface cleaner bottle panel after 87 days at 140 °F.

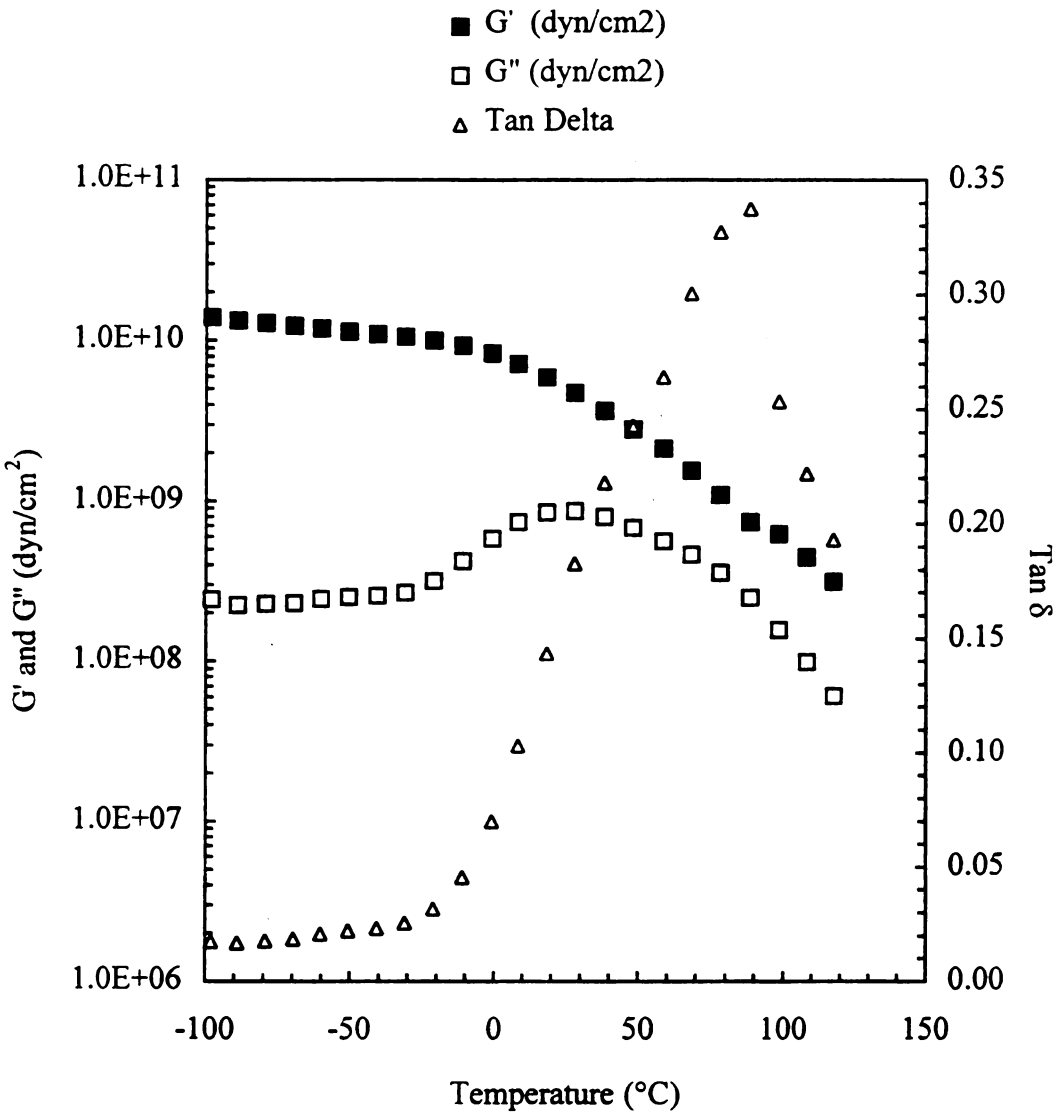

Figure 49. DMA plot for glass surface cleaner bottle panel after 180 days at 120 °F.

The DMA property that would be most sensitive to any morphological changes in the HDPE comprising the bottle is tan δ as described in Chapter 3.A.3. For comparison purposes, Figures 50 and 51 display the tan δ plots for all three product/package systems stored at 140 and 120 °F, respectively, along with the tan δ plot for the control bottle. The results at both temperatures show that the tan δ plots are very similar in shape up to a temperature of approximately 70 °C, with a peak occurring in the approximate range of 60 - 80 °C. However, at higher temperatures, the plots are not as similar as at lower temperatures. This is explained by the fact that the polymer is beginning to soften as it approaches the melting point, which results in greater scatter in the data. In addition, the anti-bacterial surface cleaner tan δ plot at 140 °F, while similar in shape to the other plots, is significantly higher in magnitude than the rest of the data. It is difficult to draw a conclusion from this, but the similarity in the location of the thermal transition implies a minimal change in morphology for this sample.

The similarity in all the tan δ plots suggests that the polymer morphology does not change significantly during the aging process. This conclusion is also supported by the yield stress and modulus results described above, even though there was a minimal change in these properties, since a significant change in the morphological structure would most likely cause a significant change in each of these properties as well. Further support for this conclusion is obtained from the percent crystallinity data described in Chapter 3.E.4.

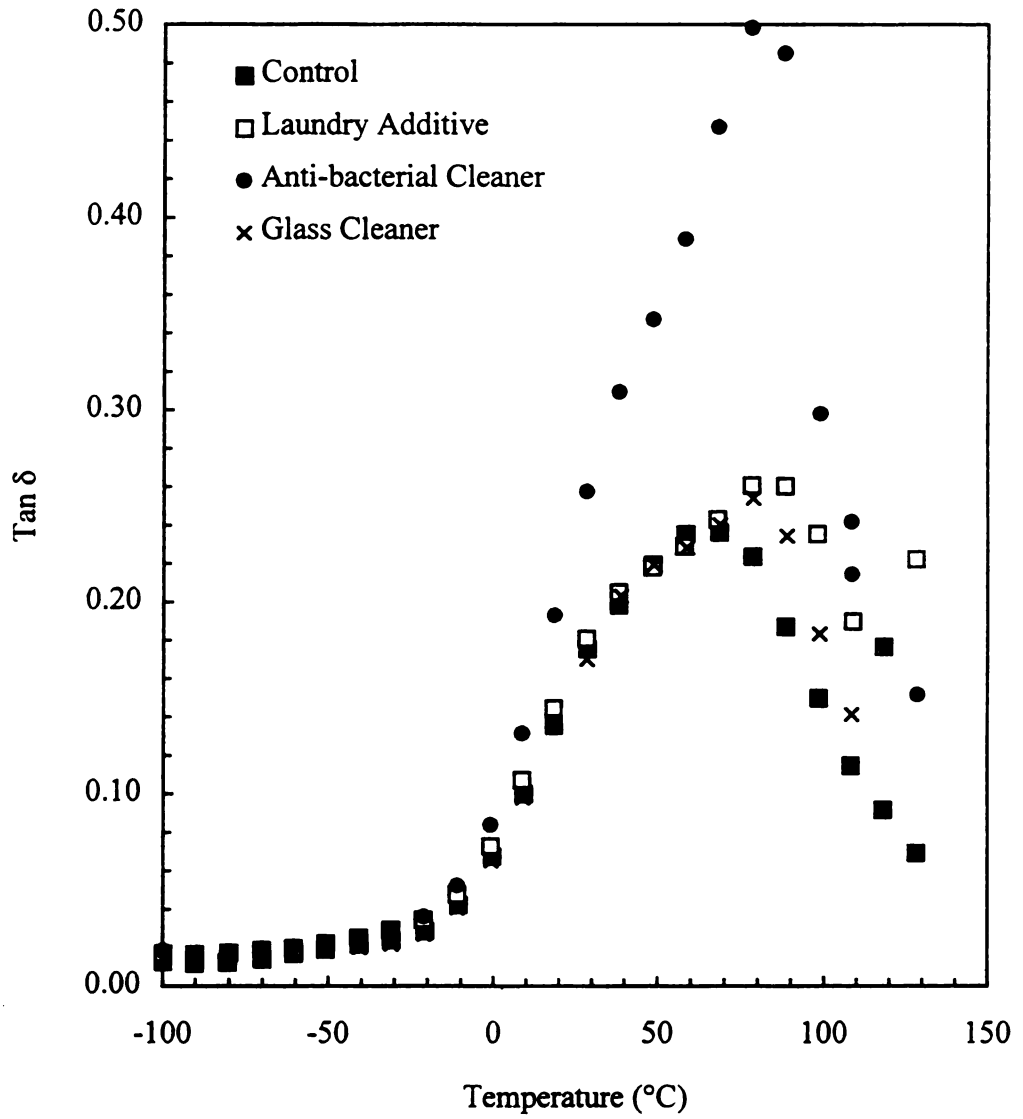

Figure 50. Tan δ plots of bottle panels for product/package systems stored at 140 °F.

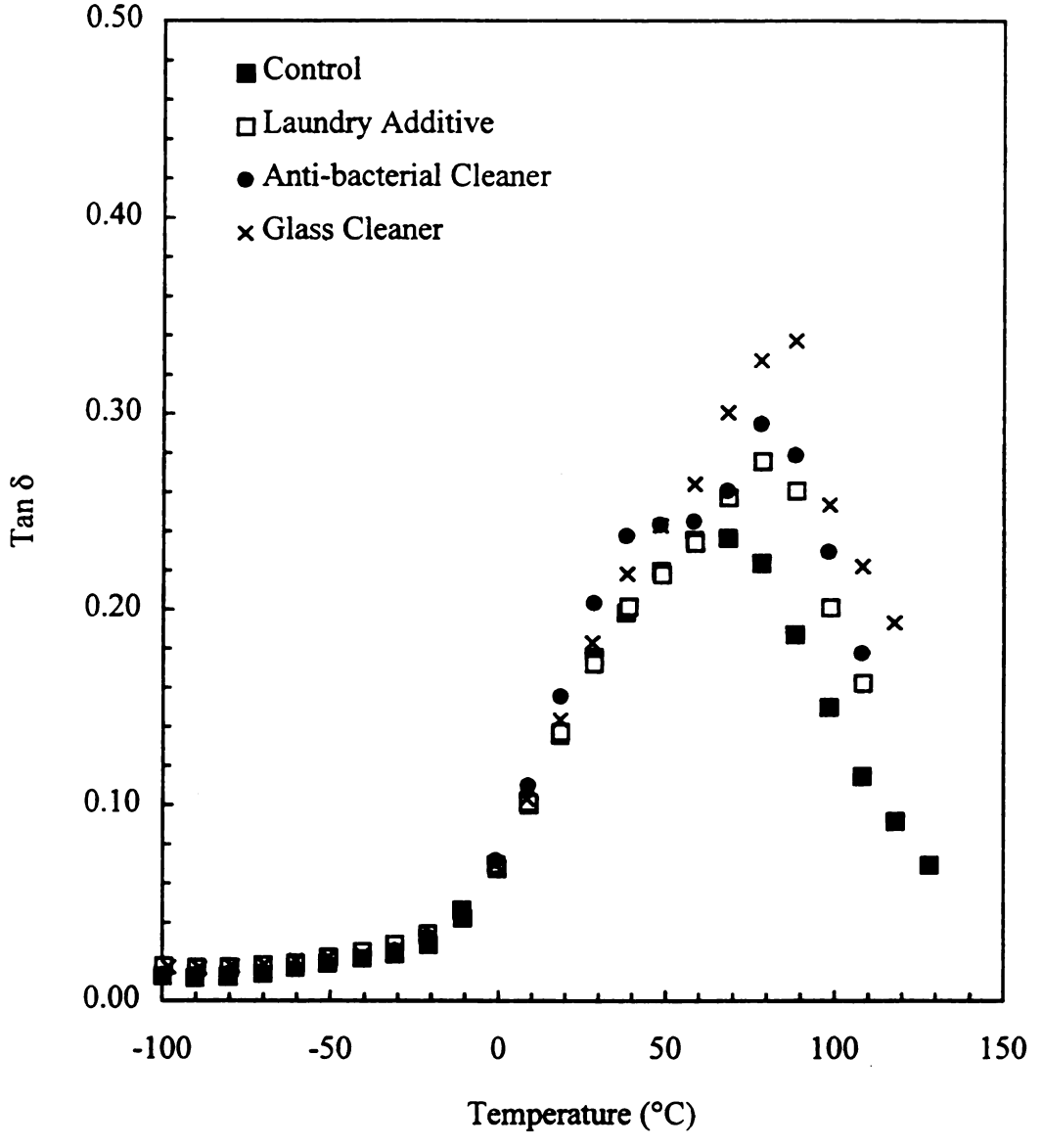

Figure 51. Tan δ plots of bottle panels for product/package systems stored at 120 °F.

3. Yellowness Index

Figures 52 - 59 display all the yellowness index data acquired during the six month study. The data shows the changes in the exterior and interior surface yellowness indices as a function of time for the four sets of product/package systems that failed during the study. This data was analyzed using the t-test in a similar fashion as the yield stress and modulus data; the results are summarized in Tables 21 and 22 for the exterior and interior surface yellowness index measurements, respectively.

Table 21. t-Test results for exterior surface yellowness index measurements.

		t-Test Probability		
Product	**Temp. (°F)**	**Control vs. SDT**	**Control vs. No SDT**	**SDT vs. No SDT**
Laundry Additive	140	0.22	0.52	0.40
	120	0.13	0.32	0.22
Surface Cleaner	140	9.2×10^{-4}	3.8×10^{-6}	0.024
Glass Surface Cleaner	140	0.10	0.018	0.11

Table 22. t-Test results for interior surface yellowness index measurements.

		t-Test Probability		
Product	**Temp. (°F)**	**Control vs. SDT**	**Control vs. No SDT**	**SDT vs. No SDT**
Laundry Additive	140	0.62	0.99	0.26
	120	8.5×10^{-3}	3.5×10^{-3}	0.53
Surface Cleaner	140	1.4×10^{-7}	1.8×10^{-10}	0.014
Glass Surface Cleaner	140	1.7×10^{-11}	9.2×10^{-11}	0.94

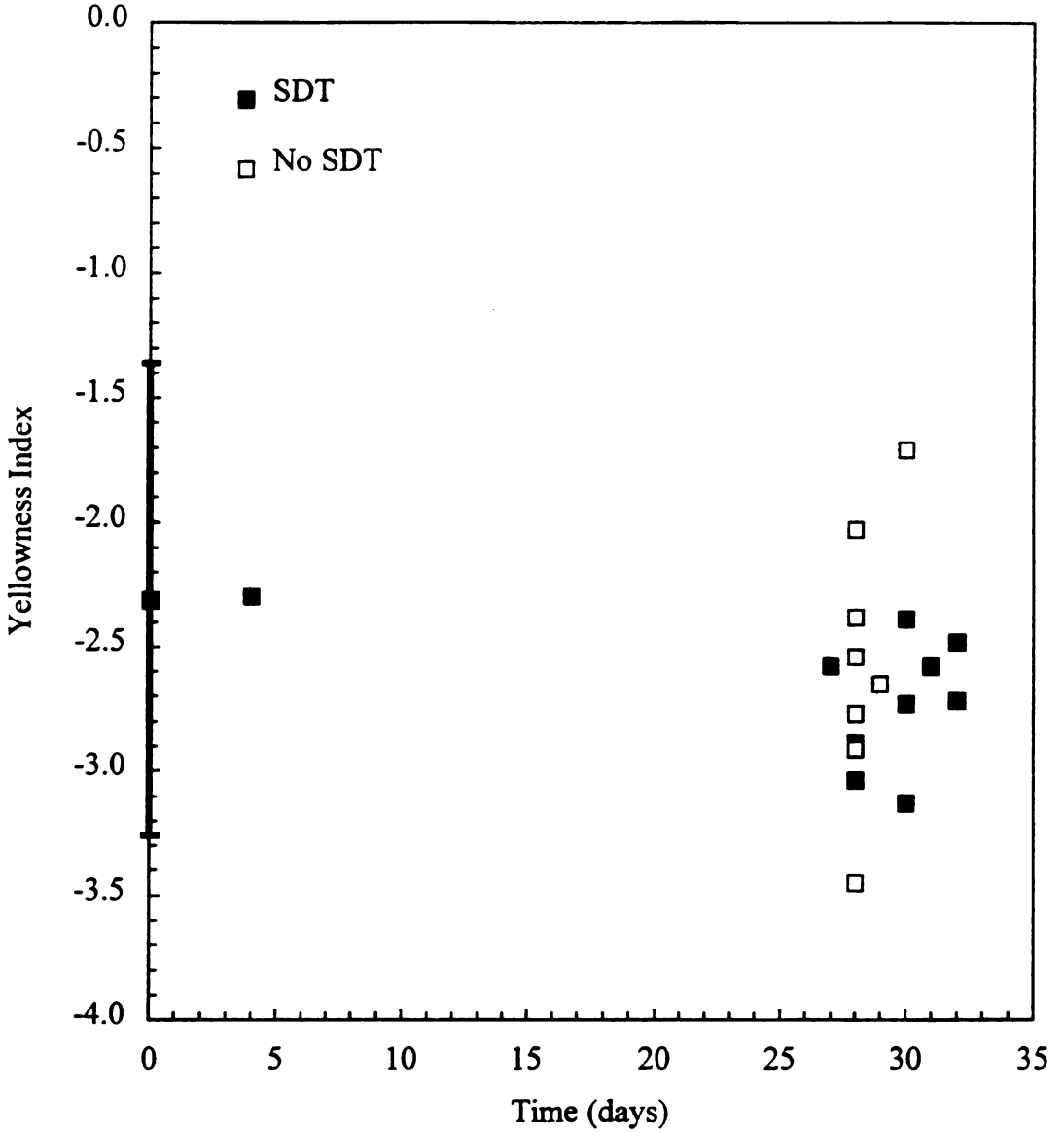

Figure 52. Exterior surface yellowness index vs. time for laundry additive bottles stored at 140 °F.

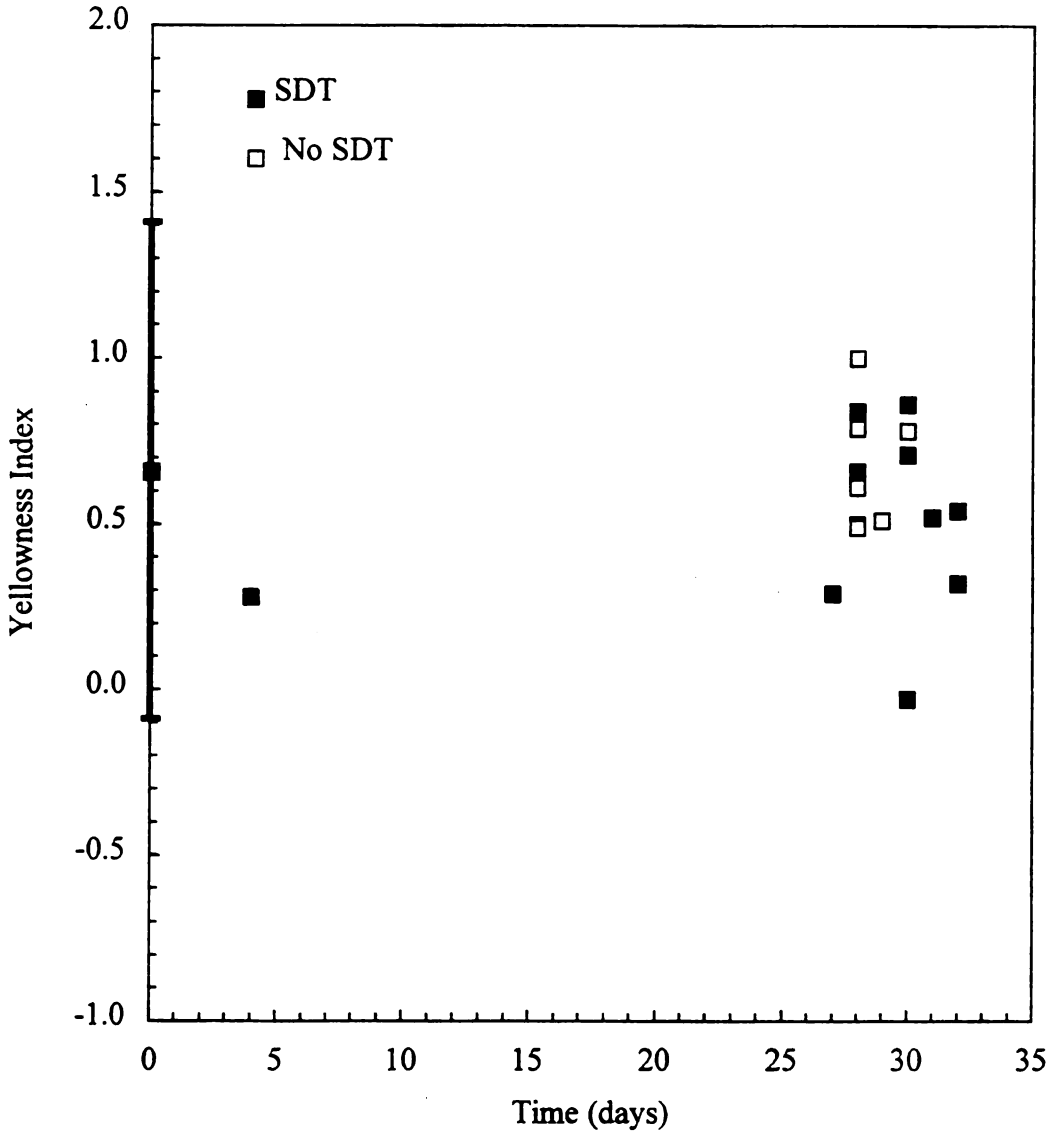

Figure 53. Interior surface yellowness index vs. time for laundry additive bottles stored at 140 °F.

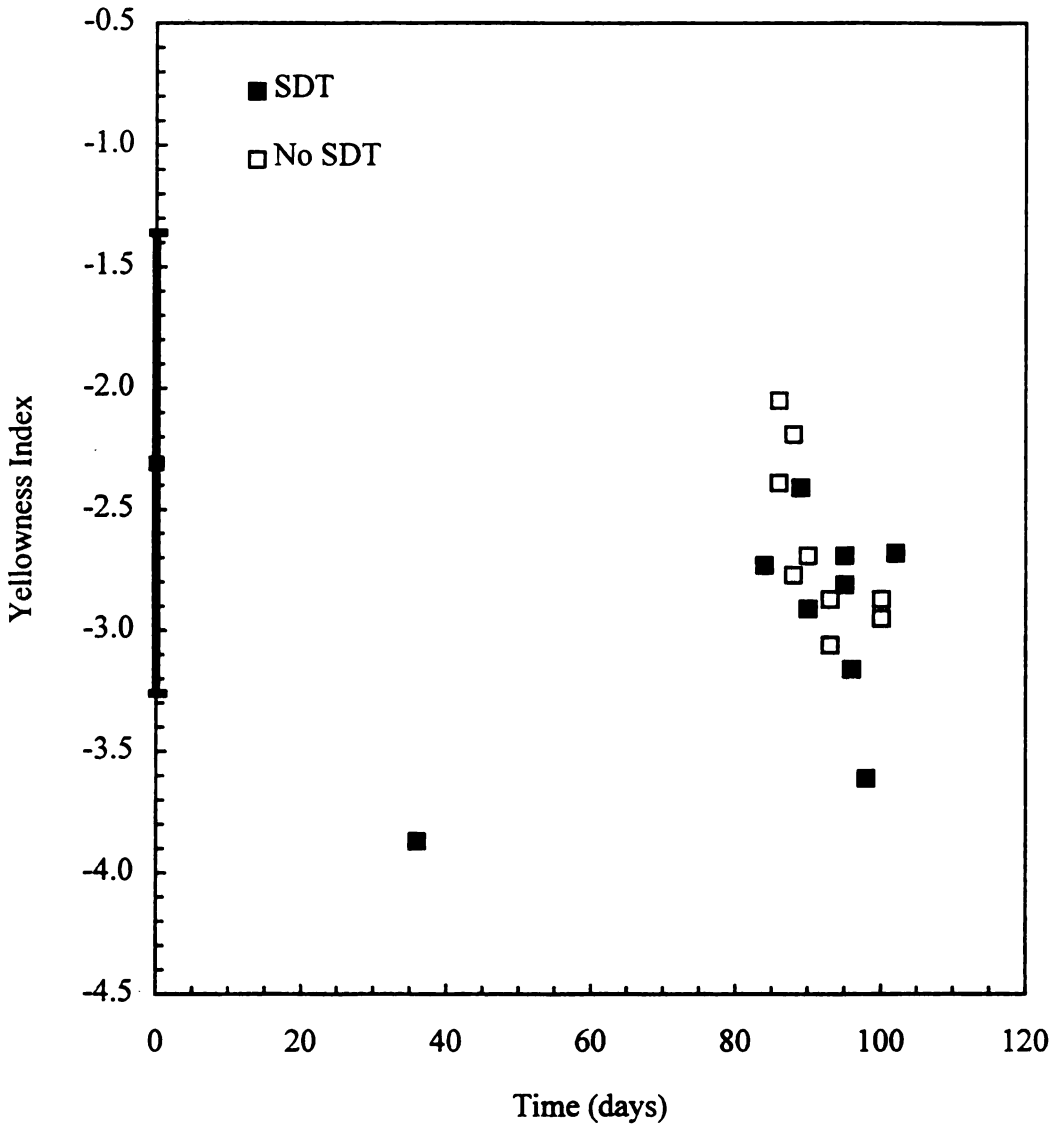

Figure 54. Exterior surface yellowness index vs. time for laundry additive bottles stored at 120 °F.

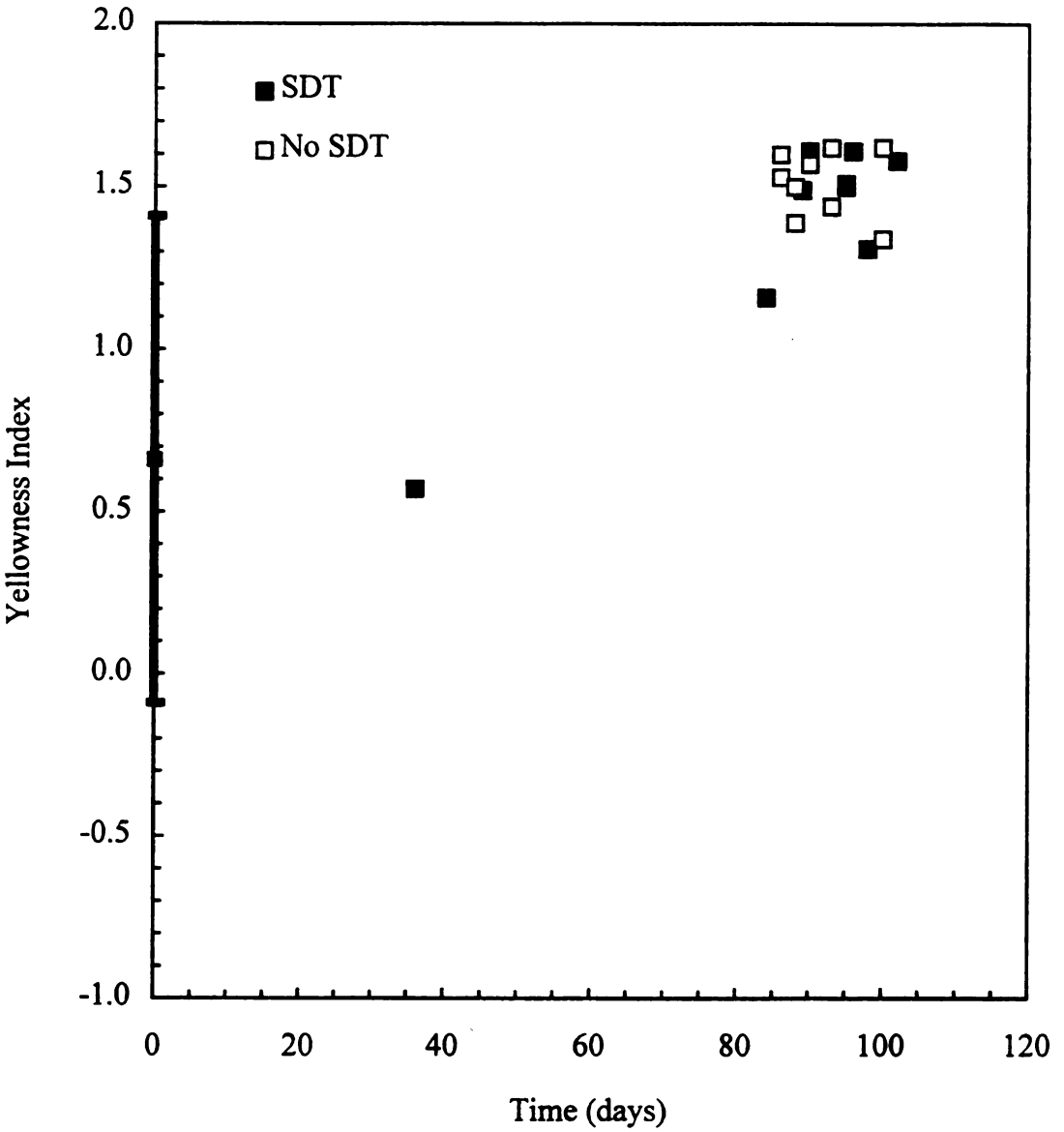

Figure 55. Interior surface yellowness index vs. time for laundry additive bottles stored at 120 °F.

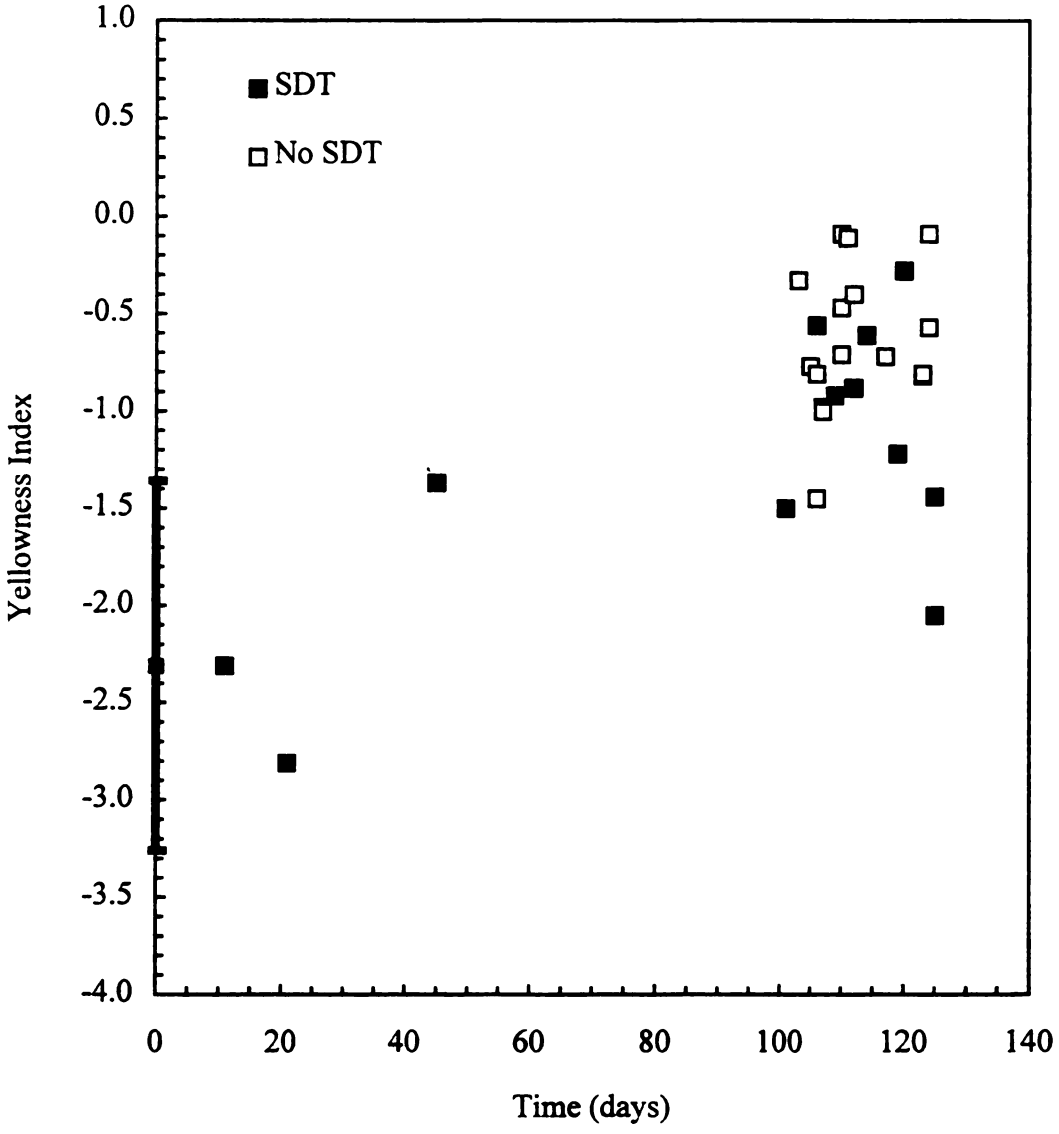

Figure 56. Exterior surface yellowness index vs. time for anti-bacterial cleaner bottles stored at 140 °F.

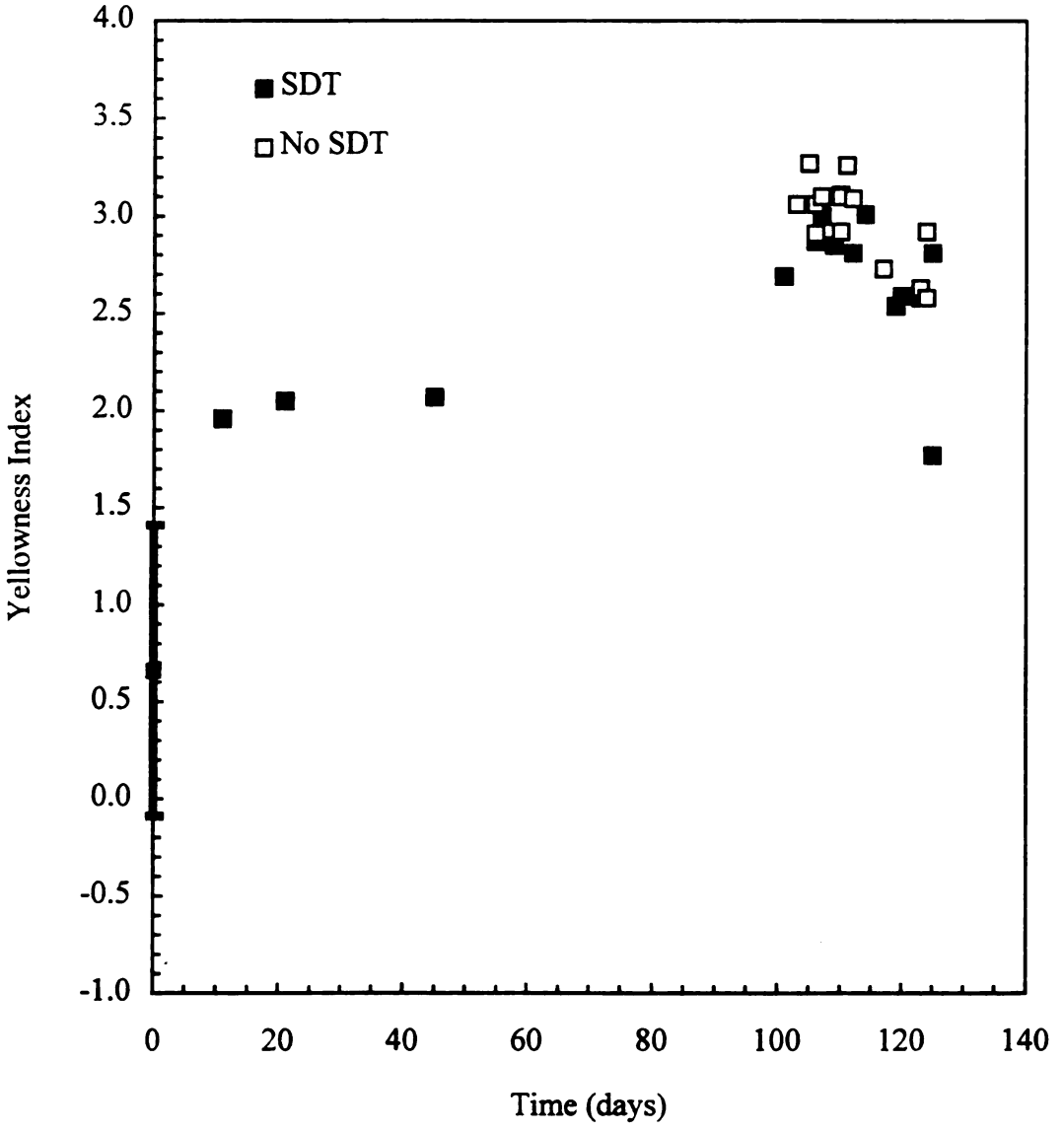

Figure 57. Interior surface yellowness index vs. time for anti-bacterial cleaner bottles stored at 140 °F.

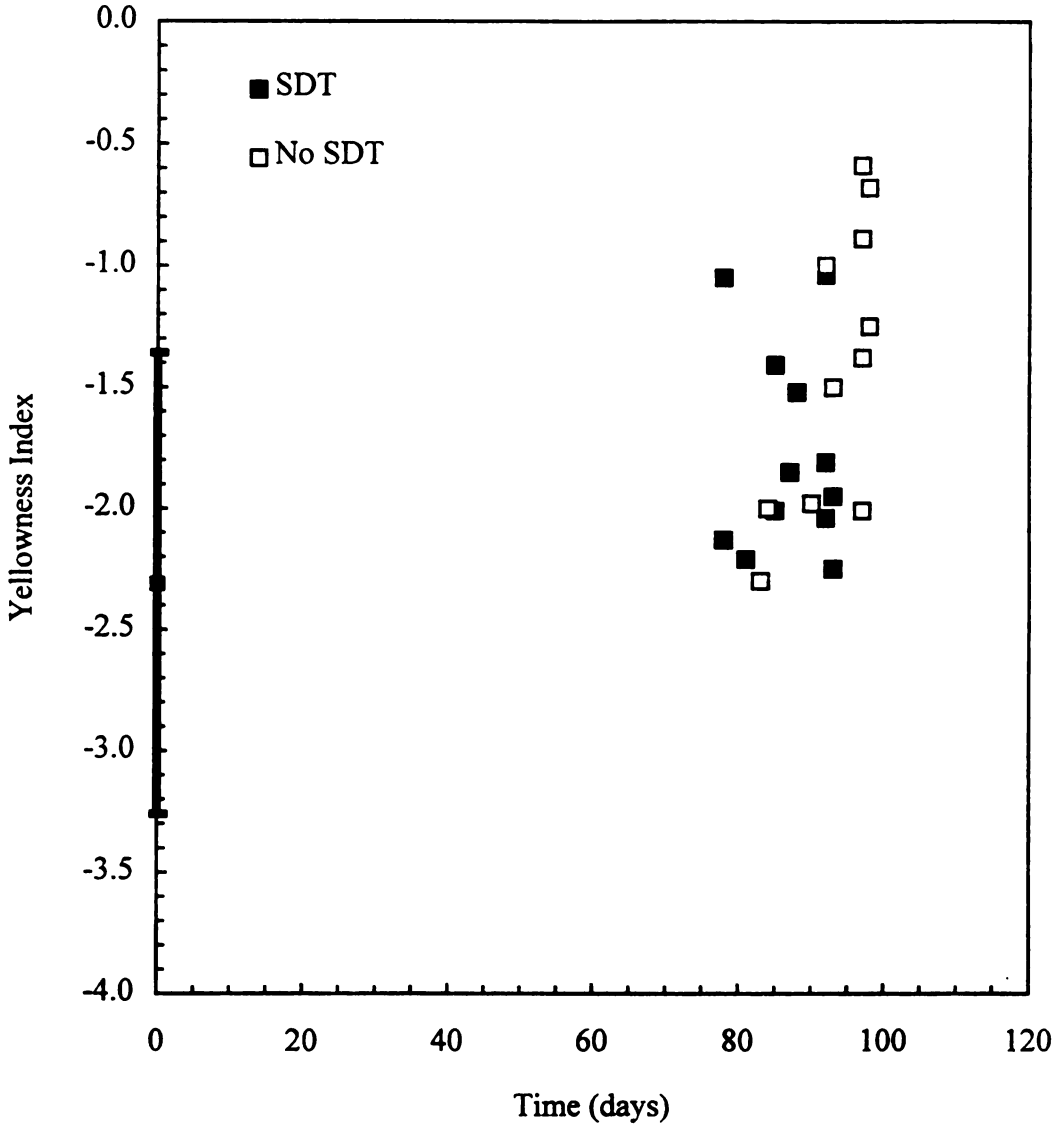

Figure 58. Exterior surface yellowness index vs. time for glass surface cleaner bottles stored at 140 °F.

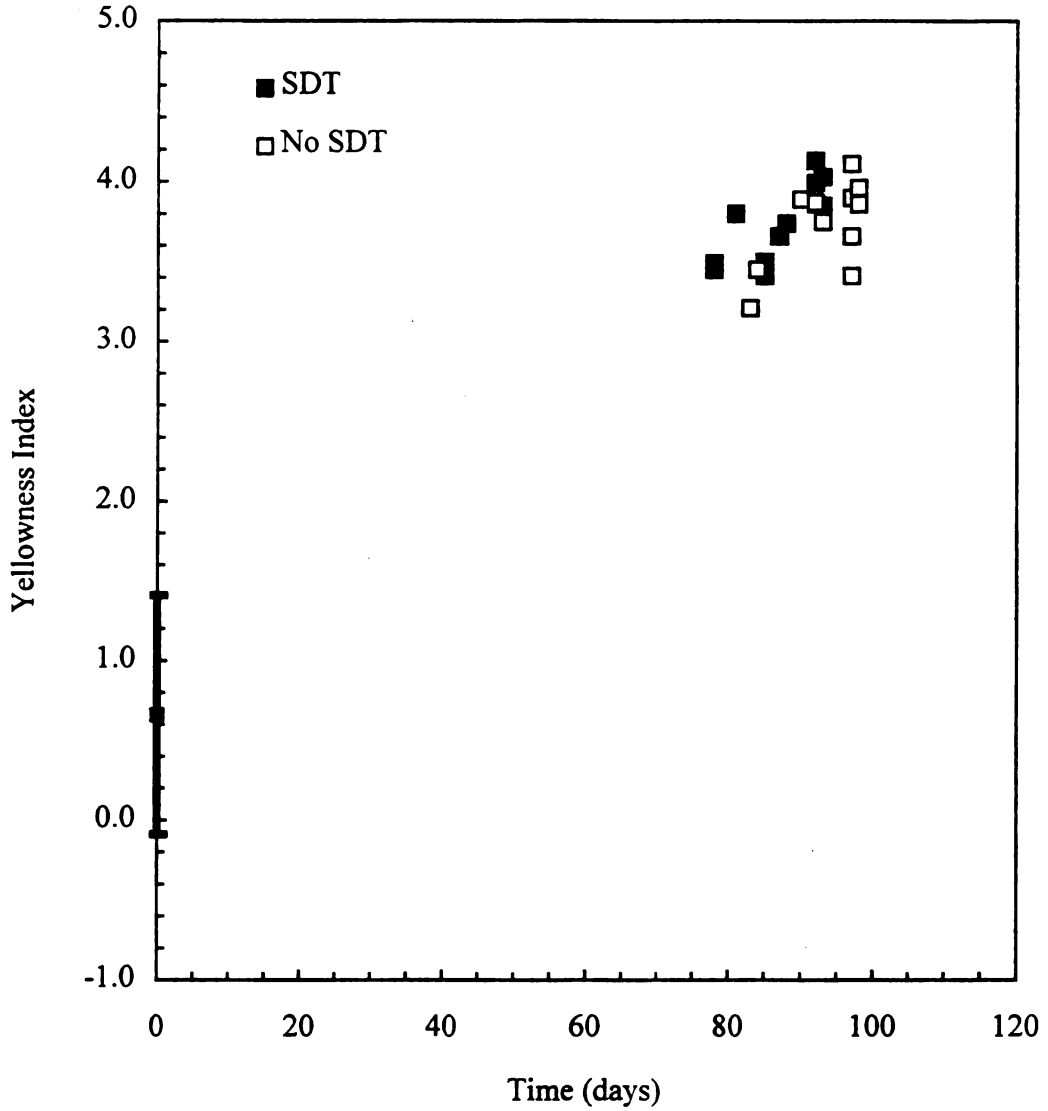

Figure 59. Interior surface yellowness index vs. time for glass surface cleaner bottles stored at 140 °F.

The data for the laundry additive and glass surface cleaner shows that the exterior and interior surface yellowness indices are not dependent on whether or not the samples were exposed to distribution testing. This result is not surprising since the physical environment is not expected to affect the chemical reaction responsible for any color changes at the interface between bottle and contact phase. In contrast, the results for the anti-bacterial surface cleaner suggest that Simulated Distribution Testing impacts the exterior and interior surface yellowness indices (t-test probabilities of 0.024 and 0.014 at 140 and 120 °F, respectively). However, since Simulated Distribution Testing is not expected to affect the yellowness index and the t-test probabilities are close to 0.05, the validity of this conclusion is certainly questionable. Furthermore, visual observation of the data shows that the "SDT" and "No SDT" results are in the same range.

The t-test probabilities displayed in Tables 21 and 22 for the bleach alternative laundry additive product/package system stored at 140 °F strongly suggest that the exterior and interior surface yellowness indices did not change during storage. This is the only failed system that did not show color change signs of the inside bottle surface. However, this system failed after only ~30 days storage time, which is a significantly shorter time than the rest of the product/package systems. The data for the laundry additive system stored at 120 °F shows that, although the exterior surface index does not change, there is strong evidence that the interior surface yellowness index is different than that of the control bottle. The change in color from the control bottle value of 0.66 ± 0.75 to approximately 1.5 (see Figure 55) indicates an increase in blue color. However, this color change could not be observed visually and therefore, the typical consumer

would probably not be affected by such a color change. The result does, however, indicate interaction between the product and packaging system.

Both surface cleaner product/package systems stored at 140 °F show compelling evidence that the interior surface yellowness index is different than that for the control bottle, as indicated by the t-test probabilities and the graphical analysis shown in Figures 57 and 59. As with the laundry additive product/package system stored at 120 °F, the color change is an increase in blue, and was not visually observed. The glass cleaner interior surface yellowness index increased to approximately 4, while the anti-bacterial surface cleaner exhibited an interior surface yellowness index of ~3. The change in exterior surface yellowness index for these product/package systems, while not as pronounced as the change in interior surface index, is still significant. The results clearly indicate that a component(s) of the product is diffusing through the packaging material to affect the color of the exterior surface of the bottle.

While the mechanism of color change was not investigated, the general results obtained imply interaction between product and package material. The practical importance of this is considered minimal, since none of the color changes detected spectrophotometrically were visually observed. However, from a theoretical standpoint, it would be interesting to attempt to correlate the permeation of product constituents with color change.

4. Crystallinity

The crystallinity of HDPE samples taken from several product/package systems was determined by calculating the percent crystallinity from DSC data, as described in Chapter 2.B.7. Due to the length of time required to collect the DSC data, product/package systems were selectively sampled for percent crystallinity determination. To this end, some packaging systems that failed due to environmental stress cracking were evaluated, along with systems that did not fail but were evaluated at the end of the study.

Table 23 displays the percent crystallinity data obtained for failed product/package systems that were stored at 140 °F. All data shown in this table, except for one value of 64%, falls within one standard deviation of the mean for the control

Table 23. Percent crystallinity of 140 °F samples.

Laundry Additive			**Anti-Bacterial Surface Cleaner**			**Glass Surface Cleaner**		
Time (days)	**% Cryst.**	**Failed (Y/N)**	**Time (days)**	**% Cryst.**	**Failed (Y/N)**	**Time (days)**	**% Cryst.**	**Failed (Y/N)**
0	59	-	0	59	-	0	59	-
30	60	Y	21	61	Y	76	61	Y
32	62	Y	45	64	Y	81	61	Y
			101	56	Y	87	59	Y
			106	60	Y	92	61	Y
			107	58	Y	93	56	Y
			111	61	Y	95	59	Y
			120	58	Y	97	58	Y
			124	56	Y	97	60	Y
			124	60	Y	98	57	Y
			125	56	Y	98	57	Y

bottle percent crystallinity (59 ± 3%). In addition, a clear-cut trend of increasing or decreasing percent crystallinity is not observed. These two observations strongly suggest that the percent crystallinity did not change during storage at 140 °F for any of the product/package systems investigated.

Similar percent crystallinity data for the three product/package systems stored at 120 °F are shown in Table 24. The data in this table include product/package systems

Table 24. Percent crystallinity of 120 °F samples.

Laundry Additive			Anti-Bacterial Surface Cleaner			Glass Surface Cleaner		
Time (days)	**% Cryst.**	**Failed (Y/N)**	**Time (days)**	**% Cryst.**	**Failed (Y/N)**	**Time (days)**	**% Cryst.**	**Failed (Y/N)**
0	59	-	0	59	-	0	59	-
36	62	Y	21	61	Y	31	59	Y
84	61	Y	81	61	Y	178	63	N
93	57	Y	178	61	N	180	64	N
95	60	Y	180	66	N			
100	54	Y						
100	61	Y						
102	56	Y						

that were sampled at the end of the six month study, in addition to those that failed during the study. Except for a few values, the data in this table also fall within one standard deviation of the control bottle mean, indicating that the percent crystallinity of the HDPE did not change for samples stored at 120 °F. For completeness, the percent crystallinity was measured at the end of the study on samples taken from product/package systems stored at 100 °F and ambient conditions. The results are shown in Table 25 and again suggest no change in percent crystallinity.

Table 25. Percent crystallinity at the end of study of 100 °F and ambient samples.

Laundry Additive			Anti-Bacterial Surface Cleaner			Glass Surface Cleaner		
	% Crystallinity			% Crystallinity			% Crystallinity	
Time (days)	100 °F	Amb.	Time (days)	100 °F	Amb.	Time (days)	100 °F	Amb.
180	58	-	179	60	-	179	63	-
182	-	58	182	-	62	182	-	60

The percent crystallinity results presented above are consistent with conclusions made relating to the mechanical properties of the product/package systems. A significant change in polymer morphology would most likely cause a change in the overall percent crystallinity of the HDPE. Such a change would result in large changes in the tensile and dynamic mechanical properties, in addition to percent crystallinity. Although mechanical property changes were detected in some cases, these changes were fairly small and would not be expected to show up in percent crystallinity measurements. A further conclusion is that crystallinity is probably not a material property that is directly related to package integrity since dramatic changes in this property were not observed for failed product/package systems.

5. Sorption of d-Limonene for Anti-Bacterial Surface Cleaner

The sorption of d-limonene into HDPE bottle panel samples was determined for several anti-bacterial surface cleaner product/package systems during the course of the six month investigation. Measurements were made on samples that failed during storage

(140 and 120 °F) and on samples that did not fail but were sampled at the end of the study (100 °F and ambient). The concentration of d-limonene in HDPE bottle samples, as determined by gas chromatographic analysis (see Chapter 2.B.8), were then plotted as a function of time for each storage environment.

Figure 60 displays the concentration of d-limonene in HDPE bottle samples for the anti-bacterial surface cleaner system as a function of time during storage under each environmental condition. The data obtained at 140 and 120 °F are for samples that were removed from storage because of failure, while the 100 °F and ambient data are for systems that did not fail but were removed from storage for analysis. Most of the data presented in this plot are single measurements, and therefore error bars could not be associated with the measurements.

Each set of data in Figure 60 shows the same general behavior, which was independent of storage conditions, in that there is a gradual decrease in the d-limonene concentration with time. Since d-limonene was not detected in the control bottles (see Table 3, page 35), it is obvious that there was a rapid increase in concentration prior to the first data points being measured for each storage environment. After this time period, the concentration gradually decreases until eventually there is no measurable level of d-limonene detected.

Comparing the d-limonene results obtained from the four different storage conditions shows that there is no particular concentration level in which package failure would be expected to occur. Data for product/package systems stored at 100 °F and ambient show that these HDPE bottles exhibited extremely high concentrations of

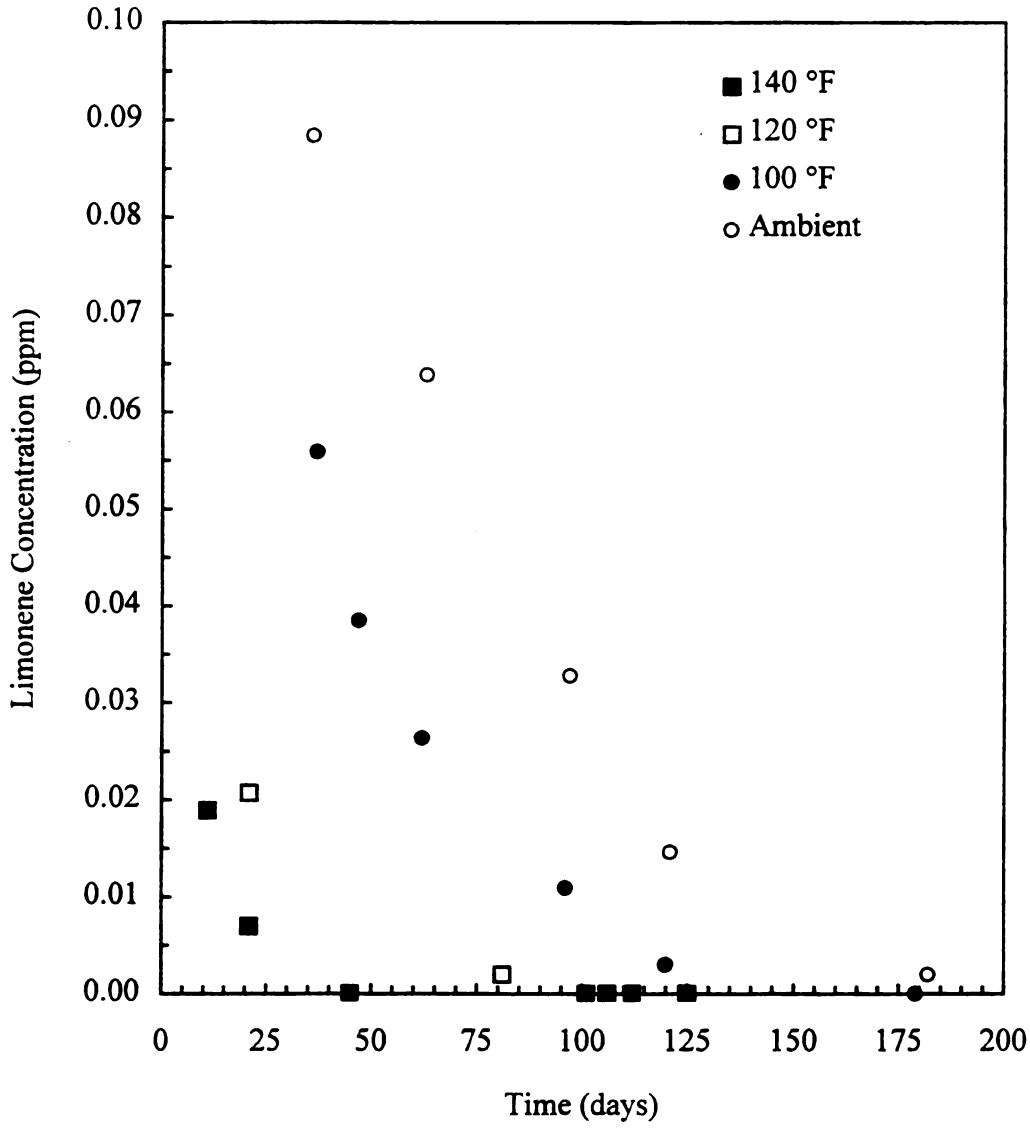

Figure 60. d-Limonene concentration in bottle panels of anti-bacterial cleaner product/package system as a function of temperature.

d-limonene when compared to the 140 and 120 °F systems that failed, even though they did not fail at the time when these high concentrations occurred. In addition, when the concentration levels at these lower temperature storage conditions drop to values similar to the failed systems, these systems still did not fail. Therefore, the data implies that the sorption of d-limonene into the plastic packaging material is not directly related to product/package integrity.

The mechanism responsible for the general shape of the curves shown in Figure 60 has been discussed previously [26] and can be described by understanding the mechanism of permeation as described in Chapter 3.C.3. Initially, since there is no permeant (i.e., d-limonene) in the packaging material, there will be a rapid increase in permeant concentration due to the high concentration gradient between contact phase and package. However, the product/package system is a dynamic system because, as the permeation process proceeds, permeant is depleted from the contact phase thereby causing decreased concentration in the product. This reduction in concentration leads to a decrease in sorption, and hence, a decrease in the amount of permeant in the packaging material. Eventually all of the permeant will permeate through the packaging material, or the driving force will be so small that permeant will not be sorbed into the packaging material, and little, if any permeant will be detected in the packaging material. This mechanism will result in a gradual decrease in d-limonene concentration, with an ultimate concentration approaching zero. This entire process will be accelerated at higher storage temperatures. This is exactly the behavior that is observed as shown in Figure 60.

CHAPTER 4

CONCLUSIONS

Studies identifying the effect of chemical and physical environments on the integrity of product/package systems during accelerated and long-term storage conditions can provide the fundamental basis for rational material selection for new products and/or package system designs. The research presented in this dissertation is the initial phase in further developing this type of fundamental understanding.

The physical environment resulted in several types of package system defects which were due to the shock and vibration forces associated with Simulated Distribution Testing. Defects occurring in the bottle included dents, abrasions, and creases. The most prevalent types of defects were creases, which were located in the neck, bottom, shoulder, and panel regions of the bottle, and occurred in approximately 85% of the package systems. Dents in the shoulder and bottom corner of the bottle were observed in approximately 16% and 9% of the bottles, respectively. Abrasion defects, which included panel, bottom, and shoulder abrasions, were detected in approximately 12%, 4%, and 3% of the bottles, respectively.

Closure defects were observed less frequently than defects to the bottle component of the package system. The most severe closure defect, in which the closure was physically sheared off from the bottle, occurred in 2.8% of the bottles. Less severe

closure defects included damage to the nozzle cover and cracks in the closure body. Each type of defect in these categories was observed in less than 1% of the package systems, except for closures in which the nozzle cover was broken off (4.3%).

Package system failure during storage, defined as product leaking from the bottle, resulted from environmental stress cracking. Damage to the product/package systems due to the physical environment was determined to seriously impact package stability during long-term storage only when the defect type was a bottle dent. All other defects caused by Simulated Distribution Testing did not affect product/package system integrity. An *initiation period* was observed, during which time only package systems with a distribution dent failed. The primary location where failure was observed for package systems that did not fail from distribution dents was near the center of the bottom edge of the bottle. This result was independent of Simulated Distribution Testing, unless there was a dent in the bottle, and it was shown that this bottom center location had the minimum bottle thickness.

Product/package system integrity was also shown to be affected by the chemical nature of the contact phase. The bleach alternative laundry additive system was clearly the most aggressive product, as these product/package systems failed significantly earlier than the two surface cleaner product/package systems. Although these two later product/package systems exhibited similar storage stability, the glass surface cleaner systems failed prior to the anti-bacterial surface cleaner samples. This was attributed in part to higher pressure build-up, causing greater stress in the glass surface cleaner package systems.

Performance criteria, including tensile yield stress, modulus of elasticity, and dynamic mechanical properties, which were evaluated for failed product/package systems during the study did not show significant differences from control samples. Minor changes estimated to be at most ~10% were observed in the tensile yield stress and modulus of elasticity on samples taken from a panel of failed bottles. However, these minor changes in properties did not influence product/package stability, and therefore, are most likely not significant from a practical standpoint. Similarly, significant changes in dynamic mechanical properties and percent crystallinity were not observed. In contrast, sizable changes in yellowness indices were observed on the interior and exterior surfaces of most product/package systems investigated. The color changes detected spectrophotometrically were not visually observed and therefore are also probably not significant from a practical standpoint. However, this result implies product/package interaction due to sorption of product constituents and subsequent chemical reaction.

In conclusion, the research presented in this dissertation has defined many of the important techniques and considerations necessary in advancing the fundamental understanding relating chemical, physical, and climatic environmental effects to product/package interaction and integrity. However, additional research is required to further increase the usefulness of such an experimental design and to fulfill the ultimate goal of providing the foundation for systematic material selection for new product/package systems. For example, more detailed studies are required to allow the application of the Arrhenius approach to estimate package system failure. In addition, research on other packaging materials used for rigid applications such as PCR resins,

poly(ethylene terephthalate), poly(vinyl chloride), and poly(propylene) could be investigated. Similarly, other types of packaging systems and components could be studied such as flexible and corrugated packaging materials, closures, and finishes. Finally, investigation of several different simulated distribution test procedures could provide evidence of the impact of product distribution environment on product/package system integrity.

LIST OF REFERENCES

LIST OF REFERENCES

1. *Packaging World* July, 1997, D2.

2. *Modern Plastics* **1990**, 67, 46.

3. Lustiger, A. In "Failure of Plastics"; Brostow, W.; Corneliussen, R. D., Eds.; Hanser: Munich, 1986; Chapter 16.

4. Wright, D. C. "Environmental Stress Cracking of Plastics"; Rapra Technology Limited: United Kingdom, 1996.

5. *Packaging World* April, 1997, 26-28.

6. Choudhry, S.; Lox, F.; Decroly, P. *Packaging Technology and Science* **1994**, 7, 163-167.

7. Singh, S. P.; Syal, V. P. *J. Test. Eval.* **1996**, 24, 241-244.

8. Schuluter, A. R.; Miller, M. F.; Jones, D. K.; Meade, M. K.; Ramsey, C. B.; Patterson, L. L. *Meat Science* **1994**, 37, 257-270.

9. "Standard Practice for Performance Testing of Shipping Containers and Systems"; ASTM D 4169-94, Annual Book of ASTM Standards: Philadelphia, PA, 1995; Vol. 15.09, pp 551-561.

10. "Preshipment Test Procedures - For Domestic Shipments Within the Continent of Origin"; International Safe Transit Association, April, 1996.

11. "Preshipment Test Procedures - For Export Shipments Outside the Continent of Origin"; International Safe Transit Association, April, 1996.

12. Singh, S. P.; Voss, T. *J. Test. Eval.* **1992**, 20, 382-387.

13. Imai, T. M.S. Thesis, Michigan State University, 1988.

14. "Good Practices Manual for Packaging in Plastic Bottles"; Plastic Bottle Institute, 1980.

15. "Standard Test Method for Flow Rates of Thermoplastics by Extrusion Plastomer"; ASTM D 1238-90b, Annual Book of ASTM Standards: Philadelphia, PA, 1994; Vol. 08.01, pp 272-280.

16. Brandrup, J.; Immergut, E. H. (Eds.) "Polymer Handbook"; J. Wiley and Sons: New York, 1989; p V/23.

17. "Standard Test Method for Tensile Properties of Plastics"; ASTM D 638-91, Annual Book of ASTM Standards: Philadelphia, PA, 1994; Vol. 08.01, pp 52-64.

18. "Standard Test Method for Yellowness Index of Plastics"; ASTM D 1925-70, Annual Book of ASTM Standards: Philadelphia, PA, 1994; Vol. 08.01, pp 489-491.

19. Wunderlich, B. "Thermal Analysis"; Academic Press: New York, 1990; p 418.

20. Birley, A. W.; Haworth, B.; Batchelor, J. "Physics of Plastics: Processing, Properties, and Materials Engineering"; Oxford University Press: New York, 1992; p 310.

21. Nielsen, L. E.; Landel, R. F. "Mechanical Properties of Polymers and Composites"; Marcel Dekker: New York, 1994; Chapter 4.

22. Bogdanov, B. G.; Michailov, M. In "Handbook of Polyolefins: Synthesis and Properties"; Vasile, C; Seymour, R. B., Eds.; Marcel Dekker: New York, 1993; Chapter 10.

23. DeLassus, P. T. *Polymers, Laminations & Coatings Conference*, **1985**, 445-450.

24. SAS® User's Guide. Version 6. 1990. SAS Inst., Inc., Cary, NC.

25. Schultz, J. "Polymer Materials Science"; Prentice-Hall: New Jersey, 1974; Chapter 11.

26. Booma, M.; Hoojjat, P.; Giacin, J. R. *J. of Plastic Film & Sheeting* **1995**, 11, 58-78.